

ARTHUR LAKES LIBRARY
COLORADO SCHOOL OF MINES
GOLDEN, CO 80401

**SPINODAL DECOMPOSITION FOR THE
SPATIALLY DISCRETE CAHN-HILLIARD
EQUATION**

by
Brian E. Moore

ProQuest Number: 10794463

All rights reserved

INFORMATION TO ALL USERS

The quality of this reproduction is dependent upon the quality of the copy submitted.

In the unlikely event that the author did not send a complete manuscript and there are missing pages, these will be noted. Also, if material had to be removed, a note will indicate the deletion.



ProQuest 10794463

Published by ProQuest LLC (2018). Copyright of the Dissertation is held by the Author.

All rights reserved.

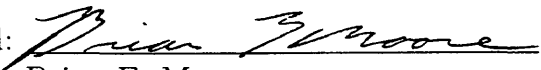
This work is protected against unauthorized copying under Title 17, United States Code
Microform Edition © ProQuest LLC.

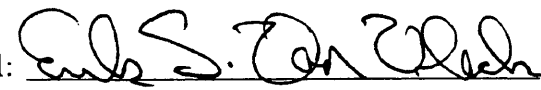
ProQuest LLC.
789 East Eisenhower Parkway
P.O. Box 1346
Ann Arbor, MI 48106 – 1346

A thesis submitted to the Faculty and the Board of Trustees of the Colorado School of Mines in partial fulfillment of the requirements for the degree of Master of Science (Mathematical and Computer Sciences).

Golden, Colorado

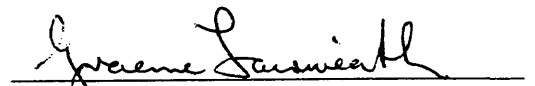
Date 9/8/99

Signed: 
Brian E. Moore

Approved: 
Dr. Erik Van Vleck
Professor of Mathematics
Thesis Advisor

Golden, Colorado

Date 9/8/99

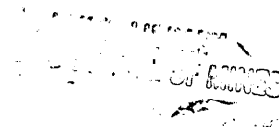

Dr. Graeme Fairweather
Professor and Head
Department of Mathematical and
Computer Sciences

ABSTRACT

The process of phase separation with a characteristic wavelength is a phenomenon known as spinodal decomposition. In this thesis, spinodal decomposition is studied for a discretized fourth-order parabolic partial differential equation known as the spatially discrete Cahn-Hilliard equation. Here, an extensive and mathematically rigorous analysis of when and how spinodal decomposition occurs in this equation is performed.

First, a linearization of the nonlinear problem is considered for the spatially discrete equation. It is shown that the eigenvalues for the discrete linear equation are almost equal to the eigenvalues of the continuous linear equation for a sufficiently fine discretization of the domain. Then, using results obtained for the continuous problem to make conclusions about the discrete problem, a probability estimate is derived. This estimate says that, with a probability close to one, an initial condition chosen at random inside a particular neighborhood of an equilibrium in the spinodal interval will lead to spinodal decomposition, provided the number of grid points for the spatially discrete domain is large enough. An estimate of the wavelength of spinodally decomposed states is also derived. These results are then used to prove a similar probability estimate for the nonlinear problem.

Following this theoretical analysis, two time discretizations, as well as a spatial discretization, will be considered for the Cahn-Hilliard equation. At this point, two different time stepping techniques will be used to give examples of the dependence of the theoretical results on the equilibrium point used to linearize the problem, the distance the initial condition is from that point, and the size of the spatial mesh. These numerical simulations offer confidence in both the numerics used to solve the problem and the theory developed in this thesis. Finally, a comparison of the Crank-



Nicolson method and a gradient stable splitting method presented by David Eyre, which are used for the numerics of this thesis, are compared. It is found that these methods give nearly the same results for each experiment, even though each solves the problem very differently.

TABLE OF CONTENTS

ABSTRACT	ii
LIST OF FIGURES	vi
LIST OF TABLES	vii
ACKNOWLEDGMENTS	viii
Chapter 1 INTRODUCTION	1
Chapter 2 THE LINEARIZED EQUATION	5
2.1 Spectral Analysis	5
2.1.1 The Continuous Laplacian Operator	6
2.1.2 The Discrete Laplacian Operator	13
2.1.3 The Dominating Subspace	18
2.2 Dynamics of the Linear Problem	20
2.2.1 Choosing a Spatial Mesh	20
2.2.2 Probability Estimates	24
2.3 Wavelength Estimates	33
Chapter 3 NONLINEAR DYNAMICS	44
3.1 The Abstract Equation	44
3.1.1 Properties of the Linear Operator	45
3.1.2 Estimates for the Nonlinearity	50
3.2 Spinodal Decomposition	52
3.2.1 The Flow on the Invariant Manifold	53
3.2.2 Probability Estimates for the Nonlinear Equation	69
Chapter 4 TIME STEPPING SCHEMES	73
4.1 The Cahn-Hilliard Equation as a Gradient System	74
4.2 One-Step Gradient Stable Methods	78
4.2.1 Crank-Nicolson Method	79
4.2.2 Eyre's Method	80

Chapter 5	NUMERICAL EXPERIMENTS AND RESULTS . . .	86
5.1	Outline of Experimental Setup	87
5.2	Crank-Nicolson Method	90
5.2.1	Results for the Parameter m	91
5.2.2	Results for the Perturbation from m	91
5.2.3	Results for the Product $(\epsilon n)^2$	93
5.3	Eyre's Method	94
5.4	Discussion of the Numerical Results	94
Chapter 6	CONCLUSIONS AND FUTURE WORK	103
	REFERENCES	106

LIST OF FIGURES

5.1	Varying values of concentration with “-”: $m = 0$, “- -”: $m = .1$, “-.”: $m = .3$, “..”: $m = .4$, “+”: $m = .5$, where $\tilde{\rho} = 10^{-1}$ and $(\epsilon n)^2 = 1$. . .	92
5.2	Varying values of perturbation $\tilde{\rho}$ from the concentration with “..”: $\tilde{\rho} = 10^{-3}$, “- -”: $\tilde{\rho} = 10^{-2}$, “-”: $\tilde{\rho} = 10^{-1}$, “-.”: $\tilde{\rho} = 1$, where $m = 0$ and $(n\epsilon)^2 = 1$	93
5.3	Varying values of the product $(\epsilon n)^2$ with “-.”: $(\epsilon n)^2 = .5$, “- -”: $(\epsilon n)^2 = 1$, “-”: $(\epsilon n)^2 = 10$, where $\tilde{\rho} = 10^{-1}$ and $m = 0$	95
5.4	Varying values of concentration with “-”: $m = 0$, “- -”: $m = .1$, “-.”: $m = .3$, “..”: $m = .4$, “+”: $m = .5$, where $\tilde{\rho} = 10^{-1}$ and $(\epsilon n)^2 = 1$. . .	96
5.5	Varying values of perturbation $\tilde{\rho}$ from the concentration with “..”: $\tilde{\rho} = 10^{-3}$, “- -”: $\tilde{\rho} = 10^{-2}$, “-”: $\tilde{\rho} = 10^{-1}$, “-.”: $\tilde{\rho} = 1$, where $m = 0$ and $(n\epsilon)^2 = 1$	97
5.6	Varying values of the product $(\epsilon n)^2$ with “- -”: $(\epsilon n)^2 = .5$, “-”: $(\epsilon n)^2 = 10$, where $\tilde{\rho} = 10^{-1}$ and $m = 0$	98
5.7	Varying the error tolerance (tol) for the Crank-Nicolson method for $\tilde{\rho} = 10^{-4}$ and $\tilde{\rho} = 10^{-2}$ with “..” : $\text{tol} = 10^{-4}$, “- -” : $\text{tol} = 10^{-3}$, and “-” : $\text{tol} = 10^{-2}$	101
5.8	Comparison of Eyre’s method “- -” and the Crank-Nicolson method “-”, with $m = 0$, and $(n\epsilon)^2 = 1$ where $\tilde{\rho} = 10^{-3}$ for the top lines, and $\tilde{\rho} = 10^{-1}$ for the bottom lines	102

LIST OF TABLES

5.1	Average time step size for each method as $\tilde{\rho}$ was varied given an error tolerance	100
-----	--	-----

ACKNOWLEDGMENTS

I would like to express my most sincere thanks to Dr. Erik Van Vleck for his enduring support, patience, and encouragement throughout the course of this project, and for his helpful insight and constant guidance. I would also like to thank Dr. Stanislaus Maier-Paape for the lecture he gave at Colorado School of Mines on spinodal decomposition, which sparked my interest in this study, and for his notes that got me started on the subject of this thesis. Further thanks are due to fellow students and the faculty members of the Colorado School of Mines Department of Mathematical and Computer Sciences, who have helped me in many different ways complete this work, and I appreciate the office, resources, and facilities offered by the school. I am forever grateful for the loving support of my family, especially from my wife, Wendy. This research was supported in part by a Colorado State Fellowship along with funding given by the Colorado School of Mines Department of Mathematical and Computer Sciences.

Chapter 1

INTRODUCTION

When a high-temperature homogeneous mixture of two metals is quenched to a lower temperature, the mixture may exhibit a phase separation which will occur in two stages. In the first stage, the mixture quickly becomes inhomogeneous as it decomposes into a fine-grained structure, which exhibits a characteristic length scale. This phenomenon is known as spinodal decomposition. Following this stage, the mixture will go through a coarsening process in which the characteristic length scale grows. Cahn and Hilliard [8, 10] proposed a fourth-order parabolic partial differential equation, which describes this process of phase separation and is given by

$$u_t = -\Delta(\epsilon^2 \Delta u + f(u)), \forall x \in \Omega, \quad (1.1)$$

$$\frac{\partial u}{\partial \nu} = \frac{\partial \Delta u}{\partial \nu} = 0, \forall x \in \partial\Omega,$$

where ν is the unit outward normal, ϵ is a small parameter, and $-f$ is the derivative of a double-well potential W , the standard example being the nonlinear cubic function $f(u) = u - u^3$. Here and throughout the paper, Δ denotes the standard Laplacian, $u_t = \partial u / \partial t$, and $\Omega \subset \mathbb{R}^d$ is a bounded domain with sufficiently smooth boundary given by $\partial\Omega$, where $d \in \{1, 2, 3\}$. Cahn and Hilliard [8, 10] first derived this equation through Fick's law of diffusion using the van der Waals free energy functional

$$E[u] := \int_{\Omega} \left(\frac{\epsilon^2}{2} |\nabla u|^2 + W(u) \right) dx, \quad (1.2)$$

which was introduced in [42], where ∇u denotes the gradient of u , and (1.1) is a gradient system with respect to this functional. The derivation of this equation can also be found in Elliott [13].

In the so-called Cahn-Hilliard equation (1.1), the variable u represents the concentration of one of the two metallic components, which implies that $\int_{\Omega} u dx$ represents the total mass of that component. Now, using Green's Theorem and the given boundary conditions, we can write

$$\begin{aligned} \frac{d}{dt} \int_{\Omega} u dx &= \int_{\Omega} \frac{\partial u}{\partial t} dx \\ &= \int_{\Omega} -\Delta(\epsilon^2 \Delta u + f(u)) dx \\ &= \int_{\partial\Omega} -\frac{\partial}{\partial \nu}(\epsilon^2 \Delta u + f(u)) ds = 0. \end{aligned}$$

Thus, mass is conserved, and the concentration of the other component \check{c} can be determined by the equation $\check{c} = (1 - u)/2$. This means that a concentration of 0 or 1 in one of the components corresponds to u being -1 or 1, depending on which component is being considered.

Spinodal decomposition is the process in which the values of u approach the minima of the potential function $W(u)$. The phase separation that occurs in this process can be seen when a vat of two well-mixed molten metals are cooled to a lower temperature. When separation takes place initially, a characteristic length scale is observed for spinodally decomposed states. For more on spinodal decomposition refer to [8], and [23]

Every constant function is a stationary solution or equilibrium of (1.1), and if an equilibrium is contained in the spinodal interval, which is the set of all $m \in \mathbb{R}$ such that $f'(m) > 0$, then it is unstable. (Notice that the spinodal interval for

$f(u) = u - u^3$ is the open interval $(-1/\sqrt{3}, 1/\sqrt{3})$.) Thus, if $u_0 = m$ is contained in the spinodal interval, any orbit starting close to it will soon leave a neighborhood of that equilibrium. This is when phase separation for (1.1), and in particular spinodal decomposition, takes place. In fact, understanding how this happens is central to understanding spinodal decomposition, because most orbits exiting the neighborhood mentioned above will exit close to an invariant manifold. Thus, the behavior of these orbits is very similar to that of the orbits on the manifold, and we will show that these orbits exhibit spinodal decomposition.

The Cahn-Hilliard equation (1.1) has been the subject of much study since its derivation, over 40 years ago. Existence and uniqueness of solutions of (1.1) have been proven by Elliott and Zheng [15], Nicolaenko and Scheurer [30], Rankin [33], and Temam [41]. Results on steady state solutions of (1.1) can be found in Novick-Cohen and Segel [31], Modica [27], and Zheng [44]. There are many results concerning the coarsening process mentioned above, which are due to Alikakos et al. [1], Alikakos et al. [2], Bates and Xun [5, 6], Bronsard and Hilhorst [7], Pego [32], and Stoth [38], among others. Numerical results that exhibit spinodal decomposition and coarsening for one, two, and three dimensions can be found in Cahn et al. [9], Elliott and French [14], Elliott [13], and Sander and Wanner [36]. Analytic results on spinodal decomposition have been presented by Grant [19], and Maier-Paape and Wanner [25], [26].

Despite this extensive amount of study, to the best of my knowledge there are no analytic results concerning spinodal decomposition of the spatially discrete Cahn-Hilliard equation. An analysis of this sort would be beneficial, because numerical results are essential for visualizing the behavior of the equation. Knowing when and how the equation portrays a given property for the discrete case will help the analysis

when it comes to solving the equation numerically. Our aim in this paper is to present a complete and mathematically rigorous analysis of when and how spinodal decomposition occurs for the spatially discrete Cahn-Hilliard equation.

Our approach in this paper is as follows. In chapter 2, we will consider a linearization of (1.1) at the homogeneous equilibrium $u_0 = m$. For this linearization, we derive a probability estimate for when an initial condition starting inside a certain ball will lead to spinodal decomposition, and we derive a wavelength estimate for spinodally decomposed states depending on the parameter ϵ . The results for the linearized equation give an idea of what is to be expected for the nonlinear equation. In the third chapter, a similar probability estimate is proven for the nonlinear equation, using three basic assumptions about the domain Ω and the nonlinearity $f(u)$. Next, we follow up the analysis of the spatially discretized equation with a discussion on time discretization of the equation. In this discussion we describe the Crank-Nicolson method as well as a splitting method due to Eyre [17] for solving the problem. Then we follow up these theoretical results with a numerical analysis of (1.1), in which we juxtapose these two methods, and get a better idea of how well our theoretical results hold in practice. To conclude this thesis we discuss our results, compare the theory derived in the second and third chapters with the numerics done in the fourth, and discuss the two discretizations explored throughout.

In order to accomplish this, we consider both the continuous Cahn-Hilliard equation as well as the spatially discrete equation. Much of our analysis depends on the eigenvalues for the Laplacian operator, and our approach is to show that the eigenvalues of the discrete Laplacian are almost equal to the eigenvalues of the continuous Laplacian. In doing this, we can use many of the results derived for the continuous problem to make conclusions about the discrete problem.

Chapter 2

THE LINEARIZED EQUATION

The ideas in this chapter are based upon the work done on spinodal decomposition for the continuous Cahn-Hilliard equation, found in [25]. We begin our analysis by first considering a linearization of the Cahn-Hilliard equation at a homogeneous equilibrium $u_0 = m$, where m is contained in the spinodal interval, i.e. $f'(m) > 0$. This linearization is given by

$$v_t = -\Delta(\epsilon^2 \Delta v + f'(m)v), \forall x \in \Omega, \quad (2.1)$$

with the Neumann boundary conditions

$$\frac{\partial v}{\partial \nu} = \frac{\partial \Delta v}{\partial \nu} = 0, \forall x \in \partial\Omega.$$

Though results similar to those obtained in this paper may hold for different boundary conditions, these will be the only boundary conditions considered, hence, they are to be assumed whenever they are not stated.

2.1 Spectral Analysis

First, notice that because of the previously discussed mass constraint on the Cahn-Hilliard equation, the linear operator associated with the problem given in

(2.1) is acting on the space

$$X := \left\{ u \in L^2(\Omega) : \int_{\Omega} u dx = 0 \right\}. \quad (2.2)$$

Before we consider the spatially discrete version of this equation itself, we must first understand the Laplacian operator for both the linearized discrete and continuous problems.

2.1.1 The Continuous Laplacian Operator

We start with the continuous Laplacian as we take into account our first lemma, which is built upon the ideas of Courant and Hilbert [11].

Lemma 2.1 *Let $\Omega \subset \mathbb{R}^d$, for $d \in \{1, 2, 3\}$, denote a bounded domain with piecewise C^1 -boundary, such that if $d = 2$; then Ω is a two-dimensional rectangle, and if $d = 3$, the Ω is a three-dimensional rectangle. Then the spectrum of the operator $-\Delta$ consists of an infinite sequence of real eigenvalues, $0 < \kappa_1 \leq \kappa_2 \leq \dots \rightarrow \infty$ with corresponding normalized eigenfunctions ψ_1, ψ_2, \dots that form a complete orthonormal set in X . Furthermore, if $N_d(\lambda)$ denotes the number of eigenvalues less than $\lambda \in \mathbb{R}$, then we have*

$$\lim_{\lambda \rightarrow \infty} \frac{N_d(\lambda)}{\lambda^{d/2}} = c_d \Upsilon^{(d)}(\Omega), \quad (2.3)$$

where $\Upsilon^{(d)}(\Omega)$ denotes a standard Euclidian volume, and the constants c_d are given by $c_1 = 1/\pi$, $c_2 = 1/4\pi$, and $c_3 = 1/6\pi^2$.

Proof: For $d = 1$, we can assume that Ω is the interval $[0, a]$. Then for the eigenvalue problem

$$\Delta\psi + \kappa\psi = 0,$$

with the boundary conditions

$$\frac{\partial\psi}{\partial x}(0) = \frac{\partial\psi}{\partial x}(a) = 0,$$

it is well known that the eigenvalues are given by

$$\kappa_k = \pi^2 \frac{k^2}{a^2},$$

where $k = 1, 2, 3, \dots$, and the corresponding normalized eigenfunctions are

$$\psi_k = \sqrt{\frac{2}{a}} \cdot \cos \frac{k\pi x}{a}.$$

So, $N_1(\lambda)$ is precisely equal to the number of lattice points with integral coordinates on the line, $\pi^2(x^2/a^2) = \lambda$. Thus,

$$x = \frac{\sqrt{\lambda}a}{\pi}$$

and we can write

$$\lim_{\lambda \rightarrow \infty} \frac{N_1(\lambda)}{\lambda^{1/2}} = \frac{a}{\pi}.$$

For the case $d = 2$, we consider the rectangle $[0, a] \times [0, b]$. Here, the eigenvalues are given by

$$\kappa_{k,\ell} = \pi^2 \left(\frac{k^2}{a^2} + \frac{\ell^2}{b^2} \right),$$

with corresponding normalized eigenfunctions

$$\psi_{k,\ell} = \sqrt{\frac{4}{ab}} \cdot \cos \frac{k\pi x_1}{a} \cdot \cos \frac{\ell\pi x_2}{b},$$

for $k, \ell \in \mathbb{N}$. Thus, $N_2(\lambda)$ is equal to the number of lattice points with integral coordinates in the sector of the ellipse

$$\frac{x^2}{a^2} + \frac{y^2}{b^2} = \frac{\lambda}{\pi^2}$$

in the quadrant $x \geq 0, y \geq 0$. For large λ , the area of this sector is arbitrarily close to the number of lattice points in it. Now, let there be a unit square above and to the right of each lattice point. Then this sector of the ellipse is contained in the region formed by these squares, and if we omit the squares that the ellipse passes through, and let the number of these squares be $R(\lambda)$, then the remaining region lies entirely inside this sector of the ellipse. The area of the sector is given by

$$V = \int_0^\alpha \left(\beta^2 - \frac{\beta^2}{\alpha^2} x^2 \right)^{\frac{1}{2}} dx,$$

where

$$\alpha^2 = (\lambda a^2)/\pi^2 \tag{2.4}$$

and

$$\beta^2 = (\lambda b^2)/\pi^2. \tag{2.5}$$

Evaluation of this integral gives

$$V = \left[\frac{x}{2} \left(\beta^2 - \frac{\beta^2}{\alpha^2} x^2 \right)^{\frac{1}{2}} + \frac{\alpha\beta}{2} \arcsin \frac{x}{\alpha} \right]_0^\alpha = \frac{\alpha\beta\pi}{4},$$

and since $\alpha\beta = (\lambda ab)/\pi^2$ we have

$$V = \lambda \frac{ab}{4\pi}.$$

Thus, we can write the inequality

$$N_2(\lambda) - R(\lambda) \leq \lambda \frac{ab}{4\pi} \leq N_2(\lambda),$$

which gives us the asymptotic expression

$$\lim_{\lambda \rightarrow \infty} \frac{N_2(\lambda)}{\lambda} = \frac{ab}{4\pi}.$$

Now, we approach the case when $d = 3$ in a similar manner. First, notice that the eigenvalues for this case are given by

$$\kappa_{k,\ell,m} = \pi^2 \left(\frac{k^2}{a^2} + \frac{\ell^2}{b^2} + \frac{m^2}{c^2} \right),$$

and corresponding normalized eigenfunctions are given by

$$\psi_{k,\ell,m} = \sqrt{\frac{8}{abc}} \cdot \cos \frac{k\pi x_1}{a} \cdot \cos \frac{\ell\pi x_2}{b} \cdot \cos \frac{m\pi x_3}{c},$$

for $k, \ell, m \in \mathbb{N}$. The volume of the ellipsoid

$$\frac{x^2}{\alpha^2} + \frac{y^2}{\beta^2} + \frac{z^2}{\gamma^2} = 1,$$

where α^2 and β^2 are defined in (2.4) and (2.5) respectively, and $\gamma^2 = (c^2\lambda)/\pi^2$, is given by the double integral

$$V = \gamma \int_0^\beta \int_0^\alpha \left(1 - \frac{x^2}{\alpha^2} - \frac{y^2}{\beta^2} \right)^{\frac{1}{2}} dx dy.$$

If we let $\xi^2 = \gamma^2(\beta^2 - y^2)/\beta^2$ and $(\gamma x)/\alpha = \xi \sin \theta$, then we can rewrite this integral as

$$V = \frac{\alpha}{\gamma} \int_0^\beta \int_0^{\pi/2} (\xi^2 - \xi^2 \sin^2 \theta)^{\frac{1}{2}} \xi \cos \theta d\theta dy.$$

Since $1 - \sin^2 \theta = \cos^2 \theta$, we have

$$V = \frac{\alpha}{\gamma} \int_0^\beta \xi^2 \int_0^{\pi/2} \cos^2 \theta d\theta dy = \frac{\alpha\pi}{4\gamma} \int_0^\beta \xi^2 dy = \frac{\alpha\gamma\pi}{4} \int_0^\beta \left(1 - \frac{y^2}{\beta^2}\right) dy.$$

Thus,

$$V = \frac{\alpha\beta\gamma\pi}{6} = \lambda^{3/2} \frac{abc}{6\pi^2},$$

and following the same procedure we used for the case $d = 2$, we get

$$\lim_{\lambda \rightarrow \infty} \frac{N_3(\lambda)}{\lambda^{3/2}} = \frac{abc}{6\pi^2},$$

completing the proof of our first lemma. \diamond

This brings us to the eigenvalues of the linear operator associated with the linearized Cahn-Hilliard equation.

Lemma 2.2 *Let A_ϵ be the linear operator such that*

$$A_\epsilon v = -\Delta(\epsilon^2 \Delta v + f'(m)v), \tag{2.6}$$

and A_ϵ is acting on the set

$$D(A_\epsilon) = \left\{ u \in X \cap H^4(\Omega) : \frac{\partial u}{\partial \nu}(x) = \frac{\partial \Delta u}{\partial \nu}(x) = 0, \forall x \in \partial\Omega \right\},$$

where X is given in (2.2). Then $-A_\epsilon$ is a selfadjoint sectorial (cf. [21]) operator.

Furthermore, the spectrum of A_ϵ consists of real eigenvalues $\lambda_1 \geq \lambda_2 \geq \dots \rightarrow -\infty$

given by

$$\lambda_i := \kappa_i(f'(m) - \epsilon^2 \kappa_i)$$

for $i \in \mathbb{N}$, and the corresponding eigenfunctions ϕ_1, ϕ_2, \dots are formed from the eigenfunctions ψ_i given in Lemma 2.1.

Proof: First notice that using the L^2 inner product

$$\langle u, v \rangle = \int_0^a u(x)v(x)dx,$$

we get

$$\langle -A_\epsilon u, v \rangle = \epsilon^2 \int_0^a u''''v dx + f'(m) \int_0^a u''v dx.$$

Now, it is well known that

$$\int_0^a u''v dx = \int_0^a v''u dx$$

and

$$\int_0^a u''''v dx = \int_0^a v''''u dx,$$

whenever $u'(x) = u'''(x) = 0$ for $x \in \partial\Omega$. Notice that Ω in this case is the interval $[0, a]$. This implies that

$$\langle -A_\epsilon u, v \rangle = \langle u, -A_\epsilon v \rangle.$$

Following this same procedure for higher space dimensions yields the same result; thus, the linear operator $-A_\epsilon$ is selfadjoint.

Since A_ϵ is given by (2.6), we can use the eigenvalues for the operator $-\Delta$ that were found in the proof of Lemma 2.1 to obtain

$$A_\epsilon v = -\Delta(\epsilon^2 \Delta v + f'(m)v) = \kappa_i(f'(m) - \epsilon^2 \kappa_i)v = \lambda_i v$$

for $i \in \mathcal{N}$. Thus, the eigenvalues of the linear operator A_ϵ are given by

$$\lambda_i = \kappa_i(f'(m) - \epsilon^2 \kappa_i),$$

and will have the ordering $\lambda_1 \geq \lambda_2 \geq \dots \rightarrow -\infty$. This ordering implies that the spectrum of $-A_\epsilon$ is bounded below, and according to Henry [21], since $-A_\epsilon$ is also a self adjoint densely defined operator in a Hilbert space, $-A_\epsilon$ is sectorial. This completes the proof of the lemma. \diamond

We can now make three important conclusions based on these two lemmas. First, using the definition of λ_i given above, and the assumption that $f'(m) > 0$, we can conclude that the eigenvalues of the operator A_ϵ are zero when $\kappa_i = f'(m)/\epsilon^2$, negative when $\kappa_i > f'(m)/\epsilon^2$, and positive when $0 < \kappa_i < f'(m)/\epsilon^2$. Thus, the homogeneous equilibrium $u_0 = m$ is unstable whenever

$$0 < \epsilon < \sqrt{\frac{f'(m)}{\kappa_1}}.$$

Using these results, and the result from Lemma 2.1 we arrive at our next conclusion.

As $\epsilon \rightarrow 0$, the dimension of the unstable manifold is of the order

$$\frac{f'(m)^{d/2} c_d \text{vol}^{(d)}(\Omega)}{\epsilon^d}.$$

Finally, we can conclude that the largest eigenvalue of the operator A_ϵ is half way between the points where the eigenvalues are zero. Hence, if we choose $\kappa_i = f'(m)/2\epsilon^2$ then the largest eigenvalue of A_ϵ is bounded by

$$\lambda_\epsilon^{max} := \frac{f'(m)^2}{4\epsilon^2}. \quad (2.7)$$

where Δ_n is the symmetric tridiagonal matrix given in (2.9), and $\varphi \in \mathbb{R}^{n+1}$. It is well known that the eigenvalues for this matrix are given by

$$\mu_j = \frac{2}{h^2} \left(1 - \cos \left(\frac{j\pi}{n+1} \right) \right), \quad (2.10)$$

and the corresponding normalized eigenfunctions are given by

$$\varphi_j^{(k)} = \sqrt{\frac{2}{n+1}} \cos \left(\frac{jk\pi}{n+1} \right)$$

for $j = 0, 1, \dots, n$, and $0 \leq k \leq n$.

In order to understand the asymptotics of μ_j and φ_j , notice that

$$\cos \left(\frac{j\pi}{n+1} \right) = 1 - \frac{1}{2} \left(\frac{j\pi}{n+1} \right)^2 + \frac{1}{4!} \left(\frac{j\pi}{n+1} \right)^4 + O(n^{-6}),$$

which leads us to

$$\left(\frac{j\pi}{n+1} \right)^2 n^2 - \frac{2}{4!} \left(\frac{j\pi}{n+1} \right)^4 n^2 \leq \mu_j \leq \left(\frac{j\pi}{n+1} \right)^2 n^2 \leq (j\pi)^2. \quad (2.11)$$

Since we have $\kappa_j = (j\pi)^2$, we use the Squeeze Theorem to get $\mu_j \rightarrow \kappa_j$ as $n \rightarrow \infty$. In addition, the normalized eigenfunctions for the continuous case given in Lemma 2.1 can be written as

$$\psi_j(x) = \hat{c} \cos(j\pi x)$$

for some constant \hat{c} , which implies that we can write $\varphi_j^{(k)}$ in the form

$$\varphi_j^{(k)} = \psi_j \left(\frac{k}{n+1} \right).$$

Notice that similar results hold for the higher space dimensions $d = 2, 3$, where the

eigenvalues and eigenfunctions are obtained from the eigenvalues and eigenfunctions for one dimension as in the proof of Lemma 2.1. Now we consider the following result which relates the eigenvalues of the discrete Laplacian to those of the continuous Laplacian.

Lemma 2.3 *Let $0 < \hat{\rho} \ll 1$, and suppose $0 \leq (j\pi)^2 \leq 6\hat{\rho}n^2$ and $n \geq 6/\hat{\rho}$. Then the eigenvalues of the continuous and discrete Laplacian operators, given in Lemma 2.1 and (2.10) respectively, satisfy*

$$\left| \frac{\mu_j}{\kappa_j} - 1 \right| \leq \hat{\rho}.$$

Proof: From (2.11), we see that

$$\left| \mu_j - \kappa_j \left(\frac{n}{n+1} \right)^2 \right| \leq \frac{2}{4!} \left(\frac{j\pi}{n+1} \right)^4 n^2,$$

which implies

$$\left| \frac{\mu_j}{\kappa_j} - 1 + 1 - \left(\frac{n}{n+1} \right)^2 \right| \leq \frac{2}{4!} (j\pi)^2 \frac{n^2}{(n+1)^4}.$$

From this it follows that, $|\mu_j/\kappa_j - 1| \leq \hat{\rho}$ if

$$\left| 1 - \left(\frac{n}{n+1} \right)^2 \right| \leq \frac{\hat{\rho}}{2}, \tag{2.12}$$

and

$$\frac{2}{4!} (j\pi)^2 \frac{n^2}{(n+1)^4} \leq \frac{\hat{\rho}}{2}. \tag{2.13}$$

First, notice that (2.12) is true if

$$\frac{2n+1}{(n+1)^2} \leq \frac{\hat{\rho}}{2},$$

or equivalently,

$$\frac{(n+1)^2}{2n+1} \leq \frac{2}{\hat{\rho}}.$$

Clearly, this is satisfied if

$$\frac{n^2}{3n} \geq \frac{2}{\hat{\rho}} \iff n \geq \frac{6}{\hat{\rho}}.$$

Now, consider (2.13). Clearly, it is satisfied if

$$(j\pi)^2 \leq \hat{\rho} \frac{4!}{4} \frac{(n+1)^4}{n^2} = 6\hat{\rho} \frac{(n+1)^4}{n^2},$$

and since we have $(j\pi)^2 \leq 6\hat{\rho}n^2$, this statement is true. \diamond

The next step in our analysis is to consider the eigenvalues of the spatially discrete Cahn-Hilliard equation, linearized at $u = m$. We can write (1.1) in spatially discrete form as

$$\dot{u} = -n^2 \Delta_n (\epsilon^2 n^2 \Delta_n u + f(u)). \quad (2.14)$$

Here and throughout, we define $\dot{u} = du/dt$. Now, if we define the linear operator \hat{A}_ϵ by

$$\hat{A}_\epsilon \varphi = -n^2 \Delta_n (\epsilon^2 n^2 \Delta_n \varphi + f'(m)\varphi),$$

then the eigenvalues for the discrete linear operator \hat{A}_ϵ are given by

$$\xi_j = \xi(\mu_j) = \mu_j (-\epsilon^2 \mu_j + f'(m))$$

for one space dimension, and since $\kappa_j \sim \mu_j$, we have $\lambda_j \sim \xi_j$.

In order to better understand the linearized equation, we briefly discuss the solutions to the abstract equations for both the discrete and continuous cases, which

will be useful in our analysis. The continuous abstract equation is given by

$$v_t = A_\epsilon v, \quad (2.15)$$

$$v(0) = \bar{v},$$

and we know from Lemma 2.2 that this equation generates an analytic semigroup $S_\epsilon(t)$, cf. Henry [20]. Hence, the solution of problem (2.15) is given by $v(t) = S_\epsilon(t)\bar{v}$, and we can write \bar{v} as a Fourier series given by

$$\bar{v} = \sum_{k=1}^{\infty} \langle \bar{v}, \phi_k \rangle \phi_k,$$

where the set $\{\phi_k\}$ is orthonormal and $\langle \cdot, \cdot \rangle$ denotes the scalar product in $L^2(\Omega)$. Therefore, the solution of (2.15) is given by

$$v(t) = \sum_{k=1}^{\infty} e^{\lambda_k t} \langle \bar{v}, \phi_k \rangle \phi_k,$$

for all $t \geq 0$, cf. [25]. Similarly, for the discrete equation

$$\dot{v} = \hat{A}_\epsilon v,$$

we have

$$\bar{v} = \sum_{k=1}^n \langle \bar{v}, \varphi_k \rangle \varphi_k, \quad (2.16)$$

and

$$v(t) = \sum_{k=1}^n e^{\xi_k t} \langle \bar{v}, \varphi_k \rangle \varphi_k, \quad (2.17)$$

for all $t \geq 0$.

2.1.3 The Dominating Subspace

Let Y be the space for the discrete problem corresponding to X . Then we define the dominating subspace of Y in the following way. First, notice that $Y = \mathbb{R}^{n^d}$ and $\xi(2f'(m)/\epsilon^2) < \lambda_\epsilon^{max}$. Fix constants $\gamma^{--} \sim -1 < 0 \ll \gamma^- < \gamma^+ < 1$, and consider those values of $\epsilon > 0$ such that the spectrum of \hat{A}_ϵ , defined by $\sigma(\hat{A}_\epsilon)$, is disjoint from the set $\{\gamma^{--}, \gamma^-, \gamma^+\} \cdot \lambda_\epsilon^{max}$. This allows us to divide the spectrum of \hat{A}_ϵ into four parts such that

$$\sigma(\hat{A}_\epsilon) = \sigma_\epsilon^{--} \cup \sigma_\epsilon^- \cup \sigma_\epsilon^+ \cup \sigma_\epsilon^{++},$$

where $\sigma_\epsilon^{--} = \sigma(\hat{A}_\epsilon) \cap (-\infty, \gamma^{--})$, $\sigma_\epsilon^- = \sigma(\hat{A}_\epsilon) \cap (\gamma^{--}, \gamma^-)$, $\sigma_\epsilon^+ = \sigma(\hat{A}_\epsilon) \cap (\gamma^-, \gamma^+)$, and $\sigma_\epsilon^{++} = \sigma(\hat{A}_\epsilon) \cap (\gamma^+, \infty)$. Hence, if we let Y_ϵ^{--} , Y_ϵ^- , Y_ϵ^+ , and Y_ϵ^{++} be subspaces of Y that are generated by the eigenfunctions of \hat{A}_ϵ corresponding to the eigenvalues in σ_ϵ^{--} , σ_ϵ^- , σ_ϵ^+ , and σ_ϵ^{++} , respectively, then we can write

$$Y = Y_\epsilon^{--} \oplus Y_\epsilon^- \oplus Y_\epsilon^+ \oplus Y_\epsilon^{++}. \quad (2.18)$$

Furthermore, if $v : \mathbb{R} \rightarrow Y$ is a full orbit of (2.14), then we can decompose $v(t)$ in the following way:

$$v(t) = v^{--}(t) + v^-(t) + v^+(t) + v^{++}(t), \quad (2.19)$$

where the superscript on v corresponds to the appropriate subspace of Y . In addition, since X is the space on which the continuous problem is acting, we can define a similar decomposition of X . Specifically, we can write

$$X = X_\epsilon^{--} \oplus X_\epsilon^- \oplus X_\epsilon^+ \oplus X_\epsilon^{++}, \quad (2.20)$$

where X_ϵ^{--} is infinite dimensional. Notice that as $n \rightarrow \infty$, the discrete problem approaches the continuous problem, and the subspace Y_ϵ^{--} is of considerably higher dimension than that of the other subspaces.

It is important to be careful here because it could happen that μ_j contributes to Y_ϵ^{++} , but κ_j contributes to X_ϵ^+ . Nevertheless, the difference between eigenvalues for the discrete and continuous operators can be controlled, and this is shown in our next lemma.

Lemma 2.4 *Suppose*

$$n \geq \max \left[\sqrt{\frac{2f'(m)}{6\hat{\rho}} \frac{1}{\epsilon}}, \frac{6}{\hat{\rho}} \right]. \quad (2.21)$$

and

$$\kappa_j \leq (2f'(m))/\epsilon^2 \quad (2.22)$$

for all j . Then $|\mu_j/\kappa_j - 1| \leq \hat{\rho}$ for $0 < \hat{\rho} \ll 1$.

Proof: Inequality (2.21) implies

$$\frac{2f'(m)}{\epsilon^2} \leq 6\hat{\rho}n^2,$$

and by (2.22) $\kappa_j \leq 6\hat{\rho}n^2$. An application of Lemma 2.3 completes the proof of the lemma. \diamond

Note that this result does not rely on the specific finite difference discretization being considered. However, the analysis here does rely on having good approximations to the eigenvalues of the discrete Laplacian operator. In fact, a similar analysis should follow, using the same procedure used here, for other spatial discretizations, including non-uniform finite differences, collocation, and finite elements.

2.2 Dynamics of the Linear Problem

Our purpose here is to study the stability of the equilibrium point m . Recall that positive eigenvalues imply instability, and negative eigenvalues imply stability. We will show that, even though the stable subspace, given by $Y_\epsilon^{--} \oplus Y_\epsilon^-$, may be of considerably higher dimension than that of the unstable subspace $Y_\epsilon^+ \oplus Y_\epsilon^{++}$, especially as $n \rightarrow \infty$, $Y_\epsilon^+ \oplus Y_\epsilon^{++}$ is still the dominating subspace. In other words, an orbit starting close to the equilibrium will exit a certain neighborhood of that equilibrium close to the subspace $Y_\epsilon^+ \oplus Y_\epsilon^{++}$. When this happens, we observe spinodal decomposition.

2.2.1 Choosing a Spatial Mesh

From Lemma 2.4, we conclude that all eigenvalues contributing to X_ϵ^- , X_ϵ^+ , and X_ϵ^{++} are $\hat{\rho}$ -accurate, meaning that they are almost equal to the eigenvalues contributing to Y_ϵ^- , Y_ϵ^+ , and Y_ϵ^{++} . This, along with Lemma 2.1, gives the following estimates for the dimensions of the subspaces of Y

$$\dim Y_\epsilon^{++} \sim \dim X_\epsilon^{++} \sim \epsilon^{-d}$$

$$\dim Y_\epsilon^+ \sim \dim X_\epsilon^+ \sim \epsilon^{-d}$$

$$\dim Y_\epsilon^- \sim \dim X_\epsilon^- \sim \epsilon^{-d}.$$

It is clear that, due to the infinite dimension of the subspace X_ϵ^{--} , we begin to lose the ρ -accuracy of the eigenvalues corresponding to the Y_ϵ^- or Y_ϵ^{--} subspaces depending on our choice for n . In other words, if we let μ_{j_y} and κ_{j_x} be the j th eigenvalues corresponding to Y and X , respectively, then we obviously do not have

$\mu_{j_y} \approx \kappa_{j_x}$ as $j_y \rightarrow n$ and $j_x \rightarrow \infty$. This leads us to some important results concerning our choice for n .

We must consider the following two cases. First, if we take $n \sim 1/\epsilon$, then we have $Y = Y_\epsilon^{++} \oplus Y_\epsilon^+ \oplus Y_\epsilon^-$, and

$$\dim Y_\epsilon^{++} \sim \dim Y_\epsilon^+ \sim \dim Y_\epsilon^- \sim \epsilon^{-d} \sim n^d.$$

Thus, we need only define Y_ϵ^{++} and Y_ϵ^+ because only these two subspaces are ρ -accurate. In the second case, if $n \geq (c/\epsilon)$, where $c > 1$ is some constant, then the discrete problem is a better approximation of the continuous problem and we have Y given by (2.18). In particular, we need the subspace Y_ϵ^{--} and the dimensions of the subspaces are

$$\dim Y_\epsilon^{++} \sim \dim Y_\epsilon^+ \sim \dim Y_\epsilon^- \sim \epsilon^{-d}$$

and

$$\dim Y_\epsilon^{--} \sim n^d \gg \epsilon^{-d}.$$

However, all eigenvalues in Y_ϵ^{++} , Y_ϵ^+ , and Y_ϵ^- are ρ -accurate.

As we consider these two cases, we will need the following propositions, which are based on C1 and C2 in [25]. Before we present these claims, we must introduce the following notation. Letting v be a full orbit of (2.15), we denote the initial condition corresponding to this orbit by $\bar{v} = v(0)$. In addition, let $B_R(0)$ be a ball centered at zero with radius R , and suppose that this orbit leaves the ball $B_R(0)$ at time $t^* > 0$. Then we let $v^* = v(t^*)$ denote the point where $v(t)$ exits the ball $B_R(0)$. Furthermore, we can decompose \bar{v} and v^* analogously to (2.19).

Proposition 2.1 *If $r < (\rho R^{-\gamma^{--}})^{1/(1-\gamma^{--})}$, then $\|v^{*,--}\| < \rho$. In other words, every orbit starting in $B_r(0)$ has a small Y_ϵ^{--} -component upon leaving $B_R(0)$.*

Proof: Since $\bar{v} \in B_r(0)$, we have

$$\left\| \sum_{k=1}^{\infty} \langle \bar{v}, \varphi_k \rangle \varphi_k \right\| \leq r$$

by (2.16). Using this and the fact that the largest eigenvalue of A_ϵ is bounded above by λ_ϵ^{max} of (2.7), and that

$$\|v(T^*)\| = \left\| \sum_{k=1}^{\infty} \exp^{\lambda_k \cdot T^*} \langle \bar{v}, \varphi_k \rangle \varphi_k \right\| = R$$

by (2.17), we have

$$R \leq e^{\lambda_\epsilon^{max} \cdot T^*} \left\| \sum_{k=1}^{\infty} \langle \bar{v}, \varphi_k \rangle \varphi_k \right\| \leq r e^{\lambda_\epsilon^{max} \cdot T^*}.$$

Because $\gamma^{--} < 0$, this gives us

$$\left(\frac{R}{r}\right)^{\gamma^{--}} \geq e^{\gamma^{--} \lambda_\epsilon^{max} \cdot T^*}.$$

Now, due to our choice for r , we have

$$r < \varrho \left(\frac{R}{r}\right)^{\gamma^{--}},$$

which implies that

$$\|v_\epsilon^{*,--}\| = \|S_\epsilon^{--}(T^*)\bar{v}^{--}\| \leq r e^{\gamma^{--} \lambda_\epsilon^{max} \cdot T^*} \leq r \left(\frac{R}{r}\right)^{\gamma^{--}} < \varrho,$$

and verifies Proposition 2.1. \diamond

Proposition 2.2 *Let r be as in Proposition 2.1, and suppose that $\bar{v} \in B_r(0)$ such that*

$$\|\bar{v}^{++}\| > R\varrho^\gamma \|\bar{v}^-\|^\gamma,$$

where $\gamma = \frac{\gamma^+}{\gamma^-}$, then the orbit through \bar{v} exits $B_R(0)$ near the dominating subspace $Y_\epsilon^{++} \oplus Y_\epsilon^+$. Thus, we have $\|v_\epsilon^{*,-}\| < \varrho$.

Proof: Using the spectral representation for v given in (2.17), we derive the estimate

$$\|v^{++}(t)\| \leq e^{\gamma^+ \lambda_\epsilon^{\max} t} \|\bar{v}^-\|$$

for all $t \leq 0$, which implies

$$\|v^{++}(t)\| \leq \|v^{*,++}\| \cdot e^{\gamma^+ \cdot \lambda_\epsilon^{\max} \cdot (t-T^*)} \leq R e^{\gamma^+ \cdot \lambda_\epsilon^{\max} \cdot (t-T^*)}.$$

Using (2.17), we can also derive

$$\|v^-(t)\| \geq e^{\gamma^- \lambda_\epsilon^{\max} t} \|\bar{v}^-\|,$$

for all $t \leq 0$, which gives

$$\|v^-(t)\| \geq \|v^{*,-}\| \cdot e^{\gamma^- \cdot \lambda_\epsilon^{\max} \cdot (t-T^*)},$$

for all $t < T^*$. Thus, if we let $t = 0$, we obtain the estimates

$$\|\bar{v}^-\| \cdot e^{\gamma^- \cdot \lambda_\epsilon^{\max} \cdot T^*} \geq \|v^{*,-}\|$$

and

$$\|\bar{v}^{++}\| e^{-\gamma^+ \lambda_\epsilon^{\max} T^*} \leq R,$$

which is equivalent to

$$\|\bar{v}^{++}\|^{\gamma^-/\gamma^+} e^{-\gamma^- \lambda_\epsilon^{\max} T^*} \leq R^{\gamma^-/\gamma^+},$$

and, by our assumption on \bar{v} , we have

$$\|\bar{v}^-\| < \varrho \left(\frac{\|v^{*,++}\|}{R} \right)^{\gamma^-/\gamma^+}.$$

This implies the estimate

$$\|v^{*, -}\| \leq \|\bar{v}^-\| \cdot e^{\gamma^- \cdot \lambda_\epsilon^{\max} \cdot T^*} < \varrho \cdot \left(\frac{\|\bar{v}^{++}\|}{R} \right)^{\gamma^-/\gamma^+} \cdot e^{\gamma^- \cdot \lambda_\epsilon^{\max} \cdot T^*} \leq \varrho,$$

and completes the proof of the proposition. \diamond

For the first case $n \sim 1/\epsilon$, use Proposition 2.2 to get $\|\bar{v}^{*, -}\| < \varrho$. The second case with $n \geq c/\epsilon$ is similar to that of the continuous case, hence, we can use Proposition 2.1 and Proposition 2.2 to get $\|\bar{v}^{*, -}\| < \varrho$ and $\|\bar{v}^{*, -}\| < \varrho$. Thus, the Y_ϵ^{--} and the Y_ϵ^- components of an orbit are small at exiting, and we can ignore the effects of these spaces.

2.2.2 Probability Estimates

The Propositions 2.1 and 2.2 imply that most orbits starting inside a neighborhood $B_r(0)$ will leave a larger neighborhood $B_R(0)$ close to the dominating subspace $Y_\epsilon^{++} \oplus Y_\epsilon^+$, because the effects of Y_ϵ^{--} and Y_ϵ^- are small. Since most orbits will be within a distance ϱ from this subspace, they will behave similarly to those functions in $Y_\epsilon^{++} \oplus Y_\epsilon^+$. Thus, an understanding of the functions in the dominating subspace will give a better understanding of functions whose initial conditions start close to the

equilibrium. It was shown that the subspace $Y_\epsilon^{++} \oplus Y_\epsilon^+$ is spanned by the functions $\cos(k\pi x)$ or a superposition of these functions depending on the dimension of the domain Ω . According to [25], we can show that for some constants c_1 and c_2 depending on γ^- and $f'(m)$,

$$c_1 \frac{1}{\epsilon} \leq k \leq c_2 \frac{1}{\epsilon}.$$

So, the average size of nodal domains is of order ϵ . These ideas fuel our discussion on the wavelength of spinodally decomposed states, but first we must determine how often an orbit will be close to the dominating subspace.

The question now is with what probability does an initial condition, originating inside $B_r(0)$, lead to an orbit that will exit $B_R(0)$ within a ϱ -neighborhood of the dominating subspace $Y_\epsilon^{++} \oplus Y_\epsilon^+$ for a sufficiently small constant ϱ ? Before we can address this question, we must first define the measure to be used on the space $Y = Y_\epsilon^- \oplus Y_\epsilon^+ \oplus Y_\epsilon^{++}$. If we take an orthonormal bases $\{\vartheta_1, \vartheta_2, \dots, \vartheta_N\}$ in Y , where N is the dimension of Y , then the image of the N -dimensional Lebesgue measure on \mathbb{R}^N under the mapping

$$\mathbb{R}^N \ni (\beta_1, \beta_2, \dots, \beta_n) \rightarrow \sum_{i=1}^N \beta_i \vartheta_i \in Y$$

which is an isometry, will be denoted by $\Upsilon^{(N)}(\cdot)$, where \mathbb{R}^N is equipped with the Euclidian scalar product. Furthermore, let $G_r \subset B_r$ be the set of all initial conditions starting in B_r that correspond to orbits which exit B_R close to the dominating subspace. Then we can define $M_r := B_r \setminus G_r$ to be the set of all bad initial conditions which exit B_R away from the dominating subspace. Using this convention, we want

to show that, for some $0 \ll p < 1$,

$$\frac{\Upsilon^{(N)}(G_r)}{\Upsilon^{(N)}(B_r)} \geq p. \quad (2.23)$$

In order to accomplish this and answer the posed probability question, we turn to the following theorem, which is equivalent to Theorem 3.1 in [25].

Theorem 2.1 *Let $\beta, \eta \in (0, 1)$ be fixed, define $h(s) = h_{\beta, \eta}(s) := (s/\beta)^{1/\eta}$, fix $C^* > 0$, and let k, ℓ , and m be arbitrary natural numbers with $\ell \leq C^*k$. Define the set*

$$M_\varrho := \{(x, y, z) \in B_\varrho^i \subset \mathbb{R}^k \times \mathbb{R}^\ell \times \mathbb{R}^m : \|x\| \leq h(\|y\|)\},$$

where

$$B_\varrho^i := \{x \in \mathbb{R}^i : \|x\| \leq \varrho\}, \quad (2.24)$$

for $i = k + \ell + m$, $\varrho > 0$, and $\|\cdot\|$ denotes the standard Euclidean norm. Then

$$\frac{\Upsilon^{(i)}(M_\varrho)}{\Upsilon^{(i)}(B_\varrho^i)} \leq \sqrt{\frac{h(\varrho)}{\varrho}} = \beta^{\frac{-1}{2\eta}} \varrho^{\frac{1}{2}(\frac{1}{\eta}-1)},$$

for all $0 < \varrho \leq \varrho_0$ with

$$\varrho_0 := \beta^{\frac{1}{1-\eta}} \left(\min \left\{ \frac{1}{1+2C_*}, \left(\int_0^1 (1-s^2)^{C_*/2} ds \right)^2 \right\} \right)^{\frac{\eta}{1-\eta}} > 0.$$

Proof: Suppose that $m \geq 1$, and let $\theta := (\|x\|^2 + \|y\|^2)^{1/2}$. Then, if we let ∂B be the boundary of B and define the set

$$\tilde{M}_\theta = \{(x, y) \in \partial B_\theta^{k+\ell} : \|x\| \leq h(\|y\|)\},$$

we can use the definition of B_r^i in (2.24) to get

$$M_\varrho = \bigcup_{\theta \in [0, \varrho]} \left(\tilde{M}_\theta \times B_{\sqrt{\varrho^2 - \theta^2}}^m \right).$$

Using Fubini's theorem,

$$\Upsilon^{(i)}(M_\varrho) = \int_0^\varrho \Upsilon_s^{(k+\ell)}(\tilde{M}_\theta) \cdot \Upsilon^{(m)}\left(B_{\sqrt{\varrho^2 - \theta^2}}^m\right) d\theta, \quad (2.25)$$

where Υ_s^i denotes the surface area on the sphere ∂B_θ^i . Notice that we have $0 \leq \|x\| \leq \theta$, and $\|y\| = \sqrt{\theta^2 - \|x\|^2}$. Then, for arbitrary $(x, y) \in \tilde{M}_\theta$, we have

$$0 \leq \|x\| \leq h(\|y\|) \leq h\left(\sqrt{\theta^2 - \|x\|^2}\right) \leq h(\theta),$$

and if we define the set

$$\hat{M}_\theta := \left\{ (x, y) \in \partial B_\theta^{k+\ell} : \|x\| < h(\theta) \right\},$$

then it is clear that $\tilde{M}_\theta \subset \hat{M}_\theta$, and

$$\Upsilon_s^{(k+\ell)}(\tilde{M}_\theta) \leq \Upsilon_s^{(k+\ell)}(\hat{M}_\theta). \quad (2.26)$$

Now, in order to perform the integration $\Upsilon_s^{(k+\ell)}$ on (\hat{M}_θ) is explicitly, define the vector t by

$$t := [t_1, t_2, \dots, t_q]$$

such that $q = k + \ell - 1$ and

$$[t_1, \dots, t_k, t_{k+1}, \dots, t_q, y_\ell] = [x_1, \dots, x_k, y_1, \dots, y_\ell],$$

and let \mathcal{D} be the region given by

$$\mathcal{D} := \left\{ t \in \mathbb{R}^q : 0 < \|t\| < \theta, 0 < \left(\sum_{j=1}^k t_j^2 \right)^{1/2} < h(\theta) \right\}.$$

Then, using standard techniques for surface integrals, we get

$$\frac{1}{2} \Upsilon_s^{(k+\ell)} (\hat{M}_\theta) = \int_{\mathcal{D}} \frac{\theta}{\sqrt{\theta^2 - \|t\|^2}} d^q t.$$

For this we have assumed that $0 < \theta \leq \varrho_0$. Thus, if we let

$$Q = \min \left\{ \frac{1}{1 + 2C_*}, \left(\int_0^1 (1 - s^2)^{C_*/2} ds \right)^2 \right\},$$

then

$$\frac{h(\theta)}{\theta} = \frac{1}{\theta} \left(\frac{\theta}{\beta} \right)^{1/\eta} = \beta^{-1/\eta} \theta^{(1-\eta)/\eta} = \left(\beta^{-1/(1-\eta)} \theta \right)^{(1-\eta)/\eta} \leq Q, \quad (2.27)$$

and since $1/(1 + 2C_*) \leq 1$ for any $C_* > 0$, we have $Q \leq 1$, which implies that $h(\theta) \leq \theta$. Now, an application of Fubini's theorem and the standard integration formula for surface area of rotationally symmetric functions, gives

$$\frac{1}{2} \Upsilon_s^{(k+\ell)} (\hat{M}_\theta) = k \tau_1^k \int_0^{h(\theta)} \left((\ell - 1) \tau_1^{\ell-1} \int_0^{\sqrt{\theta^2 - s^2}} \frac{\theta \sigma^{\ell-2} d\sigma}{\sqrt{\theta^2 - s^2 - \sigma^2}} \right) s^{k-1} ds,$$

for $\ell \geq 2$; and

$$\frac{1}{2} \Upsilon_s^{(k+\ell)} (\hat{M}_\theta) = k \tau_1^k \int_0^{h(\theta)} \frac{\theta s^{k-1}}{\sqrt{\theta^2 - s^2}} ds, \quad (2.28)$$

for $\ell = 1$, where $\tau_r^i := \Upsilon^{(i)} (B_r^i)$.

Consider the case when $\ell \geq 2$, where we have

$$\Upsilon_s^{(k+\ell)}(\hat{M}_\theta) = 2k\tau_1^k(\ell-1)\tau_1^{\ell-1}\theta \int_0^{h(\theta)} \int_0^{\sqrt{\theta^2-s^2}} \frac{\sigma^{\ell-2}s^{k-1}}{\sqrt{\theta^2-s^2-\sigma^2}} d\sigma ds, \quad (2.29)$$

and a similar derivation gives

$$\Upsilon_s^{(k+\ell)}(\partial B_\theta^{k+\ell}) = 2k\tau_1^k(\ell-1)\tau_1^{\ell-1}\theta \int_0^\theta \int_0^{\sqrt{\theta^2-s^2}} \frac{\sigma^{\ell-2}s^{k-1}}{\sqrt{\theta^2-s^2-\sigma^2}} d\sigma ds. \quad (2.30)$$

In order to estimate (2.29) in terms of (2.30), we define the function $\Phi : \mathbb{N}_0 \rightarrow \mathbb{R}^+$ by

$$\Phi(\ell) = \int_0^1 \frac{s^\ell}{\sqrt{1-s^2}} ds.$$

Then a simple variable substitution yields

$$r^\ell \Phi(\ell) = \int_0^1 \frac{(sr)^\ell}{\sqrt{1-s^2}} ds = \frac{1}{r} \int_0^r \frac{s^\ell}{\sqrt{1-(s/r)^2}} ds = \int_0^r \frac{s^\ell}{\sqrt{r^2-s^2}} ds.$$

Hence, if we let $r = \sqrt{\theta^2-s^2}$, we get

$$\begin{aligned} \int_0^{h(\theta)} \int_0^{\sqrt{\theta^2-s^2}} \frac{\sigma^{\ell-2}s^{k-1}}{\sqrt{\theta^2-s^2-\sigma^2}} d\sigma ds &= \Phi(\ell-2) \int_0^{h(\theta)} (\theta^2-s^2)^{\frac{\ell-2}{2}} s^{k-1} ds \\ &= \theta^{k+\ell-2} \Phi(\ell-2) \int_0^{h(\theta)/\theta} (1-s^2)^{\frac{\ell-2}{2}} s^{k-1} ds, \end{aligned}$$

which implies

$$\Upsilon_s^{(k+\ell)}(\hat{M}_\theta) = 2k\tau_1^k(\ell-1)\tau_1^{\ell-1}\theta^{k+\ell-1}\Phi(\ell-2) \int_0^{\hat{\Theta}} (1-s^2)^{\frac{\ell-2}{2}} s^{k-1} ds,$$

where $\hat{\Theta} = h(\theta)/\theta$, and similarly we can rewrite (2.30) to read

$$\Upsilon_s^{(k+\ell)}(\partial B_\theta^{k+\ell}) = 2k\tau_1^k(\ell-1)\tau_1^{\ell-1}\theta^{k+\ell-1}\Phi(\ell-2)\int_0^1(1-s^2)^{\frac{\ell-2}{2}}s^{k-1}ds. \quad (2.31)$$

Now we need to estimate $\int_0^{\hat{\Theta}}(1-s^2)^{\frac{\ell-2}{2}}s^{k-1}ds$ in terms of $\int_0^1(1-s^2)^{\frac{\ell-2}{2}}s^{k-1}ds$. Another variable substitution gives

$$\int_0^{\hat{\Theta}}(1-s^2)^{\frac{\ell-2}{2}}s^{k-1}ds = \hat{\Theta}\int_0^1(\hat{\Theta}s)^{k-1}\left(1-(\hat{\Theta}s)^2\right)^{\frac{\ell-2}{2}}ds. \quad (2.32)$$

For fixed s in the interval $[0, 1]$, define a function $g_s : [\hat{\Theta}, \hat{\Theta}^{1/2}] \rightarrow \mathbb{R}_0^+$, such that $g_s(\hat{\Theta})$ is the integrand on the right hand side of equation (2.32), i.e.,

$$g_s(\chi) = (\chi s)^{k-1}\left(1-(\chi s)^2\right)^{\frac{\ell-2}{2}}. \quad (2.33)$$

Notice here that $0 < \hat{\Theta} < \hat{\Theta}^{1/2} < 1$, because $h(\theta) \leq \theta$, which follows from (2.27). Now, we want to show that g_s is monotonically increasing with respect to χ . Taking the derivative of g_s with respect to χ gives

$$\begin{aligned} g'_s(\chi) &= s(k-1)(\chi s)^{k-2}\left(1-(\chi s)^2\right)^{\frac{\ell-2}{2}} - s(\ell-2)(\chi s)^k\left(1-(\chi s)^2\right)^{\frac{\ell-4}{2}} \\ &= s(k-1)\left(1-(\chi s)^2\right)^{\frac{\ell-2}{2}}\left(1-(\chi s)^2\right)^{-1}\left((\chi s)^{k-2} - (\chi s)^k\right) \\ &\quad - s(\ell-2)(\chi s)^k\left(1-(\chi s)^2\right)^{\frac{\ell-4}{2}} \\ &= s(k-1)(\chi s)^{k-2}\left(1-(\chi s)^2\right)^{\frac{\ell-4}{2}} - s(k-1+\ell-2)(\chi s)^k\left(1-(\chi s)^2\right)^{\frac{\ell-4}{2}} \\ &= s(\chi s)^{k-2}\left(1-(\chi s)^2\right)^{\frac{\ell-4}{2}}\left((k-1) - (k+\ell-3)(\chi s)^2\right). \end{aligned}$$

Consider the case with $\ell \geq 2$ and $k \geq 2$. Then, for all $s \in [0, 1]$ and $\chi \in [\hat{\Theta}, \hat{\Theta}^{1/2}]$,

we have

$$(k-1) - (k+\ell-3)(\chi s)^2 \geq (k-1) \left(1 - \left(1 + \frac{\ell-2}{k-1} \right) \hat{\Theta} \right).$$

Since $C_* > 0$ and $2-k < 0$, we have $2/C_* > 2-k$, which implies that

$$C_*k - 2 < 2C_*k - 2C_*,$$

and using the assumption that $\ell \leq C_*k$ gives

$$\frac{\ell-2}{k-1} < 2C_*.$$

Thus,

$$(k-1) - (k+\ell-3)(\chi s)^2 > (k-1) \left(1 - (1+2C_*) \hat{\Theta} \right) \geq 0,$$

which implies $g'_s(\chi) > 0$; thus, g_s is increasing with respect to χ . Hence,

$$\begin{aligned} \hat{\Theta}^{1/2} \int_0^1 s^{k-1} (1-s^2)^{\frac{\ell-2}{2}} ds &= (\hat{\Theta})^{3/2} \int_0^{1/\hat{\Theta}} (\hat{\Theta}s)^{k-1} \left(1 - (\hat{\Theta}s)^2 \right)^{\frac{\ell-2}{2}} ds \\ &\geq \hat{\Theta} \int_0^1 (\hat{\Theta}s)^{k-1} \left(1 - (\hat{\Theta}s)^2 \right)^{\frac{\ell-2}{2}} ds, \end{aligned}$$

and, with (2.31), (2.32), and (2.33), we obtain

$$\frac{\Upsilon_s^{(k+\ell)}(\hat{M}_\theta)}{\Upsilon_s^{(k+\ell)}(\partial B_\theta^{k+\ell})} \leq \hat{\Theta}^{1/2} = \sqrt{\frac{h(\theta)}{\theta}},$$

for all $0 < \theta \leq \varrho_0$. Therefore, (2.25) and (2.26) give

$$\Upsilon^{(i)}(M_\varrho) \leq \int_0^\varrho \Upsilon_s^{(k+\ell)}(\hat{M}_\theta) \cdot \Upsilon^{(m)}\left(B_{\sqrt{\varrho^2-\theta^2}}^m\right) d\theta$$

$$\begin{aligned}
&\leq \int_0^\varrho \sqrt{\frac{h(\theta)}{\theta}} \cdot \Upsilon_s^{(k+\ell)}(\partial B_\theta^{k+\ell}) \cdot \Upsilon^{(m)}\left(B_{\sqrt{\varrho^2-\theta^2}}^m\right) d\theta \\
&\leq \sqrt{\frac{h(\varrho)}{\varrho}} \cdot \Upsilon^{(i)}(B_\varrho^i),
\end{aligned}$$

for all $0 < \varrho \leq \varrho_0$, and the theorem is proved for $\ell \geq 2$ and $k \geq 2$.

Now we can prove the remaining cases in a similar way. Consider the case $\ell \geq 2$ and $k = 1$. Then we need to estimate $\int_0^{\hat{\Theta}} (1-s^2)^{(\ell-2)/2} ds$ in terms of $\int_0^1 (1-s^2)^{(\ell-2)/2} ds$. Notice that

$$\int_0^{\hat{\Theta}} (1-s^2)^{\frac{\ell-2}{2}} ds \leq \int_0^{\hat{\Theta}} 1 ds = \hat{\Theta} \cdot \frac{\int_0^1 (1-s^2)^{\frac{\ell-2}{2}} ds}{\int_0^1 (1-s^2)^{\frac{\ell-2}{2}} ds}.$$

Since $\ell \leq C_* k$, we have $\ell - 2 \leq C_*$, and a calculation similar to that of (2.27) implies

$$\int_0^1 (1-s^2)^{\frac{C_*}{2}} ds \geq \sqrt{\hat{\Theta}},$$

for all $0 < \theta \leq \varrho_0$. Thus,

$$\int_0^{\hat{\Theta}} 1 ds \leq \hat{\Theta} \cdot \frac{\int_0^1 (1-s^2)^{\frac{\ell-2}{2}} ds}{\int_0^1 (1-s^2)^{\frac{C_*}{2}} ds} \leq \sqrt{\hat{\Theta}} \int_0^1 (1-s^2)^{\frac{\ell-2}{2}} ds,$$

and the result follows as in the previous case.

Now consider the case $\ell = 1$ and $k \geq 1$. By equation (2.28), we have

$$\Upsilon_s^{(k+\ell)}(\hat{M}_\theta) = 2k\tau_1^k \theta^k \int_0^{\hat{\Theta}} \frac{s^{k-1}}{\sqrt{1-s^2}} ds,$$

and

$$\Upsilon_s^{(k+\ell)}(\partial B_\theta^{k+\ell}) = 2k\tau_1^k \theta^k \int_0^1 \frac{s^{k-1}}{\sqrt{1-s^2}} ds.$$

In order to estimate the quotient of these integrals, we apply a change of variables to get

$$\int_0^{\hat{\Theta}} s^{k-1} (1-s^2)^{\frac{-1}{2}} ds = \hat{\Theta} \int_0^1 (\hat{\Theta}s)^{k-1} \left(1 - (\hat{\Theta}s)^2\right)^{\frac{-1}{2}} ds,$$

and notice that the integrand of the second integral here is $g_s(\hat{\Theta})$ defined in (2.33) with $\ell = 1$. Also notice that our previous calculation of $g'_s(\xi)$ follows regardless of our choice for ℓ . Hence, $g_s(\xi)$ is monotonically increasing for all $s \in [0, 1]$ and $\xi \in [\hat{\Theta}, \sqrt{\hat{\Theta}}]$, which gives the estimate

$$\hat{\Theta} \int_0^1 (\hat{\Theta}s)^{k-1} \left(1 - (\hat{\Theta}s)^2\right)^{\frac{-1}{2}} ds \leq \hat{\Theta}^{1/2} \int_0^1 s^{k-1} (1-s^2)^{\frac{-1}{2}} ds$$

for all $0 < \theta \leq \varrho_0$, and the result follows as before. This completes the proof of the theorem. \diamond

Notice that our definition of M_r , along with the result of this theorem, implies (2.23).

2.3 Wavelength Estimates

Now we are left to consider the wavelength of spinodally decomposed states. In general, when considering a cosine wave of the form

$$y = A \cos(kx),$$

we can use a standard definition of a wavelength $\hat{\ell}$ given in general physics by

$$\hat{\ell} = \frac{2\pi}{k},$$

where k is called the wave number. Recall that the eigenvalues for the continuous case are given in the proof of Lemma 2.1, and have the form $(j\pi)^2$. Thus, we can

write the wavelength for these eigenfunctions as

$$\hat{\ell} = \frac{2\pi}{j\pi} = \frac{2\pi}{\sqrt{\kappa_j}}.$$

Now we need to derive a result similar to this for sums of eigenfunctions. Furthermore, remember that the dominating subspace $X_\epsilon^+ \oplus X_\epsilon^{++}$ is generated by all eigenfunctions of A_ϵ corresponding to the eigenvalues in $\sigma^{++} \cup \sigma^+$, and by Lemma 2.2 these eigenfunctions are also eigenfunctions of $-\Delta$ corresponding to the eigenvalues κ_j , which are sufficiently close to μ_ϵ^{max} . Since the eigenfunctions for the discrete case are given by (2.10), we can make our arguments for the continuous eigenfunctions. In fact, all we need to guarantee is that

$$\gamma_1 \leq \frac{\mu_\epsilon^{max}}{\kappa_j} \leq \gamma_2, \quad (2.34)$$

for all κ_j with $\psi_j \in Y_\epsilon^+ \oplus Y_\epsilon^{++}$, where we define

$$0 \ll \gamma_1 < 1 \quad \text{and} \quad 0 \ll \frac{1}{\gamma_2} < 1, \quad (2.35)$$

and we derive

$$\mu_\epsilon^{max} = 4/\epsilon^2$$

from equation (2.10). Notice that it is essential to use κ_j in this inequality because we want to use the wavelength estimate for the continuous case. The following lemma gives us this result.

Lemma 2.5 *For γ_1 and γ_2 given by (2.35), there exists γ^- and $\hat{\rho}$ with $0 \ll \gamma^- < 1$ and $0 < \hat{\rho} \ll 1$ such that (2.34) holds.*

Proof: Consider all j with $\xi(\mu_j) \geq \gamma^- \lambda_\epsilon^{max}$. These are the eigenvalues that contribute to $Y_\epsilon^+ \oplus Y_\epsilon^{++}$, which implies that

$$1 - \delta < \frac{\mu_j}{\mu_\epsilon^{max}} < 1 + \delta$$

for $\delta > 0$ such that $\delta = \delta(\gamma^-) \rightarrow 0$ as $\gamma^- \rightarrow 1$. Thus

$$\left| \frac{\kappa_j}{\mu_\epsilon^{max}} - 1 \right| \leq \left| \frac{\kappa_j - \mu_j}{\mu_\epsilon^{max}} \right| + \left| \frac{\mu_j}{\mu_\epsilon^{max}} - 1 \right| \leq \left| \frac{\mu_j}{\mu_\epsilon^{max}} \right| \cdot \left| \frac{\kappa_j}{\mu_j} - 1 \right| + \delta < (1 + \delta)\hat{\rho} + \delta,$$

and if $0 < \hat{\rho} \ll 1$, then

$$\left| \frac{\kappa_j}{\mu_\epsilon^{max}} - 1 \right| < 2\delta.$$

Therefore, $\kappa_j/\mu_\epsilon^{max} \in (1 - 2\delta, 1 + 2\delta)$ and (2.34) is a direct result of this. \diamond

We want to establish a notion of wavelength of order ϵ for functions in the dominating subspace $X_\epsilon^+ \oplus X_\epsilon^{++}$, and our first step to doing this is in the following proposition, which follows from Proposition 4.3 in [25].

Proposition 2.3 *Let $\psi > 0$ be an arbitrary element of the subspace $X_\epsilon^+ \oplus X_\epsilon^{++}$ such that $\psi = \sum_{i \in \mathcal{I}} \beta_i \psi_i$, where $\beta_i \in \mathbb{R}$ and \mathcal{I} is the interval with $X_\epsilon^+ \oplus X_\epsilon^{++} = \text{span}\{\psi_i : i \in \mathcal{I}\}$. Suppose $B_r(x_0)$ is contained in a nodal domain of ψ , so that for some $n \in \mathbb{N}$, $(x_0) \in \Omega$, and $r > 0$, we have $\psi \in B_r(x_0) \subset \Omega \subset \mathbb{R}^n$. If $\hbar_i = \beta_i \psi_i(x_0)$ and $v = v_i$ is the unique solution of*

$$v'' + \frac{d-1}{t}v' + \kappa_i v = 0 \tag{2.36}$$

for $t \in (0, \infty)$, with initial conditions $v(0) = 1$, and $v'(0) = 0$, then

$$\tilde{\psi}(t) := \sum_{i \in \mathcal{I}} \hbar_i v_i(\sqrt{\kappa_i t}) > 0 \tag{2.37}$$

for all $t \in [0, r)$.

Proof: Using the Haar integral, define the function

$$\hat{\psi}(x) = \frac{1}{|O(d)|} \int_{O(d)} \psi \left(\frac{x}{s} + x_0 \right) ds$$

for all $x \in B_r(0)$. Since the structure of the function ψ implies that it is symmetric about x_0 , clearly $\hat{\psi}(x)$ is radially symmetric. Thus, $\hat{\psi}$ depends only on $|x|$, which allows us to define a function $\tilde{\psi} : [0, r) \rightarrow \mathbb{R}$ by $\tilde{\psi}(|x|) := \hat{\psi}(x)$ for all $x \in B_r(0)$. Notice here that $\tilde{\psi}(x) > 0$, since $\psi > 0$ on $B_r(x_0)$ implies $\psi(x + x_0) > 0$ on $B_r(0)$. In a similar way, we have symmetric eigenfunctions ψ_i , which lead to radially symmetric functions $\hat{\psi}_i : B_r(0) \rightarrow \mathbb{R}$ and in turn give us the functions $\tilde{\psi}_i : [0, r) \rightarrow \mathbb{R}$ given by $\tilde{\psi}_i(|x|) := \hat{\psi}_i(x)$. Notice here that the functions $\hat{\psi}_i$ are eigenfunctions of the linear operator $-\Delta$ on $B_r(0)$. This implies $\tilde{\psi}_i$ is a solution of the differential equation given in (2.36) with initial conditions $v(0) = \psi_i(x_0)$ and $v'(0) = 0$, and consequently $\tilde{\psi}_i = \psi_i(x_0)v_i$ where v_i solves (2.36), which furnishes (2.37) and completes the proof of the proposition. \diamond

It is well known that the solutions $v(t)$ of the differential equation given in (2.36), are given by

$$v(t) = (\sqrt{\kappa_i t})^{\frac{2-d}{2}} \cdot \mathcal{J}_{\frac{d-2}{2}}(\sqrt{\kappa_i t}) = \mathcal{B}_d(t)$$

for $t \geq 0$, cf. Lauterbach and Maier [24]. Here $\mathcal{J}_\nu(t)$ is the ν -th Bessel function of the first kind such that $t^{-\nu} \mathcal{J}_\nu(t) \rightarrow 1$ as $t \rightarrow 0$. In particular we have

$$\mathcal{B}_1(t) = \cos t, \quad \mathcal{B}_2(t) = \mathcal{J}_0(t), \quad \text{and} \quad \mathcal{B}_3(t) = \frac{\sin t}{t}. \quad (2.38)$$

We want to show that if $B_r(x_0)$ is in a nodal domain of some function in the dominating subspace, then the validity of (2.37) implies $r \leq K\epsilon$ for some $K \in \mathbb{R}^+$. This can only be done with some additional assumptions on the coefficients \hbar_i .

Before we present the theorems that give this result, we must first reformulate the problem. A rescaling of the variables such that $\tilde{t} = t\sqrt{\bar{\mu}}$ and $\tilde{r} = r\sqrt{\bar{\mu}}$, for

$$\bar{\mu} = \mu_\epsilon^{max} / \gamma_2, \quad (2.39)$$

implies that (2.37) is equivalent to

$$\sum_{i \in \mathcal{I}} \hbar_i \mathcal{B}_d \left(\sqrt{\frac{\kappa_i}{\bar{\mu}}} \tilde{t} \right) > 0$$

for all $\tilde{t} \in [0, \tilde{r})$. Notice here that

$$\sqrt{\frac{\kappa_i}{\bar{\mu}}} \in \left[1, \sqrt{\frac{\gamma_2}{\gamma_1}} \right]$$

as a result of (2.34). Thus we can write

$$\sqrt{\frac{\kappa_i}{\bar{\mu}}} = 1 + (s\alpha_i)$$

for all $i \in \mathcal{I}$, where $s \in [0, (\gamma_2/\gamma_1)^{1/2} - 1]$ and $\alpha = (\alpha_i)_{i \in \mathcal{I}}$ with $\alpha_i \geq 0$ and $\|\alpha\|_\infty = 1$.

If we let

$$v_s(t) = \sum_{i \in \mathcal{I}} \hbar_i \mathcal{B}_d((1 + s\alpha_i)\tilde{t}) \quad (2.40)$$

for $\tilde{t} \in [0, \tilde{r})$, then we want to determine if there is a constant $K > 0$ such that, if any choice of the parameters \hbar , α , and s as given above, implies $v_s(t) > 0$ for all $t \in (0, r)$, then $r \leq K$. We now look to two theorems that lead to this result, the first of which

is based on Theorem 4.6 in [25] and the second is based on Theorem 4.8 in [25].

Theorem 2.2 *Let $\hbar_i = \hbar_i^+ - \hbar_i^-$ such that*

$$\hbar_i^+ = \max\{0, \hbar_i\} \geq 0$$

and

$$\hbar_i^- = \max\{0, -\hbar_i\} \geq 0,$$

and let $I \subset \mathbb{N}$ be an arbitrary index set. In addition, choose $s_0 > 0$, let $s \in [0, s_0]$, and let $\delta > 0$ be a constant such that $\delta \rightarrow 0$ as $s_0 \rightarrow 0$ and

$$\infty > \sum_{i \in I} \hbar_i^+ \geq (1 + \delta) \sum_{i \in I} \hbar_i^- \geq 0 \quad (2.41)$$

for any choice of the coefficients \hbar_i . Then, for $\alpha \in \mathbb{R}^I$ satisfying $\alpha_i \geq 0$ and $\|\alpha\|_{\text{inf ty}} = 1$, the functions given in (2.40) have a sign change at some point t^* in the interval $[0, 2\pi]$.

Proof: First define

$$v_s^+(t) = \sum_{i \in I} \hbar_i^+ \mathcal{B}_d((1 + s\alpha_i)t)$$

and

$$v_s^-(t) = \sum_{i \in I} \hbar_i^- \mathcal{B}_d((1 + s\alpha_i)t),$$

so that $v_s(t) = v_s^+(t) - v_s^-(t)$, and define

$$\mathcal{B}_d^{\max}(t) = \max_{\eta \in [0, s_0]} \mathcal{B}_d((1 + \eta)t) \geq \mathcal{B}_d((1 + s\alpha_i)t)$$

and

$$\mathcal{B}_d^{\min}(t) = \min_{\eta \in [0, s_0]} \mathcal{B}_d((1 + \eta)t) \leq \mathcal{B}_d((1 + s\alpha_i)t).$$

Without any loss of generality, we can assume that $\sum_{i \in I} \hbar_i^+ = 1$. This implies

$$\mathcal{B}_d^{\min}(t) \leq v_s^+(t) \leq \mathcal{B}_d^{\max}(t), \quad (2.42)$$

as well as

$$\sum_{i \in I} \hbar_i^- \mathcal{B}_d^{\min}(t) \leq v_s^-(t) \leq \sum_{i \in I} \hbar_i^- \mathcal{B}_d^{\max}(t), \quad (2.43)$$

for all $t \geq 0$ and $s \in [0, s_0]$. Notice here that, by using (2.38) we get $\mathcal{B}_d(0) = 1$ for $d \in \{1, 2, 3\}$, which gives

$$v_s(0) = v_s^+(0) - v_s^-(0) = 1 - \sum_{i \in I} \hbar_i^- > 0.$$

If we can show that $v_s(t_o) < 0$ for some $t_o \in (0, 2\pi)$, then we are done. Let t_o be the first positive local minimum of \mathcal{B}_d . Again, using (2.38), we have $0 < t_o < 2\pi$ and $\mathcal{B}_d(t_o) < 0$ for all $d \in \{1, 2, 3\}$. Using (2.42) and (2.43), we get

$$v_s(t_o) = v_s^+(t_o) - v_s^-(t_o) \leq \mathcal{B}_d^{\max}(t_o) - \sum_{i \in I} \hbar_i^- \mathcal{B}_d^{\min}(t_o),$$

and then using (2.41) we have

$$v_s(t_o) \leq \mathcal{B}_d^{\max}(t_o) - \sum_{i \in I} \hbar_i^- \mathcal{B}_d^{\min}(t_o) \leq -\mathcal{B}_d^{\min}(t_o) \left(\frac{1}{1 + \delta} - \frac{\mathcal{B}_d^{\max}(t_o)}{\mathcal{B}_d^{\min}(t_o)} \right)$$

for all $s \in [0, s_0]$. If we choose $s_0 > 0$ small enough, then it is clear that we have the estimates $\mathcal{B}_d^{\min}(t_o) < 0$ and $\mathcal{B}_d^{\max}(t_o) < 0$. Thus,

$$0 < \frac{\mathcal{B}_d^{\max}(t_o)}{\mathcal{B}_d^{\min}(t_o)} < 1,$$

and if we choose δ such that

$$\frac{\mathcal{B}_d^{\min}(t_o)}{\mathcal{B}_d^{\max}(t_o)} - 1 < \delta,$$

then we always have $v_s(t_o) < 0$. In addition, we also know that $\|\mathcal{B}_d^{\max} - \mathcal{B}_d\| \rightarrow 0$ and $\|\mathcal{B}_d^{\min} - \mathcal{B}_d\| \rightarrow 0$ as $s_0 \rightarrow 0$. Therefore, δ can be chosen such that $\delta \rightarrow 0$ as $s_0 \rightarrow 0$, and this completes the proof of the theorem. \diamond

Theorem 2.3 Define $\psi = \sum_{i \in \mathcal{I}} \beta_i \psi_i$ where $\beta_i \in \mathbb{R}$, and let ψ be any element of the dominating subspace $X_\epsilon^+ \oplus X_\epsilon^{++}$, and suppose that the eigenvalues κ_i satisfy (2.34). Also, let $\delta > 0$ be a constant depending on γ_1 and γ_2 such that $\delta \rightarrow 0$ as $\gamma_1, \gamma_2 \rightarrow 1$, and let β and ψ_{x_0} be the vectors $(\beta_i)_{i \in \mathcal{I}}$ and $(\psi_i(x_0))_{i \in \mathcal{I}}$, respectively. If either

$$\frac{|\langle \beta, \psi_{x_0} \rangle|}{\|\beta\| \cdot \|\psi_{x_0}\|} \geq \delta > 0, \quad (2.44)$$

or

$$\left| \sum_{i \in \mathcal{I}} \beta_i \psi_i(x_0) \right| \geq \delta \cdot \min \left\{ - \sum_{i \in \mathcal{I}^-} \beta_i \psi_i(x_0), \sum_{i \in \mathcal{I}^+} \beta_i \psi_i(x_0) \right\}, \quad (2.45)$$

where \mathcal{I}^- and \mathcal{I}^+ are the subsets of \mathcal{I} with $\beta_i \psi_i(x_0) < 0$ and $\beta_i \psi_i(x_0) > 0$, respectively, then the radius r of any ball $B_r(x_0)$ in a nodal domain of ψ satisfies

$$r \leq \pi \epsilon \sqrt{\gamma_2}.$$

Proof: Recall that by (2.39) we have $\bar{\mu} = \mu_\epsilon^{max}/\gamma_2$, which gives

$$\sqrt{\bar{\mu}} = \frac{2}{\epsilon\sqrt{\gamma_2}}.$$

Thus, if we can show that Theorem 2.2 is applicable under the assumptions of this theorem with $I = \mathcal{I}$, and $s_0 = \sqrt{\gamma_2/\gamma_1} - 1$, then we can let $\tilde{r} \leq 2\pi$ to get

$$r \leq \frac{2\pi}{\sqrt{\bar{\mu}}} = \pi\epsilon\sqrt{\gamma_2},$$

and the proof will be complete.

First, suppose that (2.45) holds. This condition is equivalent to

$$\left| \sum_{i \in \mathcal{I}} \hbar_i^+ - \sum_{i \in \mathcal{I}} \hbar_i^- \right| \geq \delta \cdot \min \left\{ -\sum_{i \in \mathcal{I}} \hbar_i^-, \sum_{i \in \mathcal{I}} \hbar_i^+ \right\},$$

with $\beta_i \psi_i(x_0) = \hbar_i = \hbar_i^+ - \hbar_i^-$, which immediately implies condition (2.41) of Theorem 2.2 for both ψ and $-\psi$, and gives the desired upper bound on r .

Next, suppose that (2.44) holds. Again, we only need to show that (2.41) is satisfied and the proof is finished. Define

$$\Sigma_+ - \Sigma_- = \sum_{i \in \mathcal{I}^+} \beta_i \psi_i(x_0) - \sum_{i \in \mathcal{I}^-} -\beta_i \psi_i(x_0) = \sum_{i \in \mathcal{I}} \hbar_i^+ - \sum_{i \in \mathcal{I}} \hbar_i^- = \langle \beta, \psi_{x_0} \rangle,$$

where $\Sigma_+ \geq 0$ and $\Sigma_- \geq 0$, and assume that $\Sigma_+ > \Sigma_-$; otherwise we can consider $-\psi$ rather than ψ to get the same result. Now, we want to show that $\Sigma_+ \geq (1 + \delta)\Sigma_-$. This is obviously true if $\Sigma_- = 0$. Suppose $\Sigma_- > 0$, and without loss of generality assume $\|\beta\| = 1$. Then we have

$$\Sigma_+ - \Sigma_- = \langle \beta, \psi_{x_0} \rangle \geq \delta,$$

which gives

$$\Sigma_+ \geq \delta \|\psi_i(x_0)\| + \Sigma_- = \Sigma_- \left(1 + \frac{\delta \|\psi_i(x_0)\|}{\Sigma_-} \right).$$

According to the definition of δ , we only need to show that $\Sigma_- \leq \|\psi_i(x_0)\|$, in order to complete the proof. Let P be the orthogonal projection such that $P : \mathbb{R}^{\mathcal{I}} \rightarrow \mathbb{R}^{\mathcal{I}^-(x_0)}$ with $\mathbb{R}^{\mathcal{I}^-(x_0)} \subset \mathbb{R}^{\mathcal{I}}$. Then we have

$$\Sigma_- = -\langle P(\beta), P(\psi_i(x_0)) \rangle \leq \|P(\beta)\| \cdot \|P(\psi_i(x_0))\| \leq \|\psi_i(x_0)\|,$$

because $\|\beta\| = 1$, and the proof is complete. \diamond

This theorem gives a bound of order ϵ for the wavelength of functions in the dominating subspace $X_\epsilon^+ \oplus X_\epsilon^{++}$, but only with the extra assumptions (2.44) and (2.45). However, we can show that the theorem can be applied to typical points in Ω (cf. subsection 4.3 in [25]). In order to reach this end, let $\psi = \sum_{i \in \mathcal{I}} \beta_i \psi_i =: \Psi_{\mathcal{I}}$, and suppose D is a subdomain of Ω and $I \subset \mathcal{I}$. Then we have the approximation

$$\frac{1}{|D|} \int_D \Psi_{\mathcal{I}}^2(x) dx \approx \frac{1}{|\Omega|} \int_{\Omega} \Psi_{\mathcal{I}}^2(x) dx = \frac{1}{|\Omega|} \sum_{i \in \mathcal{I}} \beta_i^2. \quad (2.46)$$

If we assume that (2.45) does not hold for any point in $B := B_{r/2}(y_0)$, then we have

$$\int_B \Psi_{\mathcal{I}}^2(x) dx \leq \delta^2 \cdot \max \left\{ \int_B \Psi_{\mathcal{I}^-}^2(x) dx, \int_B \Psi_{\mathcal{I}^+}^2(x) dx \right\}. \quad (2.47)$$

Now let $B = \bigcup_{j=1}^J \hat{B}_j$, where the subsets \hat{B}_j are disjoint and for all $x \in \hat{B}_j$ we have $I_j^- := \mathcal{I}^-(x)$, for $j = 1, 2, \dots, J$. Then an application of the estimates (2.46) and (2.47) yields

$$\int_B \Psi_{\mathcal{I}^-}^2(x) dx = \sum_{j=1}^J \int_{\hat{B}_j} \Psi_{I_j^-}^2(x) dx \approx \sum_{j=1}^J \sum_{i \in I_j^-} \frac{|\hat{B}_j|}{\Omega} \beta_i^2 \leq \frac{|B|}{\Omega} \sum_{i \in I_j^-} \beta_i^2.$$

Notice that the same can be done for $i \in \mathcal{I}^+(x)$, which implies

$$\frac{|B|}{\Omega} \sum_{i \in \mathcal{I}} \beta_i^2 \leq \delta^2 \frac{|B|}{\Omega} \sum_{i \in \mathcal{I}} \beta_i^2,$$

where $0 < \delta \ll 1$. This implies that the theorem is applicable at typical points in the domain Ω . Thus we have a bound of order ϵ for the thickness of nodal domains of functions in $X_\epsilon^+ \oplus X_\epsilon^{++}$.

Chapter 3

NONLINEAR DYNAMICS

In this chapter, we use our results for the linearized Cahn-Hilliard equation to aid in our analysis of the nonlinear equation (2.14), and derive a similar probability estimate as that given in Theorem 2.1. It has, in fact, been shown in [36] and [37], that the behavior of the nonlinear equation is governed mostly by its linearization, though we will not use these ideas here. The concepts of this chapter are based on the results proven for the continuous problem in [26]. We start with the following assumptions on the nonlinear term f and the domain Ω .

Assumption 1 : Let $\Omega \subset \mathbb{R}^d$ be a bounded domain with $d \in \{1, 2, 3\}$ such that $\Omega = [0, 1]^d$.

Assumption 2 : Let $-f : \mathbb{R} \rightarrow \mathbb{R}$ be a C^4 -function that is the derivative of a double-well potential, the standard example being $f(u) = u - u^3$.

Assumption 3 : Assume that we have $f'(m) > 0$. In other words, fix a mass $m \in \mathbb{R}$ in the spinodal interval.

3.1 The Abstract Equation

Rather than looking at the original equation given by (2.1) with mass constraint $\int_{\Omega} u dx = m$, we will rewrite the equation as was done in [19]. Consider a change of variables such that $w = u - m$. Then, after we replace w by u again, we can write

the Cahn-Hilliard equation (1.1) as

$$u_t = -\Delta(\epsilon^2 \Delta u + f(m + u)), \forall x \in \Omega,$$

$$\frac{\partial u}{\partial \nu} = \frac{\partial \Delta u}{\partial \nu} = 0, \forall x \in \partial\Omega,$$

with mass constraint $\int_{\Omega} u dx = 0$. Again, let the linear operator \hat{A}_{ϵ} be such that

$$\hat{A}_{\epsilon} u = -n^2 \Delta_n (\epsilon^2 n^2 \Delta_n u + f'(m)u),$$

and let the nonlinear function $F : \mathbb{R}^{n^d} \rightarrow \mathbb{R}^{n^d}$ be given by

$$F(u) = -n^2 \Delta_n \tilde{f}(u),$$

where we have let

$$\tilde{f}(u) := f(m + u) - f'(m)u - f(m)$$

and $\tilde{f}(0) = \tilde{f}'(0) = 0$. This allows us to write (2.14) in the form

$$\dot{u} = \hat{A}_{\epsilon} u + F(u). \tag{3.1}$$

3.1.1 Properties of the Linear Operator

Since $\mu_j \sim \kappa_j$ for Y_{ϵ}^+ and Y_{ϵ}^{++} , which was shown in Lemma 2.4, our desired results for when the spatially discrete Cahn-Hilliard equation exhibits spinodal decomposition will follow as they did for the continuous problem. Notice that we can write the continuous equation in the same form as (3.1) using the operator A_{ϵ} , and recall that A_{ϵ} is a selfadjoint sectorial operator that generates an analytic semigroup $S_{\epsilon}(t)$ on X . Furthermore, we have fractional power spaces equipped with the graph

norm,

$$\|u\|_*^2 = \|u\|^2 + \|\Delta u\|^2 \quad (3.2)$$

where $\|\cdot\|$ is the L^2 norm here, cf. [20, 26, 33].

Using the fact that $\mu_j \sim \kappa_j$ and (2.3) as was shown in Chapter 2, we now look to the following result concerning spectral gaps for the linear operator \hat{A}_ϵ , which follows from Lemma 3.3 in [26].

Lemma 3.1 *Suppose that Assumptions 1 and 3 are satisfied, and fix constants $c_* < c^* < 1$. Furthermore, assume there are constants $\epsilon_0, s_0 > 0$ that depend only on c_* , c^* , Ω , and $f'(m)$, and where $0 < \epsilon \leq \epsilon_0$. Then \hat{A}_ϵ has eigenvalues λ_* and λ^* with*

$$c_* \lambda_\epsilon^{max} \leq \lambda_* \leq \lambda^* \leq c^* \lambda_\epsilon^{max}$$

and

$$\lambda^* - \lambda_* \geq s_0 \epsilon^{d-2}.$$

Proof: Let c_{**} and c^{**} be constants such that $c_* < c_{**} < c^{**} < c^*$. Then using the results of Lemma 2.1, and the fact that the eigenvalues of \hat{A}_ϵ are arbitrarily close to the eigenvalues of A_ϵ , we know that the intervals $[c_*, c_{**}] \cdot \lambda_\epsilon^{max}$ and $[c^{**}, c^*] \cdot \lambda_\epsilon^{max}$ each contain at least one eigenvalue of \hat{A}_ϵ . If we let λ^{**} be the smallest eigenvalue in the interval $[c^{**}, c^*] \cdot \lambda_\epsilon^{max}$ and let λ_{**} be the largest eigenvalue in the interval $[c_*, c_{**}] \cdot \lambda_\epsilon^{max}$, then we have

$$\lambda^{**} - \lambda_{**} \geq (c^{**} - c_{**}) \lambda_\epsilon^{max} = \frac{(f'(m))^2 (c^{**} - c_{**})}{4\epsilon^2}. \quad (3.3)$$

Also due to Lemma 2.1, we can choose a bound on ϵ such that, for all $0 < \epsilon \leq \epsilon_0$, the

number of eigenvalues of \hat{A}_ϵ in the interval $(c_{**}, c^{**}) \cdot \lambda_\epsilon^{max}$ is bounded by $C\epsilon^{-d} - 1$, where C is a constant depending on c_* , c^* , $f'(m)$, and Ω . Now let

$$\varsigma = \frac{(f'(m))^2 (c^{**} - c_{**})}{4C},$$

and for the sake of contradiction assume that the distance between any two consecutive eigenvalues, say λ^* and λ_* in the interval $[\lambda^{**}, \lambda_{**}]$ is strictly less than $\varsigma\epsilon^{d-2}$. This implies

$$\lambda^{**} - \lambda_{**} < \varsigma\epsilon^{d-2} \cdot C\epsilon^{-d} = \frac{(f'(m))^2 (c^{**} - c_{**})}{4C},$$

but this contradicts (3.3). Hence, the proof of the lemma is complete. \diamond

Thus it is possible to control the size of the gaps in the spectrum of \hat{A}_ϵ if we choose ϵ small enough. Let

$$0 \ll c^- < \bar{c}^- < c^+ < \bar{c}^+ < 1, \quad (3.4)$$

then we can define intervals

$$I_\epsilon^- := [a_\epsilon^-, b_\epsilon^-] \subset [c^-, \bar{c}^-] \cdot \lambda_\epsilon^{max},$$

$$I_\epsilon^+ := [a_\epsilon^+, b_\epsilon^+] \subset [c^+, \bar{c}^+] \cdot \lambda_\epsilon^{max}$$

, such that I_ϵ^- and I_ϵ^+ are each contained in the resolvent set of \hat{A}_ϵ , and there is a constant $C > 0$ with $b_\epsilon^- - a_\epsilon^- \geq C\epsilon^{d-2}$ and $b_\epsilon^+ - a_\epsilon^+ \geq C\epsilon^{d-2}$, where C depends on Ω , $f'(m)$, and the constants in (3.4), but not on ϵ . Now define $\bar{I}_\epsilon^- := (b_\epsilon^-, a_\epsilon^-)$, $\bar{I}_\epsilon^+ := (b_\epsilon^+, a_\epsilon^+)$, and $\bar{I}_\epsilon^{++} := (b_\epsilon^+, \lambda_\epsilon^{max}]$, and let $Y = Y_\epsilon^- \oplus Y_\epsilon^+ \oplus Y_\epsilon^{++}$, where each of these subspaces corresponds to the eigenvalues in \bar{I}_ϵ^- , \bar{I}_ϵ^+ , and \bar{I}_ϵ^{++} , and each of these

subspaces is of order $\epsilon^{-d} \sim n^d$.

Note that depending on our choice of n , there are two cases to be considered here. We must consider the case in which there is no Y_ϵ^{--} space, and the case in which we include the Y_ϵ^{--} space. We will start by considering the first case with $Y = Y_\epsilon^- \oplus Y_\epsilon^+ \oplus Y_\epsilon^{++}$, and finish by showing that when we include the Y_ϵ^{--} space, our results are the same. With this in mind consider the following lemma which is based on Lemma 3.6(b) in [26] and will be essential for proving our main result in the chapter.

Lemma 3.2 *Suppose that Assumptions 1 and 2 hold, and let \hat{A}_ϵ be a self-adjoint sectorial operator acting on Y , where $\hat{S}_\epsilon(t)$ is the corresponding analytic semigroup for $t \geq 0$. Then, for some ϵ_0 depending on $f'(m)$, Ω , and the constants in (3.4), such that $0 < \epsilon \leq \epsilon_0$, we have the following For every $u^{++} \in Y_\epsilon^{++}$, $u^+ \in Y_\epsilon^+$, and $u^- \in Y_\epsilon^-$,*

$$\|\hat{S}_\epsilon^{++}(t)u^{++}\| \leq e^{b_\epsilon^+ t} \cdot \|u^{++}\|, \forall t \geq 0,$$

$$\|\hat{S}_\epsilon^+(t)u^+\| \leq e^{a_\epsilon^+ t} \cdot \|u^+\|, \forall t \geq 0,$$

$$\|\hat{S}_\epsilon^+(t)u^+\| \leq e^{b_\epsilon^- t} \cdot \|u^+\|, \forall t \leq 0,$$

$$\|\hat{S}_\epsilon^-(t)u^-\| \leq e^{a_\epsilon^- t} \cdot \|u^-\|, \forall t \geq 0,$$

$$\|\hat{S}_\epsilon^-(t)u^-\| \leq e^{b_\epsilon^{--} t} \cdot \|u^-\|, \forall t \leq 0,$$

where $\|\cdot\|$ denotes the Euclidean norm.

Proof: First let ξ_1 be the largest eigenvalue of \hat{A}_ϵ , and let ξ_1, \dots, ξ_i be the eigenvalues in the interval \bar{I}_ϵ^{++} . Similarly, let ξ_{i+1}, \dots, ξ_j be the eigenvalues in \bar{I}_ϵ^+ , and let $\xi_{j+1}, \dots, \xi_{n+1}$ be the eigenvalues in \bar{I}_ϵ^- , where $1 < i < j < n$ and $i, j \in \mathbb{N}$. Using the Fourier series

representations given in (2.16) and (2.17), we have

$$u = \sum_{k=1}^{n+1} \chi_k \varphi_k,$$

and

$$\hat{S}_\epsilon(t)u = \sum_{k=1}^{n+1} e^{\xi_k t} \chi_k \varphi_k$$

for $t \geq 0$, where $\chi_k = \langle \bar{v}, \varphi_k \rangle$. This implies

$$\|S_\epsilon^{++}(t)u^{++}\| = \left\| \sum_{k=1}^i e^{\xi_k t} \chi_k \varphi_k \right\| \geq e^{b_\epsilon^+ t} \left\| \sum_{k=1}^i \chi_k \varphi_k \right\| = e^{b_\epsilon^+ t} \|u^{++}\|,$$

for all $t \geq 0$, because $b_\epsilon^+ < \xi_i$ and ξ_i is the smallest eigenvalue of the interval \bar{I}_ϵ^{++} . This automatically implies the first of our desired results, and the other four inequalities of this lemma can be proven in precisely the same manner. \diamond

We know that the linear part of (3.1) satisfies the statements that \hat{A}_ϵ is sectorial on Y , and that Y has a spectral decomposition as we have stated with fractional power spaces of Y from Lemma 2.2 and (2.18). Now define

$$C_\epsilon^+ := \frac{\min[b_\epsilon^- - a_\epsilon^-, b_\epsilon^+ - a_\epsilon^+]}{6 + \sigma + \frac{1}{\sigma}}. \quad (3.5)$$

Then we can verify that $C_\epsilon^+ \geq C\epsilon^{d-2}$, where C depends on Ω , $f'(m)$, σ , and the constants in (3.4). This implies that if $L_f \leq C\epsilon^{d-2}$, then $L_f \leq C_\epsilon^+$, and since $\epsilon^{d-2} \geq \epsilon^d$ for $\epsilon \rightarrow 0$, we have a larger neighborhood where the result holds than we did for the continuous case with $L_F \leq \epsilon^d$.

3.1.2 Estimates for the Nonlinearity

Now, as we consider properties of the nonlinearity that will be essential for proving our main result, we need the following lemma, which is based on Lemma 1 in [18].

Lemma 3.3 *Suppose that Assumption 1 is true. Let $g : \mathbb{R} \rightarrow \mathbb{R}$ be a C^4 -function with $g(0) = g'(0) = 0$, and define a mapping G such that $G(u)(x) := (-\Delta g(u))(x)$. If $\alpha > 0$ is a constant depending only on Ω and g , then, for every $L > 0$, there is a continuously differentiable mapping \hat{G} that satisfies the inequality*

$$\|\hat{G}(u) - \hat{G}(v)\| \leq L\|u - v\|,$$

and $\hat{G}(u) = G(u)$ for all u such that $\|u\| \leq \alpha L$.

Proof: First, notice that the definition of G implies G is continuously differentiable and the derivative of G is given by $DG(u)h = -\Delta(g'(u)h)$ with $G(0) = DG(0) = 0$. Now define the function $\zeta : \mathbb{R} \rightarrow [0, 1]$ to be a C^∞ -function such that, $\zeta(u) = 1$ for all $u \in [-1, 1]$, $\zeta(u) = 0$ for all $u \in (-\infty, -4] \cap [4, \infty)$, and $|\zeta'(u)| \leq 1$ for all $u \in \mathbb{R}$. In addition, let $\rho > 0$ be some constant such that for every $L > 0$ we have

$$\|DG(u)\| \leq \frac{L}{9}$$

whenever $\|u\| \leq \rho$. From the mean value theorem,

$$G(b) - G(a) = DG(c)(b - a),$$

for some $a < c < b$. This implies that G has a Lipschitz constant $L_G \leq L/9$ on the ball centered at zero with radius ρ . Suppose the function \hat{G} is given by

$$\hat{G}(u) = \zeta\left(\frac{4\|u\|^2}{\rho^2}\right)G(u).$$

Then $\hat{G}(u) = G(u)$ whenever $\|u\| \leq \rho/2$, and $\hat{G}(u) = 0$ whenever $\|u\| \geq \rho$. Using this definition for $\hat{G}(u)$, we can calculate its derivative explicitly to be

$$D\hat{G}(u)h = \frac{8}{\rho^2}\zeta'\left(\frac{4\|u\|^2}{\rho^2}\right)\langle u, h\rangle G(u) + \zeta\left(\frac{4\|u\|^2}{\rho^2}\right)DG(u)h,$$

which implies that

$$\|D\hat{G}(u)\| \leq \frac{8}{\rho^2}\left|\zeta'\left(\frac{4\|u\|^2}{\rho^2}\right)\right|\|u\|\|G(u)\| + \left|\zeta\left(\frac{4\|u\|^2}{\rho^2}\right)\right|\|DG(u)\|.$$

By the definition of ζ , and using the assumption that $\|u\| < \rho$, we get

$$\|D\hat{G}(u)\| \leq \frac{8}{\rho}\|G(u)\| + \|DG(u)\| \leq \frac{8}{\rho}\|G(u)\| + \frac{L}{9}.$$

Since G has a Lipschitz constant $L_G \leq L/9$, we have $\|G(u)\| \leq (L/9)\|u\| \leq (L/9)\rho$, which gives the estimate

$$\|D\hat{G}(u)\| \leq \frac{8L}{9} + \frac{L}{9} = L.$$

Then, using the mean value theorem as before, we conclude that \hat{G} has a global Lipschitz constant that is no greater than L . Now, if we let $\alpha = \rho/2L$, then the proof of the theorem is complete. \diamond

Notice that F satisfies the conditions imposed on G in this lemma. Therefore, F satisfies the global Lipschitz condition on a certain neighborhood of the origin, which

is proportional to ϵ^{d-2} . Notice also that using this property of the nonlinearity F , and the fact that the linear operator A_ϵ is sectorial, we can write the unique solution of (3.1) to be the solution of the integral equation

$$u(t) = S(t)u_0 + \int_0^t S(t-s)F(u(s))ds, \quad (3.6)$$

cf. [33]. This brings us to our main results on spinodal decomposition.

3.2 Spinodal Decomposition

Keeping in mind that we are considering the simplest case in which there is no Y_ϵ^{--} space, the dimensions of Y_ϵ^{++} , Y_ϵ^+ , and Y_ϵ^- are all approximately $\epsilon^{-d} \sim n^d$. Now, we can describe the flow on the space $Y = Y_\epsilon^- \oplus Y_\epsilon^+ \oplus Y_\epsilon^{++}$ by the following system of ODEs

$$\begin{aligned} \dot{u}^- &= A^-u^- + f^-(u^- + u^+ + u^{++}), \\ \dot{u}^+ &= A^+u^+ + f^+(u^- + u^+ + u^{++}), \\ \dot{u}^{++} &= A^{++}u^{++} + f^{++}(u^- + u^+ + u^{++}), \end{aligned} \quad (3.7)$$

where $\dot{u} \equiv du/dt$. This derivation can be found in [26]. Assuming the decomposition of the space X given in (2.20), we can define f by

$$f = f^- \oplus f^+ \oplus f^{++} : X_\epsilon^- \oplus X_\epsilon^+ \oplus X_\epsilon^{++} \longrightarrow X_\epsilon^- \oplus X_\epsilon^+ \oplus X_\epsilon^{++},$$

and we have that f is Lipschitz continuous, which was shown in Lemma 3.3, with Lipschitz constant L_f , such that

$$0 \leq L_f \leq C_\epsilon^+,$$

where C_ϵ^+ is given by (3.5), $\sigma > 0$ and

$$\sigma^2 = \frac{R^2}{\rho^2} - 1. \quad (3.8)$$

3.2.1 The Flow on the Invariant Manifold

Notice that this general setting is simpler than for that of the continuous case because the equations define a flow not just a semiflow. This is true because the subspaces of Y are finite dimensional. In addition, the norm acting on the space Y in this case is the standard Euclidian norm. If we let superscripts denote the orthogonal projection of a vector onto the corresponding subspace, such that $u^{+,++}$ is the orthogonal projection of u onto $X_\epsilon^+ \oplus X_\epsilon^{++}$, then we can state the following results, which follow from the results of Lemmas 2.3 and 2.4 in [4].

Lemma 3.4 *Consider the system of equations given in (3.7), and let σ be any positive constant such that*

$$0 \leq L_f \leq \frac{b^- - a^-}{2 + \sigma + 1/\sigma}.$$

Suppose $u_0 = u_0^- + u_0^+ + u_0^{++} \in Y_\epsilon^- \oplus Y_\epsilon^+ \oplus Y_\epsilon^{++}$, such that $\|u_0^{+,++}\| \leq \sigma \|u_0^-\|$, and let $u(t)$ be a solution of (3.7) corresponding to this initial condition. Then

$$\|u^{+,++}\| \leq \sigma \|u^-\|,$$

and

$$\|u^-\| \geq \|u_0^-\| e^{\gamma^- t}$$

for all $t \leq 0$.

Proof: First, we rewrite the system of equations in (3.7) as

$$\dot{u}^- = A^- u^- + f^-(u^- + u^+ + u^{++}) \quad (3.9)$$

$$\dot{u}^{+,++} = A^{+,++} u^{+,++} + f^{+,++}(u^- + u^+ + u^{++}). \quad (3.10)$$

Using the invariance of the subspaces $X_\epsilon^+ \oplus X_\epsilon^{++}$ and X_ϵ^- , the unique solution given in (3.6) can be decomposed into solutions of the system (3.9), (3.10). These solutions are given by

$$u^-(t) = S^-(t)u_0^- + \int_0^t S^-(t-s)f^-(u^-(s) + \omega(s))ds$$

for $t \geq 0$, and write $\omega(t) = u^{+,++}(t)$ to get

$$\omega(t+\tau) = S^{+,++}(\tau)\omega(t) + \int_0^\tau S^{+,++}(\tau-s)f^{+,++}(u^-(t+s) + \omega(t+s))ds$$

for $\tau \geq -t$, which implies the estimate

$$\|u^-(t)\| \leq \|S^-(t)u_0^-\| + \int_0^t \|S^-(t-s)f^-(u^-(s) + \omega(s))\|.$$

From Lemma 3.2, we know that $\|S_\epsilon^-(t)u^-\| \leq \|u^-\| e^{a_\epsilon^- t}$, which implies that

$$\|S^-(t)u_0^-\| \leq \|u_0^-\| e^{a_\epsilon^- t}$$

and

$$\|S^-(t-s)f^-(u^-(s) + \omega(s))\| \leq \|f^-(u^-(s) + \omega(s))\|e^{a_\epsilon^-(t-s)}.$$

By the Lipschitz continuity of the function F given in Lemma 3.3, we have the estimates

$$\|f^-(v) - f^-(w)\| \leq L_f\|v^- - w^-\| + L_f\|v^{+,++} - w^{+,++}\|$$

and

$$\|f^{+,++}(v) - f^{+,++}(w)\| \leq L_f\|v^- - w^-\| + L_f\|v^{+,++} - w^{+,++}\|,$$

where $v = v^- + v^{+,++}$ and $w = w^- + w^{+,++}$. Thus, we can write

$$\|f^-(u^-(s) + \omega(s))\| \leq L_f (\|u^-(s)\| + \|\omega(s)\|),$$

which implies that

$$\|u^-(t)\| \leq \|u_0^-\| \cdot e^{a_\epsilon^- t} + L_f \int_0^t (\|u^-(s)\| + \|\omega(s)\|) e^{a_\epsilon^-(t-s)} ds.$$

Using the assumption that $\|u_0^{+,++}\| \leq \sigma\|u_0^-\|$, we get

$$\|u^-(t)\|e^{-a_\epsilon^- t} \leq \|u_0^-\| + L_f(1 + \sigma) \int_0^t \|u^-(s)\|e^{-a_\epsilon^- s} ds,$$

and Gronwall's inequality implies that

$$\|u^-(t)\| \leq \|u_0^-\| e^{[a_\epsilon^- + L_f(1+\sigma)]t},$$

for $t \geq 0$. A short calculation shows that

$$a_\epsilon^- + L_f(1 + \sigma) \leq a_\epsilon^- + \frac{b_\epsilon^- - a_\epsilon^-}{2 + \sigma + \frac{1}{\sigma}}(1 + \sigma) = \frac{a_\epsilon^-(1 + \frac{1}{\sigma}) + b_\epsilon^-(1 + \sigma)}{2 + \sigma + \frac{1}{\sigma}} \leq \gamma^-,$$

where $\gamma^- = (a_\epsilon^- + b_\epsilon^-)/2$. Thus,

$$\|u^-(t)\| \leq \|u_0^-\| e^{\gamma^- t},$$

and, if we take the case when $t \leq 0$, we have the desired result. In order to obtain the next result, assume that

$$\|u_0^-\| \leq \frac{1}{\sigma} \|u_0^{+,++}\|.$$

By the proof of Lemma 3.2, it is clear that we have the estimate

$$\|S^{+,++}(t)\omega\| \leq \|\omega\| e^{b_\epsilon^- t},$$

for all $t \leq 0$. Then, following the same procedure used for $u^-(t)$, we get

$$\|\omega(t + \tau)\| \leq \|\omega(t)\| e^{b_\epsilon^- \tau} + L_f \int_\tau^0 (\|u^-(t + s)\| + \|\omega(t + s)\|) e^{b_\epsilon^-(\tau - s)},$$

which can also be written as

$$\|\omega(t + \tau)\| e^{-b_\epsilon^-(t + \tau)} \leq \|\omega(t)\| e^{-b_\epsilon^- t} + L_f \int_\tau^0 (\|u^-(t + s)\| + \|\omega(t + s)\|) e^{-b_\epsilon^-(t - s)},$$

for $-t \leq \tau \leq 0$. Gronwall's inequality implies that

$$\|\omega(t)\| \geq \|\omega_0\| e^{[b_\epsilon^- - L_f(1 + \frac{1}{\sigma})]t},$$

and we arrive at the estimate

$$\frac{\|u^-(t)\|}{\|\omega(t)\|} \leq \frac{\|u_0^-\|}{\|u_0^{+,++}\|} e^{[a_\epsilon^- - b_\epsilon^- + L_f(2 + \sigma + \frac{1}{\sigma})]t}.$$

Notice that the inequalities $\|u_0^-\| \leq \frac{1}{\sigma}\|u_0^{+,++}\|$ and $\|u_0^{+,++}\| \leq \sigma\|u_0^-\|$ imply

$$\|u_0^{+,++}\| = \sigma\|u_0^-\|,$$

and we have

$$L_f \left(2 + \sigma + \frac{1}{\sigma}\right) \leq b_\epsilon^- - a_\epsilon^-.$$

Thus,

$$\frac{\|u_0^-\|}{\|u_0^{+,++}\|} e^{[a_\epsilon^- - b_\epsilon^- + L_f(2 + \sigma + \frac{1}{\sigma})]t} \leq \frac{1}{\sigma},$$

which gives

$$\sigma\|u^-(t)\| \leq \|\omega(t)\|$$

for $t \geq 0$, and this implies the desired result if we again let $t \leq 0$. \diamond

The dominating subspace described in Chapter 2 for the linearized equation must be replaced by a dominating invariant manifold for the nonlinear equation. The following lemma establishes the existence of this manifold, and some estimates that are needed to prove results similar to Propositions 2.1 and 2.2.

Lemma 3.5 *Consider the system given in (3.7), and suppose that*

$$0 \leq L_f \leq \frac{b^+ - a^+}{8}.$$

Then the following four results hold.

1. *There exists an invariant manifold $\mathcal{R} \subset Y_\epsilon^- \oplus Y_\epsilon^+ \oplus Y_\epsilon^{++}$, which contains all solutions of (3.7) that are bounded for $t \geq 0$ and is the graph of the mapping $h_{\mathcal{R}} : Y_\epsilon^- \oplus Y_\epsilon^+ \rightarrow Y_\epsilon^{++}$. Furthermore, the function $h_{\mathcal{R}}$ is globally Lipschitz continuous with a global Lipschitz constant that is bounded above by $3L_f/(b^+ - a^+)$.*
2. *There exists an operator $\mathcal{E} : Y_\epsilon^- \oplus Y_\epsilon^+ \oplus Y_\epsilon^{++} \rightarrow \mathcal{R}$ such that each preimage $\mathcal{E}^{-1}(v)$, for $v \in \mathcal{R}$, is the graph of the mapping $h_{\mathcal{E}^{-1}} : Y_\epsilon^{++} \rightarrow Y_\epsilon^- \oplus Y_\epsilon^+$, which is globally Lipschitz continuous with a Lipschitz constant that is bounded above by $3L_f/(b^+ - a^+)$.*
3. *If u is a solution of (3.7), then*

$$\|u(t) - \mathcal{E}(u(t))\| \leq \frac{3\sqrt{2}}{2} \|u(0) - \mathcal{E}(u(0))\| e^{\gamma t}$$

for all $t \leq 0$, and $\mathcal{E}(u)$ is also a solution of (3.7).

4. *If $u \in Y_\epsilon^- \oplus Y_\epsilon^+ \oplus Y_\epsilon^{++}$, then we have*

$$\frac{1}{\sqrt{2}} \|u^{++} - h_{\mathcal{R}}(u^{-,+})\| \leq \|u - \mathcal{E}(u)\| \leq 2\|u\|.$$

Proof: The proof of part 1 is based on Theorem 4.1 in [3]. We begin by writing the system in (3.7) as

$$\dot{u}^{-,+} = A^{-,+}u^{-,+} + f^{-,+}(u^{-,+} + u^{++}) \quad (3.11)$$

$$\dot{u}^{++} = A^{++}u^{++} + f^{++}(u^{-,+} + u^{++}), \quad (3.12)$$

and noting that we have the estimates

$$\|S^{-,+}(t)u^{-,+}\| \leq \|u^{-,+}\| e^{a^+ t}$$

for all $t \geq 0$, and

$$\|S^{++}(t)u^{++}\| \leq \|u^{++}\|e^{b^+t}$$

for all $t \leq 0$. Again, by the Lipschitz continuity of the function F given in Lemma 3.3, we obtain the estimates

$$\|f^{-,+}(v) - f^{-,+}(w)\| \leq L_f\|v^{-,+} - w^{-,+}\| + L_f\|v^{++} - w^{++}\|$$

$$\|f^{++}(v) - f^{++}(w)\| \leq L_f\|v^{-,+} - w^{-,+}\| + L_f\|v^{++} - w^{++}\|.$$

Consider (3.11), and define

$$g(u^{-,+} + u^{++}) = f^{-,+}(u^{-,+} + u^{++}) - f^{-,+}(u^{++}),$$

and

$$g_0(u^{++}) = f^{-,+}(u^{++}).$$

Then we can rewrite this equation as

$$\dot{u}^{-,+} = A^{-,+}u^{-,+} + g(u^{-,+} + u^{++}) + g_0(u^{++}),$$

with the initial condition $u^{-,+}(0) = \zeta$ where ζ is an element of $Y_\epsilon^- \oplus Y_\epsilon^+$, and we know the solution of this equation can be written in the form

$$\nu(t) = S^{-,+}(t)\zeta + \int_0^t S^{-,+}(t-s)[g(\nu(s) + \mu(s)) + g_0(\mu(s))] ds$$

for $t \geq 0$, where $\mu(t)$ is the solution of the equation (3.12) in the system. Following the procedure used in the proof of Lemma 3.4, we obtain

$$\begin{aligned} \|\nu(t)\| &\leq \|\zeta\|e^{a^+t} + \int_0^t (L_f\|\nu(s)\| + \|g_0(\mu(s))\|) e^{a^+(t-s)} ds \\ &= \|\zeta\|e^{a^+t} + L_f e^{a^+t} \int_0^t \|\nu(s)\| e^{-a^+s} ds + e^{a^+t} \int_0^t \|g_0(\mu(s))\| e^{-\gamma^+s} e^{(\gamma^+-a^+)t} ds \\ &\leq e^{a^+t} \left[\|\zeta\| + L_f \int_0^t \|\nu(s)\| e^{-a^+s} ds + \frac{\|g_0\|_{\gamma^+}^+}{\gamma^+ - a^+} e^{(\gamma^+-a^+)t} \right], \end{aligned}$$

where $\gamma^+ = (b^+ + a^+)/2$, and $\|g\|_{\gamma^+}^+ := \sup \{ \|g(t)\| e^{-\gamma^+t} : t \geq 0 \}$. In order to simplify the notation, let

$$\Lambda(t) := \|\nu(t)\| e^{-a^+t},$$

and

$$\Gamma(t) := \|\zeta\| + \frac{\|g_0\|_{\gamma^+}^+}{\gamma^+ - a^+} e^{(\gamma^+-a^+)t},$$

which gives

$$\Lambda(t) \leq \Gamma(t) + L_f \int_0^t \Lambda(s) ds.$$

An application of Gronwall's inequality yields

$$\Lambda(t) \leq \Gamma(t) + L_f \int_0^t \Gamma(s) e^{L_f(t-s)} ds$$

for all $t \geq 0$, and after integrating by parts we get

$$\Lambda(t) \leq \Gamma(t) + L_f e^{L_f t} \left[\left(-\frac{\Gamma(t)}{L_f} e^{-L_f t} + \frac{\Gamma(0)}{L_f} \right) + \frac{1}{L_f} \int_0^t \Gamma'(s) e^{-L_f s} ds \right],$$

which is equivalent to

$$\Lambda(t) \leq \Gamma(0)e^{L_f t} + e^{L_f t} \int_0^t \|g_0\|_{\gamma^+}^+ e^{(\gamma^+ - a^+ - L_f)s} ds = \|\zeta\| e^{L_f t} + \frac{\|g_0\|_{\gamma^+}^+ e^{(\gamma^+ - a^+)t}}{\gamma^+ - a^+ - L_f}.$$

Now, multiply both sides of this inequality by $e^{(a^+ - \gamma^+)t}$ to get

$$\|\nu(t)\| e^{-\gamma^+ t} \leq \|\zeta\| e^{-(\gamma^+ - a^+ - L_f)t} + \frac{\|g_0\|_{\gamma^+}^+}{\gamma^+ - a^+ - L_f} \leq \|\zeta\| + \frac{\|f^{-,+}(u^{++})\|_{\gamma^+}^+}{\gamma^+ - a^+ - L_f} \quad (3.13)$$

for all $t \geq 0$. Now, if we assume ν_1 and ν_2 are both solutions of (3.11), and μ_1 and μ_2 are both solutions of (3.12), then $\nu = \nu_1 - \nu_2$ solves the differential equation

$$\dot{u}^{-,+} = A^{-,+} u^{-,+} + f^{-,+}(u^{-,+} + \nu_2 + \mu_1) + f^{-,+}(\nu_2 + \mu_2).$$

Following the same steps used to find the bound on $\|\nu(t)\| e^{-\gamma^+ t}$, we obtain

$$\|\nu_1(t) - \nu_2(t)\|_{\gamma^+}^+ \leq \|\zeta_1 - \zeta_2\| + \frac{L_f}{\gamma^+ - a^+ - L_f} \|\mu_1(t) - \mu_2(t)\|_{\gamma^+}^+ \quad (3.14)$$

Next, consider the differential equation

$$\dot{u}^{++} = A^{++} u^{++} + \tilde{g}_0 \quad (3.15)$$

for $t \geq 0$, where

$$\tilde{g}_0(t) = f^{++}(\nu_1(t) + \mu_1(t)) - f^{++}(\nu_2(t) + \mu_2(t)).$$

Since

$$\|\tilde{g}_0\|_{\gamma^+}^+ \leq L_f \|\nu_1(t) - \nu_2(t)\|_{\gamma^+}^+ + L_f \|\mu_1(t) - \mu_2(t)\|_{\gamma^+}^+,$$

using the estimate in (3.14), gives

$$\|\tilde{g}_0\|_{\gamma^+}^+ \leq L_f \|\zeta_1 - \zeta_2\| + \frac{L_f(\gamma^+ - a^+)}{\gamma^+ - a^+ - L_f} \|\mu_1(t) - \mu_2(t)\|_{\gamma^+}^+. \quad (3.16)$$

Now assume

$$\mu(t) = - \int_t^\infty S^{++}(t-s)\tilde{g}_0(s)ds.$$

In order to show that this representation of $\mu(t)$ is a solution of (3.15), let $t_0 < t$ giving the identity

$$\int_{t_0}^t A^{++}\mu(s) + \tilde{g}_0(s)ds = - \int_{t_0}^t \int_s^\infty A^{++}S^{++}(s-\sigma)\tilde{g}_0(\sigma)d\sigma ds + \int_{t_0}^t \tilde{g}_0(s)ds. \quad (3.17)$$

Following the procedure used in the proof of Lemma 3.4, we have

$$\|A^{++}S^{++}(s-\sigma)\tilde{g}_0(\sigma)\| \leq \|A^{++}\| M e^{b^+s} e^{(b^+-\gamma^+)\sigma},$$

where $M < \infty$ and depends on L_f , $\|\nu_i\|$, and $\|\mu_i\|$ for $i = 1, 2$. Thus, we can apply Fubini's theorem to the double integral in (3.17) along with

$$\mathcal{H}(s, \sigma) = A^{++}S^{++}(s-\sigma)\tilde{g}_0(\sigma)$$

to get

$$\int_{t_0}^t \int_s^\infty \mathcal{H}(s, \sigma)d\sigma ds = \int_{t_0}^t \int_s^t \mathcal{H}(s, \sigma)d\sigma ds + \int_{t_0}^t \int_t^\infty \mathcal{H}(s, \sigma)d\sigma ds.$$

Changing the order of integration on the right hand side gives

$$\begin{aligned} \int_{t_0}^t \int_s^\infty \mathcal{H}(s, \sigma)d\sigma ds &= \int_{t_0}^t \int_{t_0}^\sigma \mathcal{H}(s, \sigma)ds d\sigma + \int_t^\infty \int_{t_0}^t \mathcal{H}(s, \sigma)ds d\sigma \\ &= \int_{t_0}^t [S^{++}(\sigma - \sigma)\tilde{g}_0(\sigma) - S^{-++}(t_0 - \sigma)\tilde{g}_0(\sigma)] d\sigma \end{aligned}$$

$$+ \int_t^\infty [S^{++}(t-\sigma)\tilde{g}_0(\sigma) - S^{++}(t_0-\sigma)\tilde{g}_0(\sigma)] d\sigma.$$

This implies

$$\int_{t_0}^t \int_s^\infty \mathcal{H}(s, \sigma) d\sigma ds = \mu(t) - \mu(t_0) - \int_{t_0}^t \tilde{g}_0(s) ds,$$

which gives

$$\mu(t) - \mu(t_0) = - \int_{t_0}^t A^{++} \mu(s) + \tilde{g}_0(s) ds,$$

and $\mu(t)$ is a solution of (3.15). Hence,

$$\begin{aligned} \|\mu(t)\|e^{-\gamma^+ t} &\leq e^{-\gamma^+ t} \int_t^\infty \|S^{++}(t-s)\tilde{g}_0(s)\| ds \\ &\leq e^{-\gamma^+ t} \int_t^\infty \|\tilde{g}_0(s)\| e^{b^+(t-s)} ds \\ &\leq e^{(b^+-\gamma^+)t} \|\tilde{g}_0\|_{\gamma^+}^+ \int_t^\infty e^{(\gamma^+-b^+)s} ds, \end{aligned}$$

and since $\gamma^+ < b^+$ we get

$$\|\mu(t)\|e^{-\gamma^+ t} \leq \frac{e^{(b^+-\gamma^+)t}}{\gamma^+ - b^+} \|\tilde{g}_0\|_{\gamma^+}^+ (-e^{(\gamma^+-b^+)t}) = \frac{1}{b^+ - \gamma^+} \|\tilde{g}_0\|_{\gamma^+}^+.$$

Now using (3.16) yields

$$\|\mu(t)\|_{\gamma^+}^+ \leq \frac{L_f}{b^+ - \gamma^+} \|\zeta_1 - \zeta_2\| + \frac{L_f(\gamma^+ - a^+)}{(b^+ - \gamma^+)(\gamma^+ - a^+ - L_f)} \|\mu(t)\|_{\gamma^+}^+,$$

where we have set $\mu(t) = \mu_1(t) - \mu_2(t)$. If we define $\delta = (b^+ - a^+)/2$, then we have $\gamma^+ - a^+ = \delta$ and $b^+ - \gamma^+ = \delta$, because $\gamma^+ = (b^+ + a^+)/2$. This allows us to write

$$\|\mu(t)\|_{\gamma^+}^+ \leq \frac{L_f}{\delta} \|\zeta_1 - \zeta_2\| + \frac{L_f}{\delta - L_f} \|\mu(t)\|_{\gamma^+}^+,$$

which is equivalent to

$$\|\mu(t)\|_{\gamma^+}^+ \leq \frac{L_f(\delta - L_f)}{\delta(\delta - 2L_f)} \|\zeta_1 - \zeta_2\|. \quad (3.18)$$

We want to show that there exists a globally Lipschitz continuous mapping $h_{\mathcal{R}} : Y_{\epsilon}^- \oplus Y_{\epsilon}^+ \rightarrow Y_{\epsilon}^{++}$ such that the graph of $h_{\mathcal{R}}$, denoted by \mathcal{R} , is an invariant manifold containing all solutions of the system given by (3.11)-(3.12). To this end let

$$\mathcal{R} := \{(\zeta, \eta) : \|\vartheta(t, \zeta, \eta)\|_{\gamma^+}^+ \leq M, \forall t \geq 0\} \quad (3.19)$$

where $0 < M \in \mathbb{R}$. By definition, \mathcal{R} is an invariant manifold if $(\zeta, \eta) \in \mathcal{R}$ for $\zeta \in Y_{\epsilon}^- \oplus Y_{\epsilon}^+$ and $\eta \in Y_{\epsilon}^{++}$ implies $\vartheta(t, \zeta, \eta) \in \mathcal{R}$, where

$$\vartheta(t, \zeta, \eta) := (\vartheta_1(t, \zeta, \eta), \vartheta_2(t, \zeta, \eta))$$

is the general solution or cocycle of the system (3.11)- (3.12) for all $t \in \mathbb{R}$. Now suppose $(\zeta, \eta) \in \mathcal{R}$, and notice that (3.18) implies

$$\|\vartheta_2(t, \zeta, \eta)\|_{\gamma^+}^+ \leq \frac{L_f(\delta - L_f)}{\delta(\delta - 2L_f)} \|\zeta_1 - \zeta_2\|, \quad (3.20)$$

and using (3.13)

$$\|\vartheta_1(t, \zeta, \eta)\|_{\gamma^+}^+ \leq \|\zeta\| + \frac{L_f (\|\vartheta_2(t, \zeta, \eta)\|_{\gamma^+}^+)}{\gamma^+ - a^+ - L_f} \leq \left(1 + \frac{L_f^2}{\delta(\delta - 2L_f)}\right) \|\zeta\|. \quad (3.21)$$

Applying the cocycle property gives

$$\vartheta_2(t, \zeta, \vartheta(t, \zeta, \eta)) = \vartheta_2(t, \zeta, \eta)$$

for all $t \in \mathbb{R}$, which implies $\vartheta(t, \zeta, \eta) \in \mathcal{R}$. Since the solution $\mu(t)$ depends on ζ , we can define $h_{\mathcal{R}}(t, \zeta) = \mu(t)$, and the cocycle property gives $\vartheta(t, \zeta, h_{\mathcal{R}}(t, \zeta)) = \mu(t)$. Thus,

$$\|h_{\mathcal{R}}(t, \zeta_1) - h_{\mathcal{R}}(t, \zeta_2)\| \leq \frac{L_f(\delta - L_f)}{\delta(\delta - 2L_f)} \|\zeta_1 - \zeta_2\|,$$

and this completes the proof of part 1 because

$$\frac{L_f(\delta - L_f)}{\delta(\delta - 2L_f)} = \frac{2L_f}{b^+ - a^+} \left(\frac{b^+ - a^+ - 2L_f}{b^+ - a^+ - 4L_f} \right) \leq \frac{3L_f}{b^+ - a^+}.$$

The proof of part 2 follows from arguments similar to those used in Lemma 2.3 and Theorem 2.2 in [42]. To begin this proof, notice that, due to the construction of the system given by (3.11)-(3.12), we can follow the same procedure used to prove the existence of \mathcal{R} , to show that there exists an invariant manifold \mathcal{S} that contains all solutions of the system, and is the graph of a globally Lipschitz continuous mapping $h_{\mathcal{S}} : X_{\epsilon}^{++} \rightarrow X_{\epsilon}^{-} \oplus X_{\epsilon}^{+}$ whose global Lipschitz constant is again bounded above by $3L_f/(b^+ - a^+)$, cf. [3]. Now, let $\eta \in X_{\epsilon}^{++}$ and define a new mapping

$$T_{\chi} : X_{\epsilon}^{++} \ni \eta \mapsto h_{\mathcal{R}}(h_{\mathcal{S}}(\eta)) \in X_{\epsilon}^{++},$$

where $\chi \in X_{\epsilon}^{-} \oplus X_{\epsilon}^{+} \oplus X_{\epsilon}^{++}$. Then by Lemma 3.5 part 1

$$\|T_{\chi}(\eta_1) - T_{\chi}(\eta_2)\| \leq \frac{3L_f}{b^+ - a^+} \|h_{\mathcal{S}}(\eta_1) - h_{\mathcal{S}}(\eta_2)\| \leq \left(\frac{3L_f}{b^+ - a^+} \right)^2 \|\eta_1 - \eta_2\|,$$

and, since $3L_f/(b^+ - a^+) \leq 3/8 < 1$, T_{χ} is a contraction on X_{ϵ}^{++} . Using Banach's fixed point theorem, this implies T_{χ} has a unique fixed point $P(\chi) \in X_{\epsilon}^{++}$, and we

know that $P(\chi)$ is a fixed point of T_χ if and only if

$$P(\chi) = h_{\mathcal{R}}(h_{\mathcal{S}}(P(\chi)))$$

which is equivalent to

$$(P(\chi), h_{\mathcal{S}}(P(\chi))) \in \mathcal{R}.$$

Thus, if we let $\tilde{P}(\chi) = (P(\chi), h_{\mathcal{S}}(P(\chi)))$ and define an operator

$$\mathcal{E} : X_\epsilon^- \oplus X_\epsilon^+ \oplus X_\epsilon^{++} \ni u \mapsto \tilde{P}(u) \in \mathcal{R},$$

then clearly each $\mathcal{E}(u)$ is the graph of a globally Lipschitz continuous mapping $h_{\mathcal{E}(u)} : X_\epsilon^- \oplus X_\epsilon^+ \rightarrow X_\epsilon^{++}$ whose Lipschitz constant is bounded above by $3L_f/(b^+ - a^+)$. This implies the desired result for part 2.

For the proof of part 3, we use Corollary 4.3 of Aulbach and Wanner [3]. First, notice from the arguments above that $\mathcal{E}(u)$ is a solution of (3.11)-(3.12), which is contained in the invariant manifold \mathcal{R} , if $u \in \mathcal{R}$. Along with the definition of \mathcal{R} in (3.19), this implies $u - \mathcal{E}(u)$ is contained in \mathcal{R} , since

$$\|u - \mathcal{E}(u)\|_{\gamma^+}^+ \leq \|u\|_{\gamma^+}^+ + \|\mathcal{E}(u)\|_{\gamma^+}^+ \leq 2M.$$

Now, assume $\omega(t)$ is a solution of (3.11), (3.12), where $\omega_1(t)$ solves (3.11) and $\omega_2(t)$ solves (3.12) with $\omega(t) = \omega_1(t) + \omega_2(t)$. Then we can use (3.21) and (3.20) to get the estimates

$$\|\omega_1(t)\| \leq \left(1 + \frac{L_f^2}{\delta(\delta - 2L_f)}\right) \|\omega_1(0)\| e^{\gamma^+ t}$$

and

$$\|\omega_2(t)\| \leq \frac{L_f(\delta - L_f)}{\delta(\delta - 2L_f)} \|\omega_1(0)\| e^{\gamma t}$$

for all $t \geq 0$, which implies

$$\|\omega(t)\| \leq \|\omega_1(t)\| + \|\omega_2(t)\| \leq \frac{\delta - L_f}{\delta - 2L_f} \|\omega_1(0)\| e^{\gamma t}.$$

Notice here that we can write ω as a two-dimensional vector with components ω_1 and ω_2 . Thus, by equivalence of norms,

$$\|\omega_1(t)\| + \|\omega_2(t)\| \leq \sqrt{2} \|\omega(t)\|, \quad (3.22)$$

and consequently

$$\|\omega(t)\| \leq \sqrt{2} \frac{\delta - L_f}{\delta - 2L_f} \|\omega(0)\| e^{\gamma t}.$$

Setting $\omega(t) = u(t) - \mathcal{E}(u(t))$ gives the desired result, because

$$\frac{\delta - L_f}{\delta - 2L_f} = \frac{b^+ - a^+ - 2L_f}{b^+ - a^+ - 4L_f} \leq \frac{3}{2}.$$

The proof of part 4, follows from the arguments in the proof of Lemma 2.5(d) of Maier-Paape and Wanner [26]. Lemma 3.5 part 1 says that $\mathcal{E}(u)$ is an element of the set \mathcal{C} , where we define

$$\mathcal{C} := \left\{ w^{++} + w^{-,+} : \|w^{++} - h_{\mathcal{R}}(u^{-,+})\| \leq \frac{3L_f}{b^+ - a^+} \|w^{-,+} - u^{-,+}\| \right\}.$$

For ease of discussion, let $\mathcal{E}(u) = w$. First, we want to minimize the distance $\|u - w\|$. Since $w \in \mathcal{C}$, we have

$$\|w^{++} - h_{\mathcal{R}}(u^{-,+})\| \leq \frac{3L_f}{b^+ - a^+} \|w^{-,+} - u^{-,+}\|, \quad (3.23)$$

and by adding $\|u^{++} - w^{++}\|$ to both sides we get

$$\|u^{++} - h_{\mathcal{R}}(u^{-,+})\| \leq \frac{3L_f}{b^+ - a^+} \|w^{-,+} - u^{-,+}\| + \|u^{++} - w^{++}\|,$$

then, using the fact that $3L_f/(b^+ - a^+) < 1$, gives

$$\|u^{++} - h_{\mathcal{R}}(u^{-,+})\| \leq \|w^{-,+} - u^{-,+}\| + \|u^{++} - w^{++}\|.$$

Finally, (3.22) implies

$$\|u^{++} - h_{\mathcal{R}}(u^{-,+})\| \leq \sqrt{2}\|u - w\|,$$

which gives the desired lower bound. Then, according to [26], a similar procedure can be followed to obtain the desired upper bound, and this completes the proof of the lemma. \diamond

Using Lemmas 3.4 and 3.5, we derive a result similar to Propositions 2.1 and 2.2, but our result this time is relative to the invariant manifold \mathcal{R} . This result is given by the following proposition, and is based on Proposition 2.6 in [26].

Proposition 3.1 *Consider (3.7) and let $L_f \leq C^+$ where C^+ is given by (3.5) for any positive constant σ . Suppose that $\|u_0^{+,++}\| \leq \sigma\|u_0^-\|$ for $u_0 = u_0^- + u_0^+ + u_0^{++} \in Y_\epsilon^- \oplus Y_\epsilon^+ \oplus Y_\epsilon^{++}$ and $u_0^- \neq 0$, and let $u(t)$ be the solution of (3.7) corresponding to*

this initial condition. Then we have

$$\|u^{++}(t) - h_{\mathcal{R}}(u^{-,+}(t))\| \leq \frac{6\|u_0\| \cdot \|u^-(t)\|^\gamma}{\|u_0^-\|^\gamma}$$

for all $t \leq 0$.

Proof: Recall from Lemma 3.5 part 3 that

$$\|u(t) - \mathcal{E}(u(t))\| \leq \frac{3}{2}\|u(0) - \mathcal{E}(u(0))\|e^{\gamma^+t},$$

and by Lemma 3.4 we have

$$\|u^-(t)\| \geq \|u_0^-\|e^{\gamma^-t},$$

which can also be written as

$$\frac{\|u^-(t)\|^\gamma}{\|u_0^-\|^\gamma} \geq e^{\gamma^+t},$$

where $\gamma = \gamma^+/\gamma^-$. This implies

$$\|u(t) - \mathcal{E}(u(t))\| \leq \frac{3}{2} \frac{\|u(0) - \mathcal{E}(u(0))\|}{\|u_0^-\|^\gamma} \|u^-(t)\|^\gamma,$$

for all $t \leq 0$. Now, from Lemma 3.5 part 4, we have

$$\|u^{++} - h_{\mathcal{R}}(u^{-,+})\| \leq \sqrt{2}\|u - \mathcal{E}(u)\| \leq 2\sqrt{2}\|u\|,$$

which implies the final result and completes the proof of the proposition. \diamond

3.2.2 Probability Estimates for the Nonlinear Equation

This leads us to the main result of this section, the probability estimate. We use the same idea of Lebesgue measure that we used in subsection 2.2.2. In addition, we

will also use the same definitions of the sets M_r , G_r and B_r , and show the validity of the estimate (2.23). The following theorem implies this result, and is based on Theorem 2.8 of [26].

Theorem 3.1 *Consider equation (3.7), let C_* , and R , be positive constants with $0 < \varrho < R$, define σ by (3.8), and let*

$$M_* := \min \left\{ \frac{1}{1 + 2C_*}, \left(\int_0^1 (1 - s^2)^{C_*/2} ds \right)^2 \right\} < 1.$$

In addition, suppose that

$$\dim Y_\epsilon^- \leq C_* \cdot \dim Y_\epsilon^{++},$$

let L_f be given as in (3.5), and let r be any number such that

$$0 < \frac{r}{R} \leq 6^{-1/(\gamma-1)} \cdot \left(\frac{\varrho}{R} \right)^{\gamma/(\gamma-1)} \cdot M_*^{1/(\gamma-1)} < \frac{\varrho}{R} < 1.$$

Define M_r to be the set of all initial conditions $u_0 \in Y_\epsilon^- \oplus Y_\epsilon^+ \oplus Y_\epsilon^{++}$ satisfying $\|u_0\| < r$ such that, for the corresponding solution of (3.7) given by $u(t)$, we have one of the following statements satisfied.

1. *If $B_R(0) = \{u \in Y_\epsilon^- \oplus Y_\epsilon^+ \oplus Y_\epsilon^{++} : \|u\| < R\}$, then the solution $u(t) \in B_R(0)$ for all $t \geq 0$.*
2. *There exists a time $t^* > 0$ such that $\|u(t^*)\| = R$ and $\|u^-(t^*)\| \geq \varrho$. In other words, the norm of the Y_ϵ^- -component of u is at least ϱ when the orbit leaves B_R .*

Then we have the estimate

$$\frac{\Upsilon(M_r)}{\Upsilon(B_r(0))} \leq \sqrt{6} \left(\frac{\varrho}{R} \right)^{\frac{-\gamma}{2}} \cdot \left(\frac{r}{R} \right)^{\frac{\gamma-1}{2}}$$

for $r \leq r_0(\rho, R, \gamma, p)$, where $\Upsilon(\cdot)$ is the standard Lebesgue measure on $Y_\epsilon^- \oplus Y_\epsilon^+ \oplus Y_\epsilon^{++}$.

Proof: First define the set

$$\tilde{M}_r = \left\{ u \in B_r(0) : \|u^{++} - h_{\mathcal{R}}(u^{-,+})\| \leq \frac{6R}{\varrho^\gamma} \|u^-(t)\|^\gamma \right\},$$

and let w_0 be an arbitrary element of M_r . Assume that w is the forward orbit associated with w_0 , and that $w \in B_R(0)$. Then, according to Lemma 3.5, w is an element of the invariant manifold \mathcal{R} , and we have $w_0 \in \tilde{M}_r$.

Now assume the second case in which the norm of the Y_ϵ^- -component of u is at least ϱ when the orbit leaves B_R . Then $\|w(t^*)\| = R$ and $\|w^-(t^*)\| \geq \varrho$. If we let $u_0 = w(t^*)$ and $t = -t^*$ in Proposition 3.1, then we get

$$\|w_0^{++} - h_{\mathcal{R}}(w_0^{-,+})\| \leq \frac{6\|w(t^*)\| \cdot \|w_0^-\|^\gamma}{\|w^-(t^*)\|^\gamma} \leq \frac{6R}{\varrho^\gamma} \|w_0^-\|^\gamma.$$

Therefore, $M_r \subset \tilde{M}_r$, and if we apply Fubini's theorem, then we get

$$\Upsilon(\tilde{M}_r) \leq \Upsilon \left\{ u \in B_r(0) : \|u^{++}\| \leq \frac{6R}{\varrho^\gamma} \|u^-\|^\gamma \right\}.$$

Now, apply Theorem 2.1 with $\gamma = 1/\eta$ and $6R\varrho^{-\gamma} = \beta^{-\gamma}$ to get the estimate

$$\left(\frac{\Upsilon(M_r)}{\Upsilon(B_r(0))} \right)^2 \leq 6R\varrho^{-\gamma} r^{\gamma-1} = 6 \left(\frac{\varrho}{R} \right)^{-\gamma} \left(\frac{r}{R} \right)^{\gamma-1},$$

and this proves the theorem. \diamond

Now consider the case when we include the Y_ϵ^{--} space with $\gamma^{--} \sim -1$. Then we must consider a system of equations similar to that in (3.7), which is given by

$$\dot{u}^{--} = A^{--}u^{--} + f^{--}(u^{--} + u^- + u^+ + u^{++}),$$

$$\dot{u}^- = A^-u^- + f^-(u^{--} + u^- + u^+ + u^{++}),$$

$$\dot{u}^+ = A^+u^+ + f^+(u^{--} + u^- + u^+ + u^{++}),$$

$$\dot{u}^{++} = A^{++}u^{++} + f^{++}(u^{--} + u^- + u^+ + u^{++}),$$

where $f = f^{--} \oplus f^- \oplus f^+ \oplus f^{++}$ is given by the mapping

$$f : Y_\epsilon^{--} \oplus Y_\epsilon^- \oplus Y_\epsilon^+ \oplus Y_\epsilon^{++} \rightarrow Y_\epsilon^{--} \oplus Y_\epsilon^- \oplus Y_\epsilon^+ \oplus Y_\epsilon^{++}.$$

Since Y_ϵ^{--} is a finite dimensional subspace of Y , the results of Lemma 3.5 follow for the equation given in (2.14) just as they did before. Therefore, we can also apply Theorem 3.1 to this system of equations acting on the space $Y_\epsilon^{--} \oplus Y_\epsilon^- \oplus Y_\epsilon^+ \oplus Y_\epsilon^{++}$, and we have the same probability estimate as before.

Chapter 4

TIME STEPPING SCHEMES

The purpose of this chapter is to discuss a complete discretization of the Cahn-Hilliard equation. In other words, we will look at time discretizations along with the spatial discretization discussed in the previous chapters. In particular, we will examine two numerical methods used to solve the problem. The first method discussed uses the well known Crank-Nicolson scheme for the time discretization, and solves the resulting nonlinear system using Newton's method. The second method discussed, which we will refer to as Eyre's method, was first presented by Eyre in [16] and [17]. In both methods, the spatial discretization will be the standard central difference approximation to the Laplacian operator.

Before proceeding to the presentation of these two methods, we must first introduce the notation that will be used throughout this chapter. Using the notation established in (2.8), let $U_i^{\hat{m}} \approx u(x_i, t_{\hat{m}})$ where \hat{m} makes reference to a specific time. Similarly, we can define $U_{i,j}^{\hat{m}} \approx u(x_i, y_j, t_{\hat{m}})$, and $U_{i,j,k}^{\hat{m}} \approx u(x_i, y_j, z_k, t_{\hat{m}})$, for the two and three-dimensional cases, respectively. Hence, if we ignore the superscript on U for now, then the spatially discrete Laplacian operator for one dimension can be written as

$$\Delta_n U_i = U_{i+1} + U_{i-1} - 2U_i. \quad (4.1)$$

Likewise, we have

$$\Delta_n U_{i,j} = U_{i+1,j} + U_{i-1,j} + U_{i,j+1} + U_{i,j-1} - 4U_{i,j},$$

and

$$\Delta_n U_{i,j,k} = U_{i+1,j,k} + U_{i-1,j,k} + U_{i,j+1,k} + U_{i,j-1,k} + U_{i,j,k+1} + U_{i,j,k-1} - 6U_{i,j,k}$$

for the two and three-dimensional cases, respectively.

For the sake of simplicity, we will only consider the one-dimensional case in this chapter, but, using the above discretizations, equivalent results will hold for the two and three-dimensional cases. This is an important note because in our implementation of these methods, in Chapter 5, we will consider only the two-dimensional case.

4.1 The Cahn-Hilliard Equation as a Gradient System

A gradient system is a system of real ordinary differential equations, given by

$$\frac{du}{dt} = -\nabla F(u) \tag{4.2}$$

$$u(0) = u_0,$$

where ∇F denotes the gradient of F , and F satisfies the restrictions

1. $F(u) \geq 0$, for all $u \in \mathbb{R}^n$, and
2. $F(u) \rightarrow \infty$ as $\|u\| \rightarrow \infty$.

Furthermore, for all gradient systems, we have the property

$$\frac{d}{dt}F(u) = \langle \nabla F(u), u_t \rangle = -\|u_t\|^2,$$

cf. [39]. Hence, we have $F(u(t)) \leq F(u(0))$ for $t \geq 0$, and we can argue that u will be driven to the critical points of (4.2). Here, we define $\langle \cdot, \cdot \rangle$ to be the inner product

on \mathbb{R}^n , and $\|\cdot\|$ is the corresponding norm.

As we stated in the introduction, the Cahn-Hilliard equation was derived using the van der Waals free energy functional (1.2). Here we will show this derivation, which was taken from [20], for the spatially discrete Cahn-Hilliard equation, and consequently show that the Cahn-Hilliard equation is a gradient system. We will start by writing the van der Waals free energy functional (1.2) in spatially discrete form as

$$E(u) = \frac{1}{n\epsilon} \sum_{i=0}^n W(u_i) + \frac{n\epsilon}{2} \sum_{i=0}^{n-1} (u_{i+1} - u_i)^2,$$

where $u \in \mathbb{R}^{n+1}$. In addition, we will rewrite the spatially discrete Cahn-Hilliard equation as

$$\dot{u} = -n^2 \Delta_n \omega(u)$$

$$\omega(u) = (n\epsilon)^2 \Delta_n u - f(u),$$

which is equivalent to the system

$$\dot{u}_i = -n^2 (\omega_{i-1} - 2\omega_i + \omega_{i+1}),$$

$$\omega_i = (n\epsilon)^2 (u_{i-1} - 2u_i + u_{i+1}) - f(u_i), \tag{4.3}$$

for $i = 0, \dots, n$, with the boundary conditions

$$u_{-1} = u_0, u_n = u_{n+1}, \omega_{-1} = \omega_0, \omega_n = \omega_{n+1}.$$

Now let ϖ be an $(n+1)$ -dimensional vector with $\varpi = [1, 1, \dots, 1]^T$, and let Δ_n^\dagger be the Moore-Penrose pseudo-inverse of Δ_n ; i.e.,

$$\Delta_n^\dagger = (\Delta_n^T \Delta_n)^{-1} \Delta_n^T. \quad (4.4)$$

Then we can define $\langle \cdot, \cdot \rangle_{-1}$ and $\langle \cdot, \cdot \rangle_2$ to be inner products on \mathbb{R}^{n+1} , such that, for $u, v \in \mathbb{R}^{n+1}$, we have

$$\langle u, v \rangle_2 = \frac{1}{n+1} \sum_{i=0}^n u_i v_i,$$

and

$$\langle u, v \rangle_{-1} = \langle \beta u, v \rangle_2$$

where we define the matrix β by

$$\beta = \frac{\varpi \varpi^T}{n+1} - \frac{\Delta_n^\dagger}{(n+1)^2}. \quad (4.5)$$

The proof that these are indeed inner products on \mathbb{R}^{n+1} can be found in [20].

If we let $\mu(t)$ be any curve in \mathbb{R}^{n+1} , then a short calculation gives

$$\begin{aligned} \frac{dE(\mu(t))}{dt} &= \dot{\mu}_0(t) \left[\frac{1}{n\epsilon} f(\mu_0(t)) - n\epsilon(\mu_0(t) - \mu_1(t)) \right] \\ &+ \sum_{i=1}^{n-1} \dot{\mu}_i(t) \left[\frac{1}{n\epsilon} f(\mu_i(t)) - n\epsilon(\mu_{i-1}(t) - 2\mu_i(t) + \mu_{i+1}(t)) \right] \\ &+ \dot{\mu}_n(t) \left[\frac{1}{n\epsilon} f(\mu_n(t)) - n\epsilon(\mu_{n-1}(t) - \mu_n(t)) \right]. \end{aligned}$$

Using the definition of ω given in (4.3), we can rewrite (4.6) as

$$\frac{dE(\mu(t))}{dt} = -\frac{1}{n\epsilon} \sum_{i=0}^n \omega_i \dot{\mu}_i = \frac{n+1}{n\epsilon} \langle \omega(\mu(t)), \dot{\mu}(t) \rangle_2.$$

If we define H^{-1} to be the Hilbert space with the inner product $\langle \cdot, \cdot \rangle_{-1}$, consisting of those elements of \mathbb{R}^{n+1} that have a mass of m_0 , then, for all $\mu(t) \in H^{-1}$, we have

$$\frac{1}{n+1} \sum_{i=0}^n \mu_i(t) = m_0$$

for all t . Differentiating this equation gives

$$\langle \varpi, \dot{\mu}(t) \rangle_2 = \frac{1}{n+1} \sum_{i=0}^n \dot{\mu}_i(t) = 0.$$

Furthermore, given the definition of Δ_n^\dagger in (4.4), we have

$$\Delta_n^\dagger \Delta_n = (\Delta_n^T \Delta_n)^{-1} (\Delta_n^T \Delta_n) = I,$$

where I is the $n \times n$ identity matrix. Thus,

$$\langle \dot{\omega}(\mu(t)), \dot{\mu}(t) \rangle_2 = \langle (-(n+1)\varpi\varpi^T + \Delta_n^\dagger) \Delta_n \omega(\mu(t)), \dot{\mu}(t) \rangle_2,$$

which gives

$$\frac{dE(\mu(t))}{dt} = \frac{(n+1)^3}{n\epsilon} \langle \beta \Delta_n \omega(\mu(t)), \dot{\mu}(t) \rangle_2 = \frac{(n+1)^3}{n\epsilon} \langle \Delta_n \omega(\mu(t)), \dot{\mu}(t) \rangle_{-1}.$$

According to Grant and Van Vleck [20], ∇G is the gradient of the function G if

$$\frac{d}{dt} G(u(t)) = \langle \nabla G, \dot{u}(t) \rangle$$

for some inner product $\langle \cdot, \cdot \rangle$. This immediately implies that ∇E is the gradient of E with respect to the inner product $\langle \cdot, \cdot \rangle_{-1}$ if we set

$$\nabla E = \frac{(n+1)^3}{n\epsilon} \Delta_n \omega(u).$$

This enables us to write the spatially discrete Cahn-Hilliard equation as a gradient system in the form

$$\dot{u} = -\frac{n^3\epsilon}{(n+1)^3} \nabla E(u) = -\nabla F(u),$$

where we let $F = (n^3\epsilon E)/(n+1)^2$.

4.2 One-Step Gradient Stable Methods

Consider the Cahn-Hilliard equation given by

$$\dot{u} = \mathcal{F}(u) \equiv -n^2 \Delta_n (n^2 \epsilon^2 \Delta_n u + f(u)). \quad (4.6)$$

Using Definition 4.3 in [39], we define gradient stability for one-step methods. To begin, one-step methods for (4.6) are time stepping schemes that do not use values of $U^{\hat{m}}$ from previous time steps, but evaluate \mathcal{F} at intermediate stages between $U^{\hat{m}}$ and $U^{\hat{m}+1}$. Thus, we can define the time step by $\tau = t_{\hat{m}+1} - t_{\hat{m}}$. It will become clear in the following sections that the schemes considered are both one-step methods.

With this in mind, a one-step numerical scheme is unconditionally gradient stable for all $\tau > 0$ and for all initial conditions, if there exists a function $F(\cdot) : \mathbb{R}^n \rightarrow \mathbb{R}$ such that the following four properties hold.

1. $F(U) \geq 0$ for all $U \in \mathbb{R}^n$
2. $F(U) \rightarrow \infty$ as $\|U\| \rightarrow \infty$

3. $F(U^{\hat{m}+1}) \leq F(U^{\hat{m}})$ for all $U^{\hat{m}} \in \mathbb{R}^n$
4. $F(U^{\hat{m}}) = F(U_0)$ for all $n \geq 0$ implies $U_0 \in \mathcal{O}$, where \mathcal{O} is the set of zeros for ∇F .

Notice that the functional F in (4.2), satisfies the first two properties of this definition. It turns out that, properties 3 and 4 are also satisfied for both of the numerical methods considered in this chapter.

4.2.1 Crank-Nicolson Method

Following the analysis in [9], we use the Crank-Nicolson method, which is a second order method in τ (cf. [28]), to discretize the Cahn-Hilliard equation, (4.6), in time. This discretization is given by

$$U^{\hat{m}+1} = U^{\hat{m}} + \frac{\tau}{2} [\mathcal{F}(U^{\hat{m}}) + \mathcal{F}(U^{\hat{m}+1})],$$

where τ is the given time step, and $\Delta_n U^{\hat{m}}$ is given by (4.1). Recall that Δ_n is the $n \times n$ tridiagonal matrix given in (2.9). Since this system is nonlinear, we use Newton's method to solve for $U^{\hat{m}+1}$. For proof that this scheme is unconditionally gradient stable see Theorem 5.6.1 of [40].

In order to implement Newton's method, let

$$G(U^{\hat{m}+1}) = U^{\hat{m}+1} - U^{\hat{m}} - \frac{\tau}{2} [\mathcal{F}(U^{\hat{m}}) + \mathcal{F}(U^{\hat{m}+1})].$$

Then we solve the system given by

$$DG(U^{\hat{m}+1,j})\delta^j = -G(U^{\hat{m}+1,j}), \quad (4.7)$$

where the extra index j refers to the number of Newton iterations for each time step. After each linear solve for the vector δ^j , $U^{\hat{m}+1}$ is updated by setting

$$U^{\hat{m}+1,j+1} = U^{\hat{m}+1,j} + \delta^j,$$

and this process is repeated until the norm of the vector G is small, relative to a tolerance that is set in Chapter 5. Then the same procedure is followed for the next time step. The matrix $DG(u)$ is the Jacobian of $G(u)$, and is given by

$$DG(U^{\hat{m}+1})\delta = \delta - \frac{\tau}{2}\mathcal{F}'(U^{\hat{m}+1})\delta,$$

where

$$\mathcal{F}'(U^{\hat{m}+1})\delta = -n^2\Delta_n \left(n^2\epsilon^2\Delta_n\delta + f'(U^{\hat{m}+1})\delta \right).$$

To get Newton's method started, we use Heun's method to derive an initial guess for each time step, cf. [18].

4.2.2 Eyre's Method

In this subsection, an unconditionally gradient stable one-step scheme for general gradient systems, given by Eyre in [17], will be presented. Consider the Cahn-Hilliard equation written as (4.2). There are two cases to be considered regarding the flow of a gradient system according to [39]. First, if

$$\langle \nabla F(u) - \nabla F(v), u - v \rangle \geq 0 \tag{4.8}$$

for all $u, v \in \mathbb{R}^n$ with $u \neq v$, then F is convex and the flow is contractive. Otherwise, if F is not convex, (4.2) may have multiple equilibria, and the flow can expand in $u(t)$.

For our purposes, we will only consider the second case, where the nature of the flow is expansive and contractive, because that is the nature of the Cahn-Hilliard equation.

We begin by writing $F(u)$ as the difference of two strictly convex functions such that

$$F(u) = F_c(u) - F_e(u) \quad (4.9)$$

with $F_c, F_e \in C^2$, and where the flow related to $-F_c$ is contractive, but the flow related to F_e is expansive. Then the numerical scheme we intend to investigate is given by

$$U^{\hat{m}+1} - U^{\hat{m}} = \tau \left[\nabla F_e(U^{\hat{m}}) - \nabla F_c(U^{\hat{m}+1}) \right], \quad (4.10)$$

where τ and $U^{\hat{m}}$ are defined as before. This numerical method for solving gradient systems is unconditionally gradient stable and has a unique solution at every time step for all $\tau > 0$ and for any initial condition. For proof of this claim, and for results on consistency and local truncation error, see Eyre [17].

Now we will apply Eyre's method for gradient systems, to the Cahn-Hilliard equation. The trick in applying this method is to find an appropriate decomposition of the function F , because the splitting given in (4.9) is not unique, but it always exists.

We choose a splitting of F such that

$$F_c = \int_0^1 \left[\frac{\epsilon^2}{2} u_x^2 + u^2 + 1 \right] dx$$

and

$$F_e = \int_0^1 \left[\frac{u^4}{4} - \frac{3u^2}{2} \right] dx,$$

in order to obtain a linear system. This splitting was used by Eyre in [17]. In order to

confirm that this decomposition satisfies the necessary requirements, we must show that the flow of the equation $\dot{u} = -\nabla F_c(u)$ is contractive, and the flow of the equation $\dot{u} = \nabla F_e(u)$ is expansive. To this end, we use (4.8) and the inner product $\langle \cdot, \cdot \rangle_{-1}$ to determine both the contractive and expansive flow, where

$$\nabla F_c(u) = -\epsilon^2 \Delta_n^2 u + 2\Delta_n u$$

and

$$\nabla F_e(u) = \Delta_n u^3 - 3\Delta_n u.$$

First, notice

$$\langle \nabla(F_c(u) - F_c(v)), u - v \rangle_{-1} = \epsilon^2 \langle \beta \Delta_n^2(u - v), u - v \rangle_2 - 2 \langle \beta \Delta_n(u - v), u - v \rangle_2, \quad (4.11)$$

where β is given in (4.5). By (4.8), the flow related to F_c is contractive if (4.11) is greater than or equal to zero. For the first term on the right hand side, we have

$$\langle \beta \Delta_n^2(u - v), u - v \rangle_2 = -\langle \Delta_n(u - v), u - v \rangle_2,$$

because $\Delta_n \varpi = 0$ and $\Delta_n^\dagger \Delta_n = I$. Recall that, by definition

$$\Delta_n(u_i - v_i) = (u_{i+1} - v_{i+1}) - 2(u_i - v_i) + (u_{i-1} - v_{i-1}),$$

and

$$\nabla(u_i - v_i) = (u_{i+1} - v_{i+1}) - (u_i - v_i).$$

Thus,

$$\langle \Delta_n(u - v), u - v \rangle_2 = \frac{1}{n+1} \sum_{i=0}^n [(u_{i+1} - v_{i+1}) - 2(u_i - v_i) + (u_{i-1} - v_{i-1})] (u_i - v_i),$$

and

$$\|\nabla(u - v)\|_2^2 = \frac{1}{n+1} \sum_{i=0}^n [(u_{i+1} - v_{i+1})^2 - 2(u_i - v_i)(u_{i+1} - v_{i+1}) + (u_i - v_i)^2].$$

Expanding these two sums and using the given boundary conditions, shows that

$$-\langle \Delta_n(u - v), u - v \rangle_2 = \|\nabla(u - v)\|_2^2 \geq 0,$$

where $\|\cdot\|_2$ is the norm induced by $\langle \cdot, \cdot \rangle_2$. For the second term on the right hand side of (4.11), we have

$$-\langle \beta \Delta_n(u - v), u - v \rangle_2 = \langle (u - v), (u - v) \rangle_2 = \|(u - v)\|_2^2 \geq 0,$$

Therefore, the flow of $\dot{u} = -\nabla F_c(u)$ is contractive.

For F_e , we have

$$\langle \nabla(F_e(u) - F_e(v)), u - v \rangle_{-1} = \langle \beta \Delta_n(u^3 - v^3), u - v \rangle_2 - 3\langle \beta \Delta_n(u - v), u - v \rangle_2, \quad (4.12)$$

and, because of the sign change, this quantity is expansive if it is greater than or equal to zero. Notice that the second term on the right hand side of (4.12) is a multiple of the second term of (4.11). Hence, we only need to consider the first term on the right

hand side of (4.12). Since $\Delta_n \varpi = 0$ and $\Delta_n^\dagger \Delta_n = I$,

$$\langle \beta \Delta_n (u^3 - v^3), u - v \rangle_2 = -\langle (u^3 - v^3), u - v \rangle_2.$$

Now, notice that

$$(u^3 - v^3)(u - v) = (u^2 + uv + v^2)(u^2 - 2uv + v^2) = \frac{1}{2} [(u + v)^2 + u^2 + v^2] (u - v)^2 \geq 0,$$

but since the solutions are generally known to lie in the region $(-1, 1)$, we have

$$\langle (u - v), (u - v) \rangle_2 \geq \langle (u^3 - v^3), u - v \rangle_2.$$

Hence, the flow of $\dot{u} = \nabla F_\epsilon(u)$ is expansive.

Now, we can use this splitting to decompose the Cahn-Hilliard equation such that Eyre's method can be applied. This particular decomposition leads to the linearly stabilized splitting scheme

$$U_j^{\hat{m}+1} - U_j^{\hat{m}} = \tau [-\epsilon^2 \mathcal{D}_n^2 + 2\mathcal{D}_n] U_j^{\hat{m}+1} + \tau [\mathcal{D}_n (U_j^{\hat{m}})^2 - 3\mathcal{D}_n] U_j^{\hat{m}}, \quad (4.13)$$

where we define $\mathcal{D}_n = n^2 \Delta_n$.

Since Newton's method will converge in a single step for a linear problem, we will employ Newton's method to solve the system in (4.13). Hence, we solve the system given in (4.7) at each time step, with

$$G(U^{\hat{m}+1}) = U^{\hat{m}+1} - U^{\hat{m}} - \tau(-\epsilon^2 \mathcal{D}_n^2 + 2\mathcal{D}_n)U^{\hat{m}+1} - \tau(\mathcal{D}_n (U^{\hat{m}})^3 - 3\mathcal{D}_n U^{\hat{m}}),$$

and

$$DG(U^{\hat{m}+1,j}) = [I + \tau(\epsilon^2 \mathcal{D}_n^2 - 2\mathcal{D}_n)] U^{\hat{m}+1,j}.$$

Again, we use Heun's method to derive $U^{\hat{m}+1,0}$.

Chapter 5

NUMERICAL EXPERIMENTS AND RESULTS

Here we apply the numerical methods discussed in Chapter 4, in order to see how accurately the theoretical results derived in this paper, describe what happens in practice. Using both of these methods will give a good basis for comparison, as we make our conclusions. Overall, these numerical results give a more complete understanding of how and when spinodal decomposition takes place for the spatially discrete Cahn-Hilliard equation.

In addition, we will compare these two methods using the numerical results obtained from the implementation of each method. We expect that the Crank-Nicolson method will offer better results, because it is solving a full nonlinear problem. However, we also expect that this method may take longer to execute as it may need to solve several linear systems at each time step using Newton's method. On the other hand, Eyre's method approximates the nonlinearity which may in turn lead to slightly less accurate results, but the time needed to execute this method is less because only one linear system is solved at each time step. In addition, the Crank-Nicolson method is second order in τ , while Eyre's method is first order. Hence, we expect Eyre's method to take more time steps than the Crank-Nicolson method in order to reach the the same final time. The performance of these methods for fixed accuracy is discussed in section 5.4.

5.1 Outline of Experimental Setup

The following numerical experiments will be done for two space dimensions only, but the same analysis can be done for one and three dimensions using the appropriate approximation for the Laplacian operator. Furthermore, the only nonlinearity considered is the standard cubic function $f(u) = u - u^3$, and all experiments are done with $n = 60$.

Notice there is a parameter on each Laplacian term of (4.6), and each of these parameters could be varied in order to explore how different values on n and ϵ effect the solution. Notice that if we multiply this equation through by h^2 , then we get

$$u_{\hat{t}} = -\Delta_n \left(n^2 \epsilon^2 \Delta_n u + f(u) \right),$$

where $\hat{t} = h^2 t$. Thus, we can consider this new equation with a different scaling of time, and vary only one parameter.

As we know, we can write a solution to the Cahn-Hilliard equation in terms of the Fourier series given by (2.16), using the normalized eigenfunctions of the Laplacian operator, that are given by $\varphi_{k,l}$ corresponding to the eigenvalues $\xi_{k,l}$ for two space dimensions. For the discrete problem we have

$$u = \sum_{k,l=1}^n \chi_{k,l} \varphi_{k,l},$$

where $\chi_{k,l} = \langle u, \varphi_{k,l} \rangle$, for the inner product

$$\langle u, v \rangle = \sum_{i,j=1}^n u_{i,j} v_{i,j}.$$

Since the $\varphi_{k,l}$ form an orthonormal basis, this immediately implies

$$\langle u, u \rangle = \sum_{k,l=1}^n \chi_{k,l}^2.$$

Now, recall that the results of Propositions 2.1 and 2.2, show that the effects of the eigenfunctions corresponding to the subspaces Y_ϵ^- and Y_ϵ^{--} , on the solution, are minimal. Hence, we should be able to describe these solutions using only the eigenfunctions corresponding to the unstable subspace $Y_\epsilon^{++} \oplus Y_\epsilon^+$. In other words, if P is the set of indices for which the eigenvalues are positive, we have

$$u = \sum_{k,l \in P} \chi_{k,l} \varphi_{k,l},$$

when spinodal decomposition takes place. Thus, using a numerical approximation of u , we get

$$0 \ll \frac{\sum_{(k,l) \in P} \langle u, \varphi_{k,l} \rangle^2}{\sum_{i,j=1}^n u_{i,j} u_{i,j}} \leq 1, \quad (5.1)$$

whenever spinodal decomposition takes place. Computation of this ratio will provide insight into several different things as we study the results.

In the following, we consider the results of three sets of numerical experiments that were performed for each method. In the first set, we take into account various values for the concentration given in the preceding discussion by the value m . In doing this, we can check the importance of having a concentration inside the spinodal interval. The second set gives attention to the size of perturbation $\bar{\rho}$ from a given concentration for the initial condition. Recall from Propositions 1 and 2 that we set a bound on the radius of the ball that initial conditions start in, by

$$r < \left(\varrho R^{-\gamma^{--}} \right)^{1/(1-\gamma^{--})}, \quad (5.2)$$

where ϱ depends on how far the orbit can be from the dominating subspace upon exiting $B_R(0)$, and R will depend on the time. These experiments will provide a better understanding of how well this derived estimate models the way solutions behave. Finally, the last set is intended to explore the relationship between n and ϵ . Recall that the previous discussion required $n \sim 1/\epsilon$ or $n \geq c/\epsilon$ in order to get results that model the actual behavior of the PDE. Since we have set n to a value of 60 in our analysis, we will consider different values of ϵ by varying the parameter $(\epsilon n)^2$. Clearly, computation of the ratio given in (5.1) will be helpful for analyzing each of the different aspects of the problem.

The initial conditions used for each experiment will depend on the values chosen for m and $\bar{\rho}$. The values of the initial vector u_0 are set to random numbers between $m + \bar{\rho}$ and $m - \bar{\rho}$. In addition, the only boundary conditions considered are the Neumann boundary conditions used throughout the paper.

In the implementation of each scheme, we do one full step and two half steps for each time step in order to estimate the local error. For the Crank-Nicolson method, we can write

$$u = u_{ex} + O(\tau^2) = u_{ex} + c\tau^2 \quad (5.3)$$

because this is a second order method (cf. [28]). Here, u is the approximate solution and u_{ex} is the exact solution. Thus, if u_1 takes two steps of size $\tau/2$, and u_2 takes one step of size τ , then we have $u_1 = u_{ex} + c(\tau/2)^2$ and $u_2 = u_{ex} + c\tau^2$, which implies

$$\frac{4(u_2 - u_1)}{3} = \frac{(c - 4c)\tau^2}{3} = -c\tau^2.$$

Eyre's method, on the other hand, is a first order method with

$$u = u_{ex} + O(\tau) = u_{ex} + c\tau \quad (5.4)$$

(cf. [17]), and we have $u_1 = u_{ex} + c(\tau/2)$ and $u_2 = u_{ex} + c\tau$ which gives

$$2(u_2 - u_1) = 2c\tau - c\tau = c\tau.$$

Finding a value for c , determines the local error. Then if the local error is greater than the tolerance 10^{-2} , we reduce the step size and start again. If the local error is less than the tolerance, we extrapolate and obtain a solution.

Conjugate gradient iterative methods (cf. [29]) for solving nonsymmetric linear systems are used at each time step for both schemes. In particular, we use the CGS method described in [35], and the CGNR method which is described in [22]. The CGS method was used as the primary solver, where CGNR was used only if CGS did not converge within the tolerance 10^{-8} . This would only occur if the norm of the right hand side was greater than 10^{-8} . If CGNR did not converge within this tolerance, then the step size was halved and the step was attempted again. We also required that Newton's method converge within a certain tolerance. If the norm of G was greater than 10^{-6} , or if the number of Newton iterates was greater than 50, then the size of the time step was reduced, and the step was attempted again.

5.2 Crank-Nicolson Method

The following contains results of the three previously described experiments performed using the Crank-Nicolson method. Each of the graphs given here is a plot of time verses the ratio given in (5.1).

5.2.1 Results for the Parameter m

Since we are only considering the nonlinearity $f(u) = u - u^3$ for the results, the spinodal interval is given by $(-1/\sqrt{3}, 1/\sqrt{3})$. Due to the symmetry of this function, we only need to perform these experiments for positive values of m . As we vary the values of m , the perturbation parameter $\tilde{\rho}$ is set to 10^{-1} , while $(\epsilon n)^2$ is set to a value of one.

Notice from Fig. 5.1 that the best results for spinodal decomposition occur for $m = .1$ and $m = 0$. As the values of m increase, we see the ratio get smaller. This is because the farther m is from zero, the farther the orbit is away from the invariant manifold upon exiting the larger neighborhood $B_R(0)$, and the less able we are to describe the orbit by the behavior on the invariant manifold where we see spinodal decomposition. Based on our analysis, this is exactly what we would expect to see. Also, since $1/\sqrt{3} \approx .577$, the ratio becomes zero for all values of m greater than this value. This is due to the fact that there are no positive eigenvalues, hence, the solution is completely described by eigenfunctions in the $Y_\epsilon^- \oplus Y_\epsilon^{--}$ subspace.

5.2.2 Results for the Perturbation from m

We notice similar results as we vary the perturbation $\tilde{\rho}$ in Fig. 5.2, and set $m = 0$ and $(n\epsilon)^2 = 1$. As the value of $\tilde{\rho}$ increases, the ratio decreases, leading to the same conclusions that were made for m . Notice, however, that the smaller $\tilde{\rho}$ is the longer the ratio stays close to one. This is what we would expect because the closer the initial condition is to the equilibrium point, the closer the corresponding orbit will be to the invariant manifold when exiting the larger ball of radius R . In addition, our analysis assumes $f'(u) \sim f'(m)$, cf. (1.1) and (2.1). However, when the perturbation is large relative to the upper bound on the spinodal interval, we can no longer make

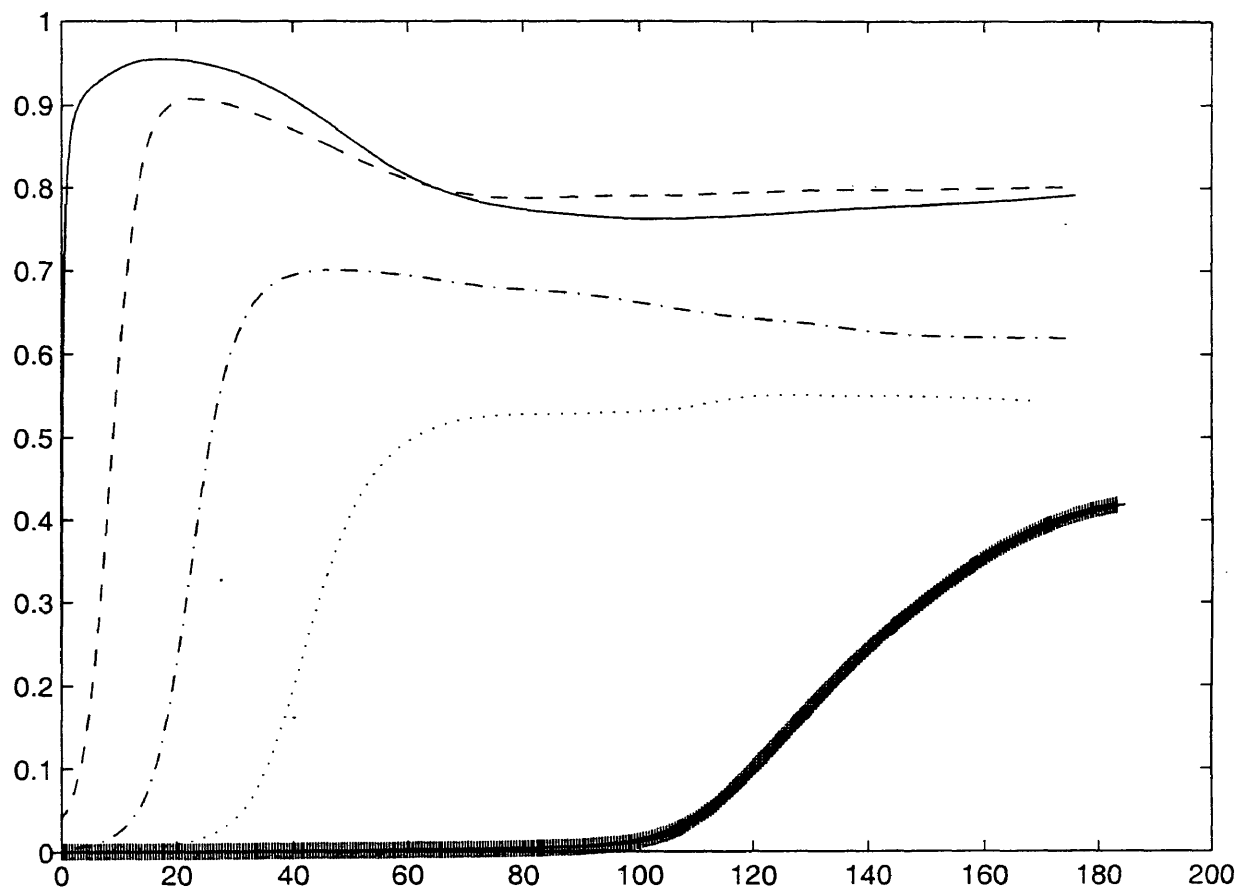


FIG. 5.1. Varying values of concentration with “-”: $m = 0$, “- -”: $m = .1$, “.-”: $m = .3$, “..”: $m = .4$, “+”: $m = .5$, where $\tilde{\rho} = 10^{-1}$ and $(\epsilon n)^2 = 1$

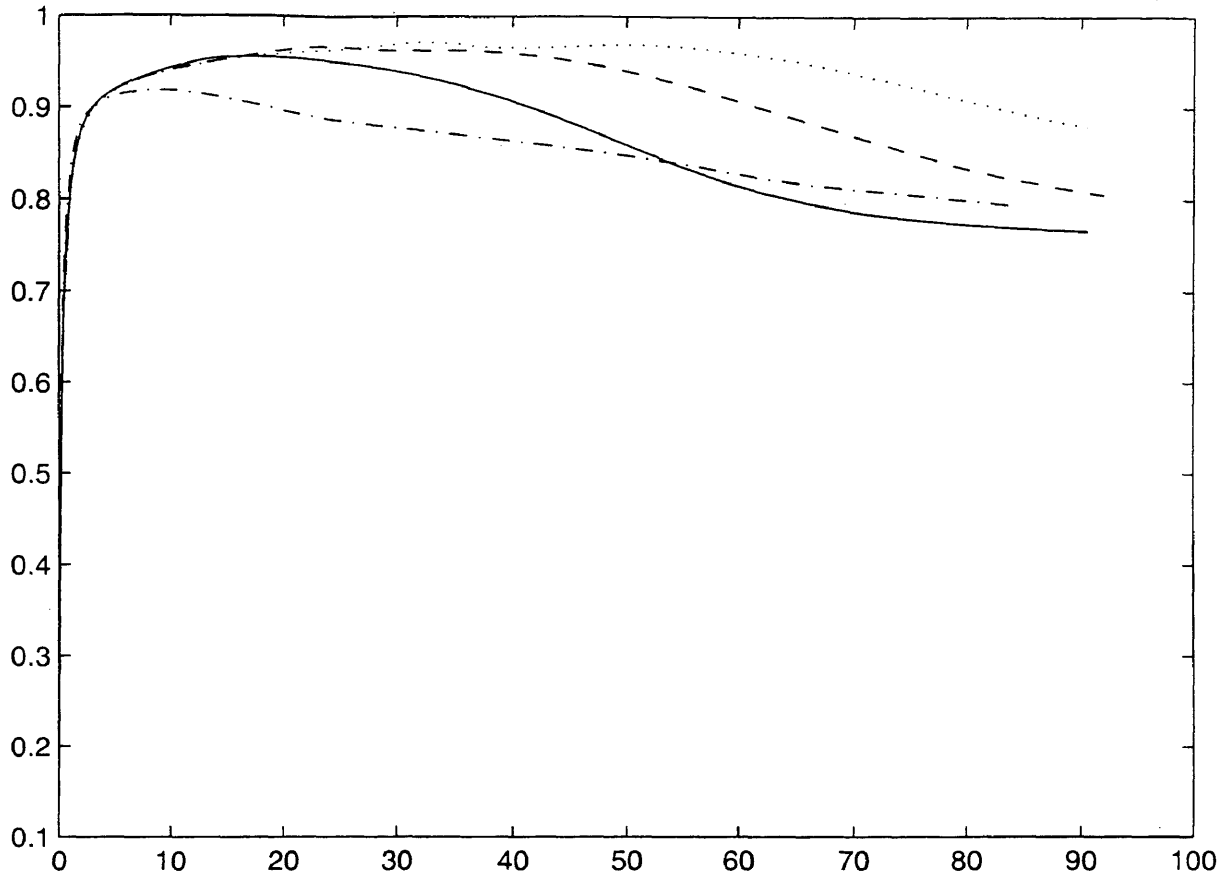


FIG. 5.2. Varying values of perturbation $\tilde{\rho}$ from the concentration with “.”: $\tilde{\rho} = 10^{-3}$, “- -”: $\tilde{\rho} = 10^{-2}$, “-·-”: $\tilde{\rho} = 10^{-1}$, “···”: $\tilde{\rho} = 1$, where $m = 0$ and $(n\epsilon)^2 = 1$

this assumption, and cannot expect our theoretical results to hold. Thus, $\tilde{\rho}$ must be small, and likewise r given by (5.2) must be small in order to get results that resemble spinodal decomposition. This can be seen as $\tilde{\rho}$ reaches a value of one, because the ratio is small and the graph is relatively flat.

5.2.3 Results for the Product $(\epsilon n)^2$

We showed in subsection 2.2.1 that we can expect to see spinodal decomposition for values of n close to $1/\epsilon$, and for $n > 1/\epsilon$. In this experiment we would like to

get an idea for how much less than $1/\epsilon$, n can be and still give good results. The parameter considered in this experiment is $(\epsilon n)^2$, hence, parameter values less than one correspond to $n < 1/\epsilon$, and parameter values greater than one correspond to $n > 1/\epsilon$. The other parameters are set with $\tilde{\rho} = 10^{-1}$ and $m = 0$.

From the plot given in Fig. 5.3 we find that for $(\epsilon n)^2 = .5$, the ratio is immediately very close to one and stays close to one for a large time. Thus, we are lead to believe that the stated bound on n could be made smaller. For the higher value $(\epsilon n)^2 = 10$, we notice that the ratio comes close to one, but takes longer to reach that point. Nevertheless, these experiments do portray what we would expect to see.

5.3 Eyre's Method

Here we present the results of the same experiments, which were done using Eyre's method. Upon observation of Fig. 5.4, Fig. 5.5, and Fig. 5.6, it becomes clear that the only notable difference between the results for each scheme is the number of time steps needed to reach a particular time, but this issue will be addressed in the discussion of our results. However, qualitatively, we note no outstanding difference, and make the same conclusions for the results obtained by way of Eyre's method as we did for the Crank-Nicolson method.

5.4 Discussion of the Numerical Results

These numerical results portray precisely what was expected given the previously established theory. As the three different parameter values were varied, we saw when spinodal decomposition takes place for the spatially discrete Cahn-Hilliard equation.

It can be seen that, on average, the ratio in each experiment reached its highest point for a relatively small time. Then the value of the ratio decreased and eventually

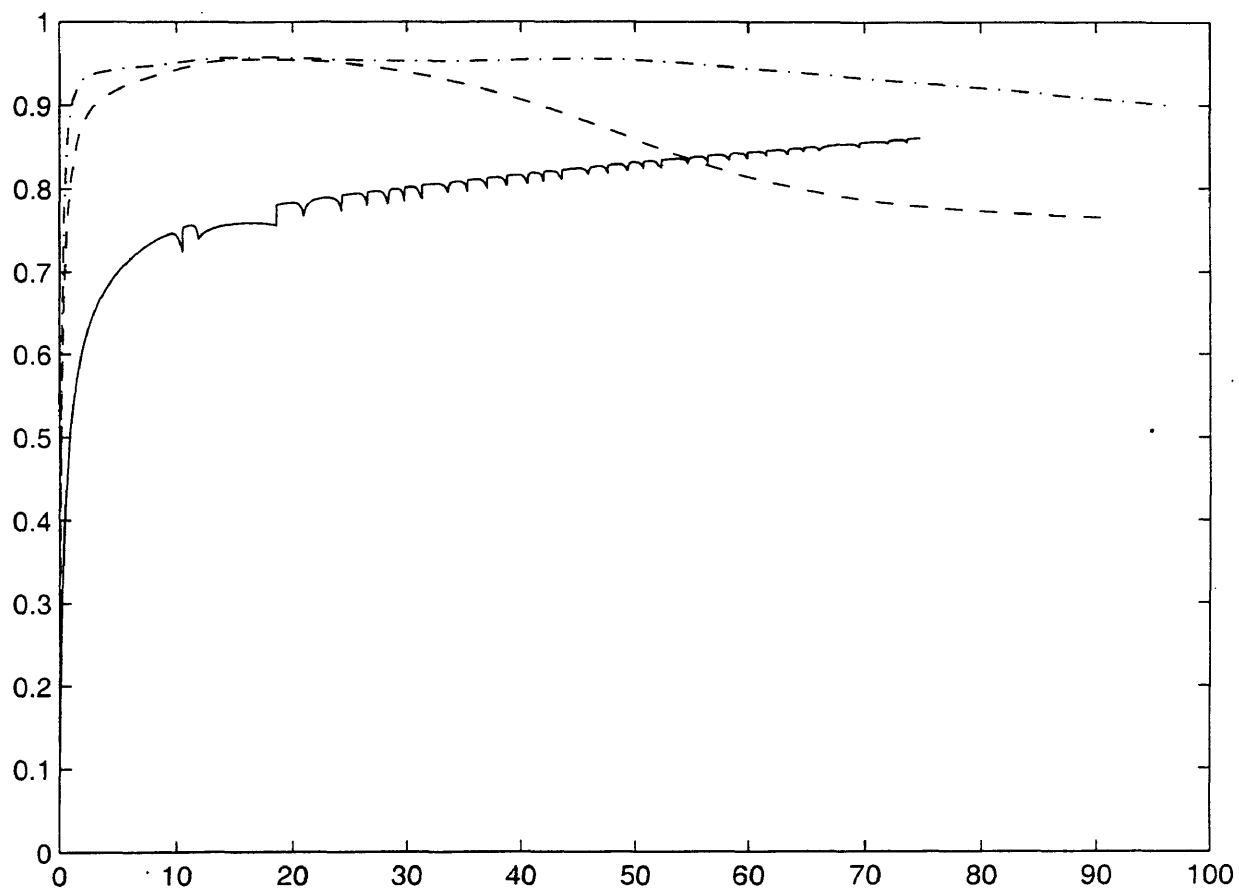


FIG. 5.3. Varying values of the product $(\epsilon n)^2$ with “-.”: $(\epsilon n)^2 = .5$, “- -”: $(\epsilon n)^2 = 1$, “_”: $(\epsilon n)^2 = 10$, where $\tilde{\rho} = 10^{-1}$ and $m = 0$

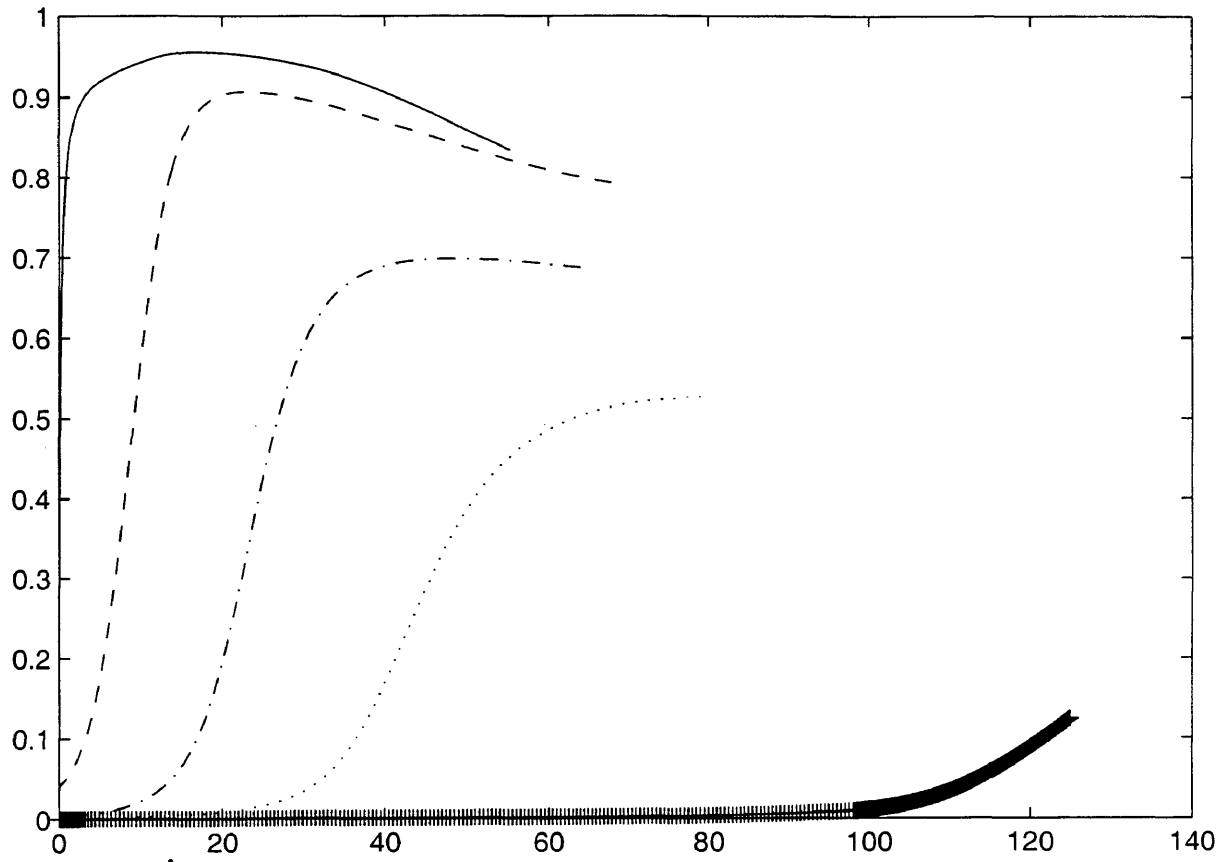


FIG. 5.4. Varying values of concentration with “-”: $m = 0$, “- -”: $m = .1$, “-.”: $m = .3$, “..”: $m = .4$, “+”: $m = .5$, where $\bar{\rho} = 10^{-1}$ and $(\dot{\epsilon}n)^2 = 1$

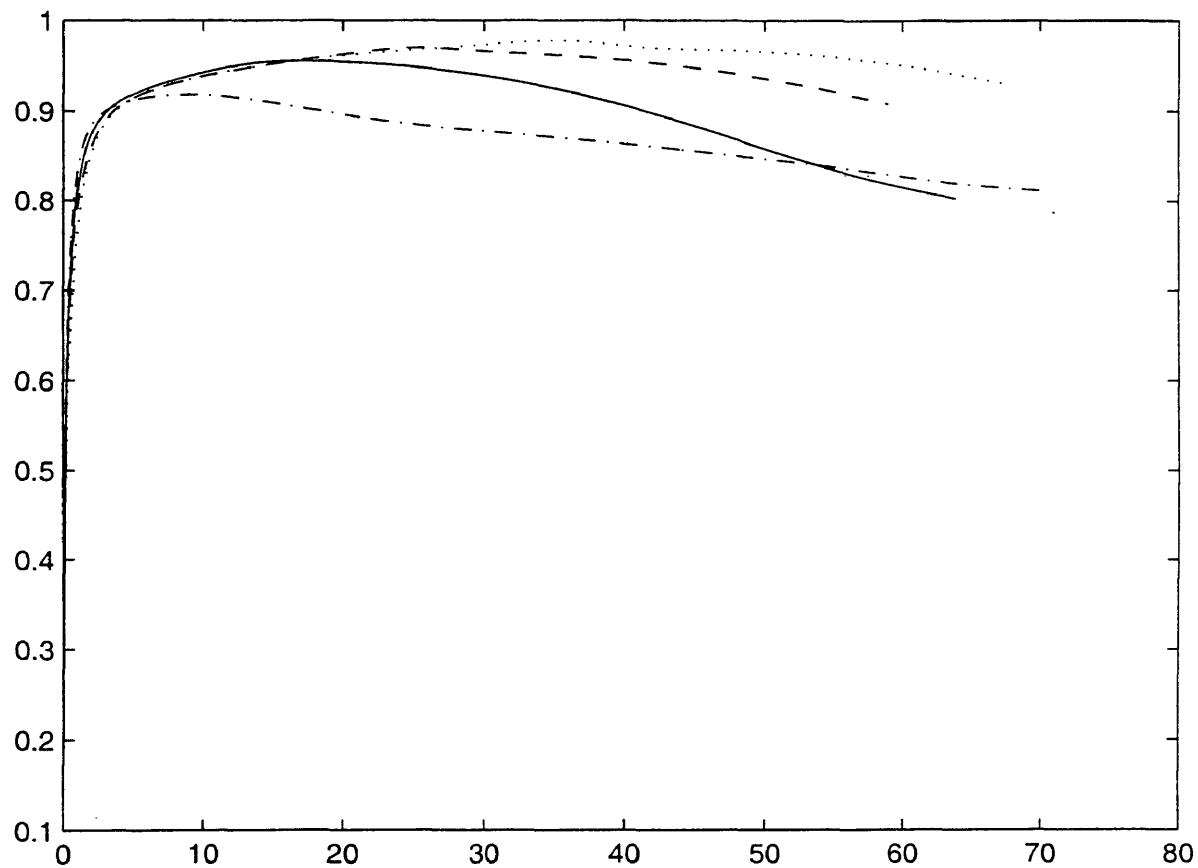


FIG. 5.5. Varying values of perturbation $\tilde{\rho}$ from the concentration with "...": $\tilde{\rho} = 10^{-3}$, "- -": $\tilde{\rho} = 10^{-2}$, "-": $\tilde{\rho} = 10^{-1}$, "-.": $\tilde{\rho} = 1$, where $m = 0$ and $(n\epsilon)^2 = 1$

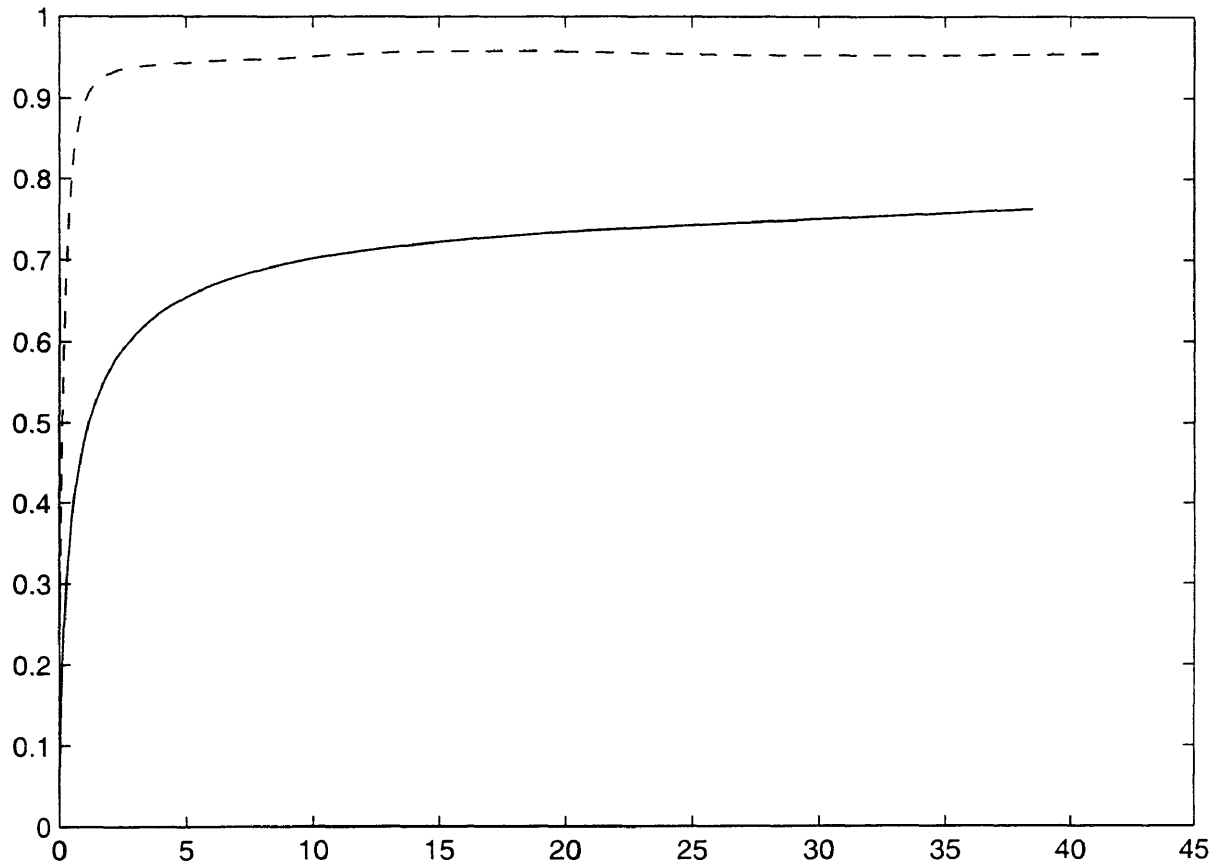


FIG. 5.6. Varying values of the product $(\epsilon n)^2$ with “- -”: $(\epsilon n)^2 = .5$, “—”: $(\epsilon n)^2 = 10$, where $\bar{\rho} = 10^{-1}$ and $m = 0$

stayed near a constant value for a large time. We refer especially to Fig. 5.1, which was taken out to a larger time than the other experiments. The ratio stays close one briefly because the coarsening process begins to take place. The nodal domains are no longer of order ϵ , and the solutions can no longer be described solely by the eigenfunctions corresponding to the positive eigenvalues.

It should be noted that the same initial condition was used for each test on the parameter $(n\epsilon)^2$, and the initial conditions for the other experiments only changed as the parameter value was changed. Something that should be considered in future analysis would be Monte Carlo simulations that give many results for many different initial conditions (cf. [36]). Another interesting experiment would be to vary the size of n directly. It is possible that a larger value of n would have led to better results.

Notice also that the norm used to calculate the ratio was the L^2 norm, but the norm used to derive our results was the graph norm given by (3.2). Clearly, these norms are very different, and would give different results. Similar experiments done using the graph norm were performed in [36]. In these experiments, solutions of the linearized Cahn-Hilliard equation are compared to the solutions of the nonlinear problem, using the Fourier series representation used in our ratio estimate. Our experiments differ because we are comparing the estimated solutions with the solutions corresponding to the positive eigenvalues, but our experiments could be done using the same norm. In fact, it would be interesting to redo our numerical analysis using the norm given by $\|\cdot\|_*$, because it is possible that the results would change.

Let the Crank-Nicolson method have an average time step of size τ_c and Eyre's method have an average time step of size τ_e . It was noted earlier that the only significant difference between the two numerical schemes used was in the number of time steps needed to reach the same final time. This can be observed in Table 5.1,

where the average step size of each method is given for different tolerances varying only $\tilde{\rho}$. Notice that $\tau_c^2 \approx \tau_e$ for each tolerance, due to the fact that Eyre's method is a lower order method. In addition, the step size decreases as the tolerance is made smaller, just as we would expect. Furthermore, Fig 5.7 plots the ratio for each different

Tolerance	τ_c	τ_e
10^{-2}	.453	.145
10^{-3}	.43	.061
10^{-4}	.3	.024

Table 5.1. Average time step size for each method as $\tilde{\rho}$ was varied given an error tolerance

error tolerance, using the Crank-Nicolson method and two values for $\tilde{\rho}$. Notice that a higher tolerance has little or no effect on the ratio.

Upon conclusion of this discussion, we compare the solutions of the two time stepping schemes. From Fig. 5.8, it is clear that the solutions for each method were the same. In this figure, both the Crank-Nicolson method and Eyre's method were plotted for the parameter values $m = 0$, $\tilde{\rho} = 10^{-1}$, and $(n\epsilon)^2 = 1$, where each method was taken out to a final time of approximately 90, and the result for each was almost the same line. We expected to see Eyre's method give less accurate results because it was solving the problem using an approximation of the nonlinearity, but the Crank-Nicolson method solved the full nonlinear problem, and gave nearly the same results. In the future, it would be interesting to see how the comparison of these two methods would change if the same experiments were performed using the extrapolated Crank-Nicolson method (cf. [12]), which uses the previous time step to approximate the nonlinearity.

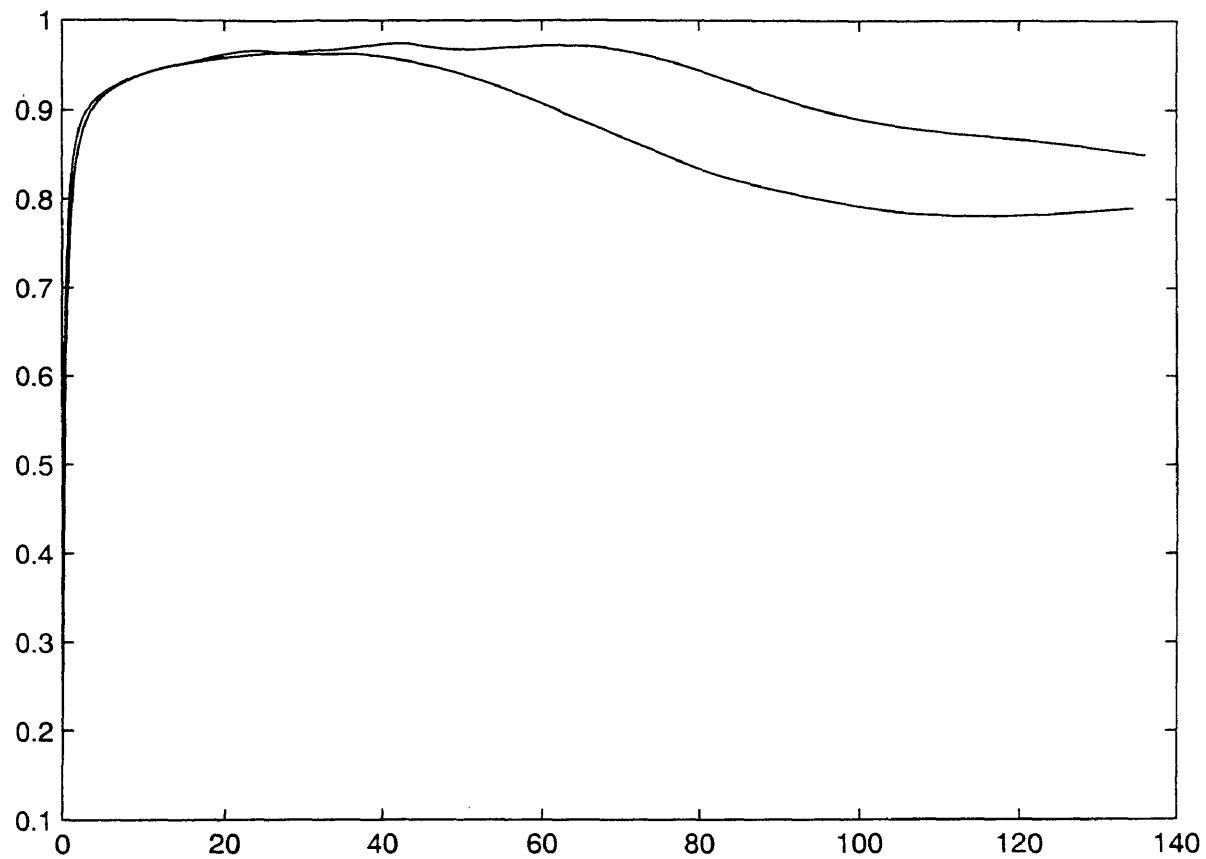


FIG. 5.7. Varying the error tolerance (tol) for the Crank-Nicolson method for $\bar{\rho} = 10^{-4}$ and $\bar{\rho} = 10^{-2}$ with “.” : tol = 10^{-4} , “- -” : tol = 10^{-3} , and “-” : tol = 10^{-2}

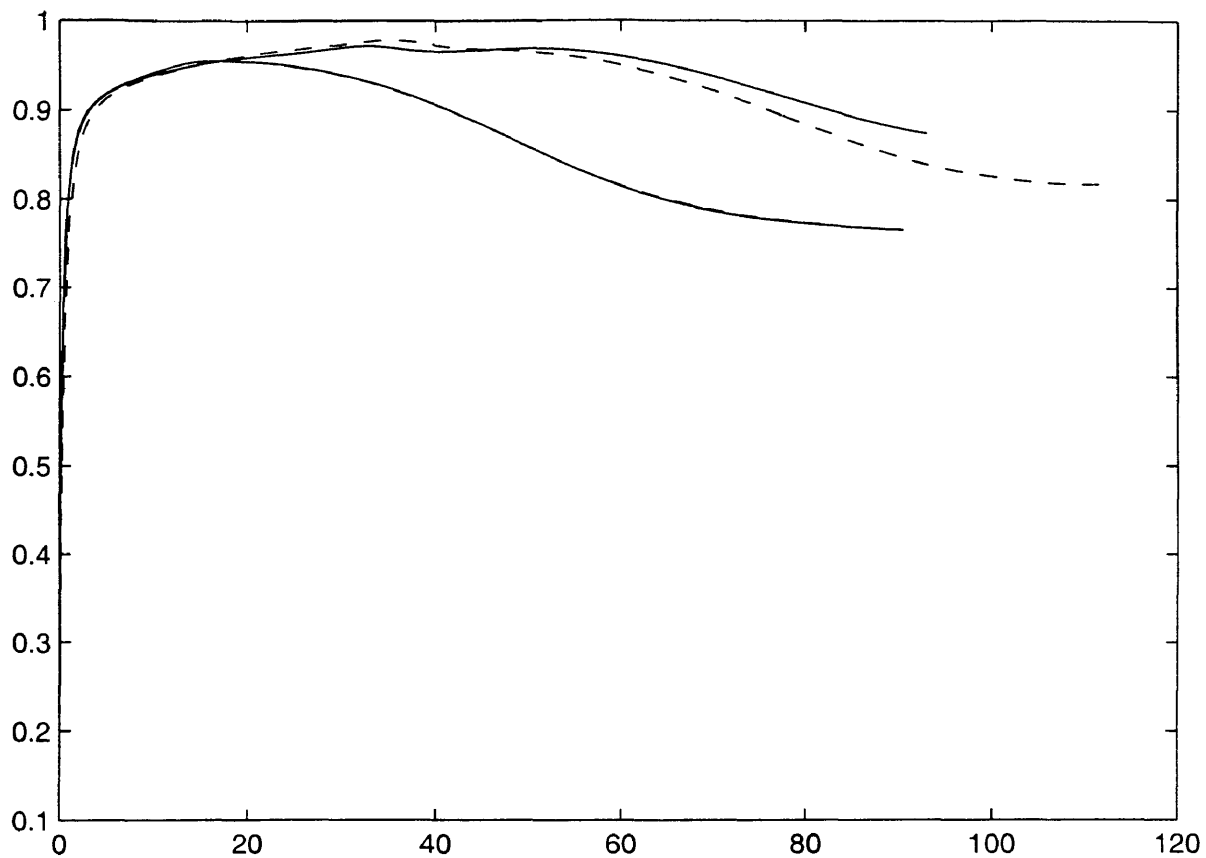


FIG. 5.8. Comparison of Eyre's method “- -” and the Crank-Nicolson method “—”, with $m = 0$, and $(n\epsilon)^2 = 1$ where $\tilde{\rho} = 10^{-3}$ for the top lines, and $\tilde{\rho} = 10^{-1}$ for the bottom lines

Chapter 6

CONCLUSIONS AND FUTURE WORK

We have studied spinodal decomposition for the spatially discrete Cahn-Hilliard equation. In this analysis, the given equation was divided into a linear part and a nonlinear part, as was done in a similar study of the continuous Cahn-Hilliard equation. The analysis for the nonlinear part followed exactly as it did for the continuous equation. For the linear part, it was shown that the positive eigenvalues of the discrete linear operator were almost equal to the positive eigenvalues of the continuous linear operator for sufficiently large n . We were concerned only with the positive eigenvalues because the negative eigenvalues have little or no effect on the solution when spinodal decomposition takes place. This enabled us to use in our analysis the results derived for the continuous linear operator.

It was shown that with a probability close to one, an initial condition chosen at random inside a neighborhood of some equilibrium in the spinodal interval would lead to an orbit that exited a larger neighborhood close to the subspace corresponding to the positive eigenvalues of the linear operator for the Cahn-Hilliard equation. For the nonlinear problem this subspace was replaced by an invariant manifold with the same probability estimate holding true. When this occurs, we get spinodal decomposition.

In our analysis, we showed what values of n would guarantee these results. From Lemma 2.4, we find a lower bound on n that enables us to use the analysis of the continuous problem. We also found that if n is close to $1/\epsilon$ or if $n > 1/\epsilon$, the effects of the negative eigenvalues are very small, giving spinodal decomposition, and our probability estimate holds. This is our main result and contribution.

We followed this theoretical analysis with numerical simulations that back these results well. In particular, the theoretical results depend on three things: the size of n relative to ϵ , the distance an initial condition started from the equilibrium point, and whether the equilibrium point was contained in the spinodal interval or not. Using two different time stepping techniques, each of these aspects was examined numerically by considering the ratio of the Fourier coefficients for the solution using only the positive eigenvalues, with that of the estimated solution. Overall, the results showed that spinodal decomposition takes place when n is close to, or greater than $1/\epsilon$, when m is in the spinodal interval, and when the initial condition starts close enough to m .

A comparison of the time stepping techniques known as Eyre's method and the Crank-Nicolson method was also performed. We found that Eyre's method offered accurate approximations, considering that it solved the equation using an approximation of the nonlinearity. We also noticed that Eyre's method required many more time steps, which was expected since it is a lower order method. This leaves us with a question of which method required the most linear system solves, because the Crank-Nicolson method solved more than one linear system per time step.

Theoretical results on when and how spinodal decomposition occur for the Cahn-Hilliard equation with both spatial and time discretizations have yet to be derived. These results would be beneficial since numerical simulations require a time discretization. We believe an analysis similar to what we have done with the spatially discrete problem, could be done for the fully discrete problem, but that has yet to be determined. Furthermore, the numerical results in this paper suggest that the lower bound we have imposed on n may be too high, meaning that we could consistently get spinodal decomposition for smaller n . The question now is how much smaller

could we let n be and still guarantee that the results will accurately model spinodal decomposition? In addition, the bound on the radius of the ball $B_r(0)$ is accurate, but what this means in terms of real values for r is still unclear. Numerically, one thing that should be considered is how different the results would be if the graph norm was used to compute the ratio rather than the L^2 norm. Another thing to be considered would be a mixed error estimate for the Newton tolerance, in which the norm of δ^j is checked as well as the norm of G .

REFERENCES

- [1] N. D. Alikakos, P. W. Bates, and X. Chen. Convergence of the Cahn-Hilliard equation to the Hele-Shaw model. *Archive for Rational Mechanics and Analysis*, 128:165–205, 1994.
- [2] N. D. Alikakos, L. Bronsard, and G. Fusco. Slow motion in the gradient theory of phase transitions via energy and spectrum. *Preprint*, 1997.
- [3] B. Aulbach and T. Wanner. Integral manifolds for Caratheodory type differential equations in Banach spaces. In *Six Lectures on Dynamical Systems*, pages 45–119. World Scientific, 1996.
- [4] P. W. Bates and C. K. Jones. Invariant manifolds for semilinear partial differential equations. *Dynamics Reported*, 2:1–38, 1989.
- [5] P. W. Bates and J. Xun. Metastable patterns for the Cahn-Hilliard equation. I. *Journal of Differential Equations*, 111:421–457, 1994.
- [6] P. W. Bates and J. Xun. Metastable patterns for the Cahn-Hilliard equation. II. Layer dynamics and slow invariant manifold. *Journal of Differential Equations*, 117:165–216, 1995.
- [7] L. Bronsard and D. Hilhorst. On the slow dynamics for the Cahn-Hilliard equation in one space dimension. *Proceedings of the Royal Society, London, Series A*, 439:669–682, 1992.
- [8] J. W. Cahn. On spinodal decomposition. *Acta Metallurgica*, 9:795–801, 1961.

- [9] J. W. Cahn, S. Chow, and E. S. Van Vleck. Spatially discrete nonlinear diffusion equations. *Rocky Mountain Journal of Mathematics*, 25(1):87–117, 1995.
- [10] J. W. Cahn and J. E. Hilliard. Free energy of a nonuniform system I. Interfacial free energy. *Journal of Chemical Physics*, 28:258–267, 1958.
- [11] R. Courant and D. Hilbert. *Methods of Mathematical Physics*. Intersciences, New York, 1953.
- [12] J. Douglas Jr. and T. Dupont. Galerkin methods for parabolic equations. *SIAM Journal of Numerical Analysis*, 7:575–626, 1970.
- [13] C.M. Elliott. The Cahn-Hilliard model for the kinetics of phase separation. *International Series of Numerical Mathematics*, 88:35–73, 1989.
- [14] C.M. Elliott and D. A. French. Numerical studies of the Cahn-Hilliard equation for phase separation. *IMA Journal of Applied Mathematics*, 38:97–128, 1987.
- [15] C.M. Elliott and S. Zheng. On the Cahn-Hilliard equation. *Archive for Rational Mechanics and Analysis*, 96:339–357, 1986.
- [16] D. J. Eyre. Unconditionally gradient stable time marching the Cahn-Hilliard equation. *Preprint*, 1998.
- [17] D. J. Eyre. An unconditionally stable one-step scheme for gradient systems. *Preprint*, 1998.
- [18] C. W. Gear. *Numerical Initial Value Problems in Ordinary Differential Equations*. Prentice-Hall, Englewood Cliffs, 1971.
- [19] C. P. Grant. Spinodal decomposition for the Cahn-Hilliard equation. *Communications in Partial Differential Equations*, 18:453–490, 1993.

- [20] C. P. Grant and E. S. Van Vleck. Slowly-migrating transition layers for the discrete Allen-Cahn and Cahn-Hilliard equations. *Nonlinearity*, 8:861–876, 1995.
- [21] D. Henry. *Geometric Theory of Semilinear Parabolic Equations*. Springer-Verlag, New York, 1981.
- [22] M. R. Hestenes and E. Stiefel. Methods of conjugate gradients for solving linear systems. *Journal Res. Nat. Bur. Stand.*, 49:409–436, 1952.
- [23] J. S. Langer. Theory of spinodal decomposition in alloys. *Annals of Physics*, 65:53–86, 1971.
- [24] R. Lauterbach and S. Maier. Symmetry-breaking at non-positive solutions of semilinear elliptic equations. *Archive for Rational Mechanics and Analysis*, 126(4):299–331, 1994.
- [25] S. Maier-Paape and T. Wanner. Spinodal decomposition for the Cahn-Hilliard equation in higher dimensions. Part I: Probability and wavelength estimate. *Preprint*, 1997.
- [26] S. Maier-Paape and T. Wanner. Spinodal decomposition for the Cahn-Hilliard equation in higher dimensions. Part II: Nonlinear dynamics. *Preprint*, 1997.
- [27] L. Modica. The gradient theory of phase transitions and the minimal interface criterion. *Archive for Rational Mechanics and Analysis*, 98:123–142, 1987.
- [28] K. W. Morton and D. F. Mayers. *Numerical Solutions of Partial Differential Equations*. Cambridge University Press, 1994.

- [29] N. M. Nachtigal, S. C. Reddy, and L. N. Trefethen. How fast are nonsymmetric matrix iterations? *SIAM Journal of Matrix Analysis and Applications*, 13:778–795, 1992.
- [30] B. Nicolaenko and B. Scheurer. Low dimensional behavior of the pattern formation Cahn-Hilliard equation. In *Trends and Practice of Nonlinear Analysis*, North Holland, 1985. Lakshimikantham.
- [31] A. Novick-Cohen and L. A. Segel. Nonlinear aspects of the Cahn-Hilliard equation. *Physica D*, 10:277–298, 1984.
- [32] R. L. Pego. Front migration in the nonlinear Cahn-Hilliard equation. *Proceedings of the Royal Society, London, Series A*, 422:261–278, 1989.
- [33] S. M. Rankin III. Semilinear evolution equations in Banach spaces with application to parabolic partial differential equations. *Preprint*.
- [34] M. Renardy and R. C. Rogers. *An Introduction to Partial Differential Equations*. Springer-Verlag, New York, 1993.
- [35] Y. Saad and M. H. Schultz. Conjugate gradient-like algorithms for solving nonsymmetric linear systems. *Mathematics of Computation*, 44:417–424, 1985.
- [36] E. Sander and T. Wanner. Monte Carlo simulations for spinodal decomposition. *Preprint*, 1998.
- [37] E. Sander and T. Wanner. Unexpectedly linear behavior for the Cahn-Hilliard equation. *Preprint*, 1999.

- [38] B. E. E. Stoth. Convergence of the Cahn-Hilliard equation to the Mullins-Sekerka problem in spherical symmetry. *Journal of Differential Equations*, 125:154–183, 1996.
- [39] A.M. Stuart and A.R. Humphries. Model problems in numerical stability theory for initial value problems. *SIAM Review*, 36:226–257, 1994.
- [40] A.M. Stuart and A.R. Humphries. *Dynamical Systems and Numerical Analysis*. Cambridge University Press, 1998.
- [41] R. Temam. Infinite-dimensional dynamical systems in mechanics and physics. In *Applied Mathematical Sciences*, volume 68, New York, 1988. Springer-Verlag.
- [42] J. D. van der Waals. The thermodynamic theory of capillarity flow under the hypothesis of a continuous variation in density. *Verhandelingen der Koninklijke Nederlandsche Akademie van Wetenschappen te Amsterdam*, 1:1–56, 1893.
- [43] T. Wanner. Linearization of random dynamical systems. *Dynamics Reported*, 4:203–269, 1995.
- [44] S. Zheng. Asymptotic behavior of solutions to the Cahn-Hilliard equation. *Applied Analysis*, 23:165–184, 1986.